UNIVERSIDADE FEDERAL DO PARANÁ

NATALIA NEUHAUS

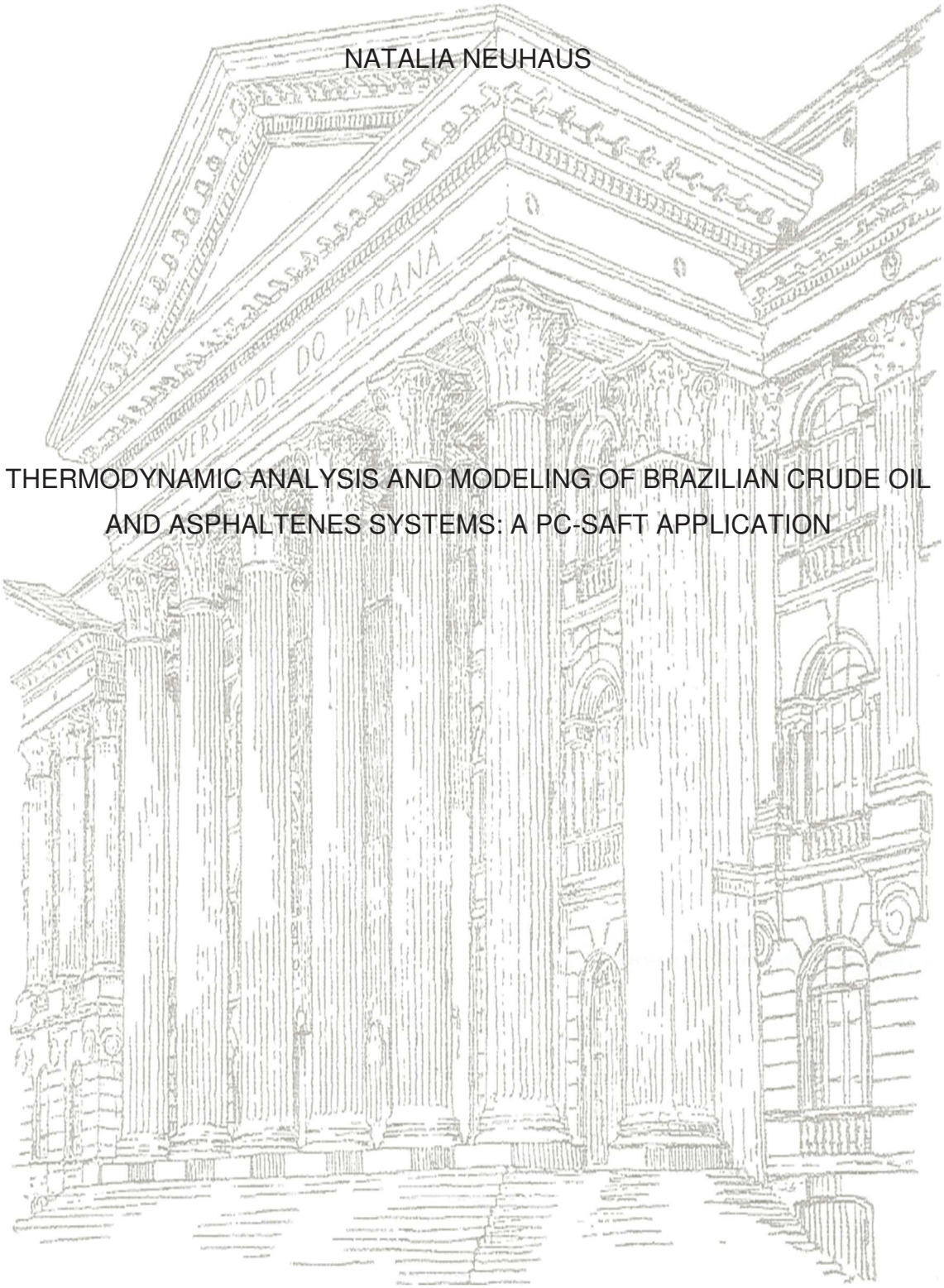

THERMODYNAMIC ANALYSIS AND MODELING OF BRAZILIAN CRUDE OIL AND ASPHALTENES SYSTEMS: A PC-SAFT APPLICATION

CURITIBA
2017

NATALIA NEUHAUS

THERMODYNAMIC ANALYSIS AND MODELING OF BRAZILIAN CRUDE OIL AND ASPHALTENES SYSTEMS: A PC-SAFT APPLICATION

Dissertação apresentada ao Programa de Pós-Graduação em Engenharia Química, Setor de Tecnologia da Universidade Federal do Paraná, como parte dos requisitos para a obtenção do título de Mestre em Engenharia Química.

Orientador: Alexandre Ferreira Santos
Co-orientador: Marcos Lúcio Corazza

CURITIBA
2017

Catalogação na Fonte: Sistema de Bibliotecas, UFPR
Biblioteca de Ciência e Tecnologia

N485t Neuhaus, Natalia
Thermodynamic analysis and modeling of brazilian crude oil and asphaltenes systems: a PC-SAFT application [recurso eletrônico] / Natalia Neuhaus. – Curitiba, 2017.

Dissertação - Universidade Federal do Paraná, Setor de Tecnologia, Programa de Pós-Graduação em Engenharia Química, 2017.

Orientador: Alexandre Ferreira Santos – Coorientador: Marcos Lúcio Corazza.

1. Petróleo - Brasil. 2. Asfalteno. 3. Perturbed-Chain Statistical Association Fluid Theory (PC-SAFT). I. Universidade Federal do Paraná. II. Santos, Alexandre Ferreira. III. Corazza, Marcos Lúcio. IV. Título.

CDD: 338.27282

Bibliotecário: Elias Barbosa da Silva CRB-9/1894

MINISTÉRIO DA EDUCAÇÃO
UNIVERSIDADE FEDERAL DO PARANÁ
PRÓ-REITORIA DE PESQUISA E PÓS-GRADUAÇÃO
Setor TECNOLOGIA
Programa de Pós-Graduação ENGENHARIA QUÍMICA

TERMO DE APROVAÇÃO

Os membros da Banca Examinadora designada pelo Colegiado do Programa de Pós-Graduação em ENGENHARIA QUÍMICA da Universidade Federal do Paraná foram convocados para realizar a arguição da dissertação de Mestrado de **NATÁLIA NEUHAUS** intitulada: **Thermodynamic analysis and modeling of brazilian crude oil and asphaltenes systems: a PC-SAFT application**, após terem inquirido a aluna e realizado a avaliação do trabalho, são de parecer pela sua APROVAÇÃO no rito de defesa.

A outorga do título de mestre está sujeita à homologação pelo colegiado, ao atendimento de todas as indicações e correções solicitadas pela banca e ao pleno atendimento das demandas regimentais do Programa de Pós-Graduação.

CURITIBA, 10 de Julho de 2017.

ALEXANDRE FERREIRA SANTOS
Presidente da Banca Examinadora (UFPR)

PAPA MATAR NDIAYE
Avaliador Externo (UFRJ)

FERNANDO AUGUSTO PEDERSEN VOLL
Avaliador Interno (UFPR)

MARCOS LÚCIO CORAZZA
Avaliador Interno (UFPR)

ACKNOWLEDGEMENTS

To God for the good health and for giving the ability to study.

I express sincere gratitude to my advisor Prof. Alexandre F. Santos for giving me the opportunity to do this master even with the distance and work. Thanks for the guidance, time and patience.

I am very thankful to Prof Marcos L. Corazza, my co-advisor, for introduce me to PC-SAFT's world, providing academicals assistance which supported me in completion of this study.

A special thanks to Priscila Nascimento for friendship and all support during the experimental tests.

I dedicate this dissertation to my partner Paulo, who has been so encouraging and supportive and my parents for their warming support through the distance.

"... nunca deixe que lhe digam que não vale a pena acreditar
no sonho que se tem ou que seus planos nunca vão
dar certo ou que você nunca vai ser alguém..."

"Quem acredita sempre alcança"

Renato Russo e Flávio Venturini

RESUMO

O petróleo ainda é a principal fonte de energia primária. A demanda global esperada para 2017 é aproximadamente 97,9 milhões de barris por dia, um crescimento equivalente a 1,3 milhões de barris por dia. Além do aumento da exploração de novos reservatórios, incluídos reservatórios de petróleo pesado, os quais são geralmente ricos em frações complexas como os asfaltenos, por exemplo, é crucial garantir a continuidade operacional da produção de petróleo. No entanto, as operações de campo enfrentam problemas devido à tendência dos asfaltenos em se associar e precipitar, causando vários problemas operacionais dispendiosos. As variações de pressão, temperatura ou composição, podem resultar em precipitação ou solubilização de asfaltenos. A precipitação e posterior deposição podem causar problemas em todas as fases de produção. Neste contexto, a principal motivação desta dissertação é modelar o petróleo brasileiro e seus asfaltenos usando a equação de estado PC-SAFT (Perturbed-Chain Statistical Association Fluid). O uso deste modelo estatístico baseado na teoria de fluidos associativos tem se mostrado altamente promissor para a modelagem do comportamento de fases de sistemas de petróleo e densidade de líquidos. Uma breve revisão desta teoria estatística é apresentada. Neste trabalho, os asfaltenos foram extraídos do petróleo bruto através da adição de diferentes n-alcanos. As densidades de tolueno e asfaltenos foram medidas utilizando o densímetro Anton Paar DMA 5000. A equação de estado mostrou-se capaz de prever com precisão a densidade dos líquidos bem como a elevação do ponto de ebulição para o petróleo em diferentes concentrações de tolueno. A precipitação de asfaltenos a partir de um óleo modelo mostrou a influência dos parâmetros de interação binária nos resultados da modelagem. A precipitação dos asfaltenos foi considerado como um processo de equilíbrio líquido-líquido onde uma das fases foi representada por asfaltenos e a outra foi caracterizada em termos de dois pseudo-componentes: saturados e (aromáticos+resinas). A influência dos agentes precipitantes (n-hexano e n-heptano) no comportamento de fase dos asfaltenos foi analisada. Os resultados demonstraram que o n-C_6 é capaz de precipitar mais asfaltenos comparado com o n-C_7, confirmando os resultados apresentados pela literatura. Os resultados encontrados pelas simulações estão em concordância com os dados obtidos experimentalmente: o erro relativo médio foi 3,75 % e 10,25 % para a porcentagem em peso de asfaltenos precipitados utilizando n-C_6 e n-C_7 como precipitante, respectivamente.

Palavras-chave: Petróleo brasileiro. Precipitação de asfaltenos. PC-SAFT.

ABSTRACT

Petroleum still is the largest source of total primary energy. The global demand in 2017 is projected at approximately 97.9 million barrels per day, a forecasted growth of 1.3 million barrels per day. Besides the increase in exploitation of new reservoirs, including heavy oil reservoirs, which are usually rich in complex fractions such as asphaltenes, it is crucial to guarantee the operational continuity of its production. However, field operations are facing problems due to the asphaltene tendency to associate and precipitate, causing several costly operational problems. Variations of pressure, temperature or composition may result in precipitation or solubilization of asphaltenes. Precipitation and subsequent deposition can cause problems in all stages of production. Therefore, the main motivation of this dissertation is to model Brazilian crude oil and asphaltene systems using the PC-SAFT equation of state. The Perturbed-Chain Statistical Association Fluid Theory (PC-SAFT) is a highly promising equation of state for modeling the phase behavior of petroleum systems and liquid densities. Asphaltenes were extracted from crude oil through the addition of different n-alkanes. Densities of toluene, asphaltenes and their mixtures were measured using a densitometer. The equation of state is capable of accurately predicting liquid density for toluene and asphaltenes and boiling point elevation for crude oil at different concentrations of toluene. Asphaltene precipitation from a model oil shows the influence of binary interaction parameters on modeling results. The system is considered in the liquid-liquid equilibrium where the asphaltene is considered in one liquid phase and the other liquid phase is characterized in terms of two pseudo-components: saturates and (aromatics+resins). The influence of precipitant agent (n-hexane and n-heptane) on the asphaltene phase behavior is analyzed. The results demonstrated that n-C6 is able to precipitate more asphaltenes than n-C7, as expected. Furthermore, simulated results are in agreement with experimental observations: the average relative error is 3.75 % and 10.25 % for the weight percentage of precipitated asphaltene using n-C6 and n-C7 as precipitant, respectively.

Key-words: Brazilian crude oil. Asphaltene precipitation. PC-SAFT.

FIGURES

TABLES

ABBREVIATIONS

ANP – National Petroleum Agency
AOP – Asphaltene Onset Precipitation
API – American Petroleum Institute
BPE – Boiling Point Elevation
CMC – Critical Micellar Concentration
CPA – Cubic-Plus-Association
DBSA – Dodecyl-benzensulphonic acid
EOS – Equation of State
ITC – Isothermal Titration Calorimetry
VLE – Vapor-Liquid Equilibrium
VL-quasi-L – Vapor-Liquid-quasi-Liquid Equilibrium
MRE – Mean relative error
MSE – Mean square error
MW – Molecular Weight
NP – Nonylphenol
OPEC – Organization of the Petroleum Exporting Countries
PR – Peng-Robinson
PC-SAFT – Perturbed-Chain Statistical Associating Fluid Theory
PVT – Pressure, Volume, Temperature
SAFT – Statistical Associating Fluid Theory
SAP – Saturate, Aromatic and Polyaromatic
SARA – Saturates, Aromatics, Resins and Asphaltenes
S-BWR – Soave-Benedict-Webb-Rubin
SRK – Soave-Redlich-Kwong
TA – Tetrameric Acid
THF – Tetrahydrofuran
TPT – Thermodynamic Perturbation Theory

SYMBOLS

[A] – Concentration of monomers

[A_2] – Concentration of dimers

a^{assoc} – Free energy of directional interactions

a^{chain} – Free energy of the chain formation

a^{segmen} – Free energy of the individual spherical "segments"

C_{Asf} – Concentration de asphaltenes

d_{ii} – Temperature-dependent size diameter

$f_{i,p}$ – Fugacity of component *i* in phase *p*

g – Gibbs free energy

g_{ii} – Radical distribution function

h – Molar enthalpy

K_A – Equilibrium constant

k – Boltzmann constant

kij – Binary interaction parameter

m – Number of segments in PC-SAFT equation of state

$\bar{m}$ – Mean number of segments

M – Number of association sites on the molecule in SAFT EOS

Mw – Molar Mass

N – Stoichiometry of reaction

P – Pressure

P_{RI} – Initial Point Precipitation

R – Universal gas constant

S – Specific gravity

s – Entropy

T – Temperature

v – Molar volume

v^{00} – Volume parameter in SAFT EOS

x – Mole fraction of component in liquid phase

y – Mole fraction of component in gas phase

z – Total mole fraction of component

Z – Compressibility factor

Z^{disp} – Dispersive Contribution

Z^{hc} – Hard-chain contribution in SAFT EOS

w – Mass fraction

ΔG – Gibbs free energy

ΔH – Enthalpy

ΔS – Entropy

γ – Aromaticity factor in PC-SAFT parameter correlations

ε – Depth of pair potential

ε/K – Segment energy parameter in PC-SAFT EOS

ρ – Density

μ – Chemical Potential

ϕ – Fugacity Coefficient

σ – Segment diameter in PC-SAFT EOS

ζ – Packing Factor

Subscripts

A – Aromatic fraction

Asp – Asphaltene fraction

b – Boiling point

C – Cumulative

hs – Hard-sphere

i – Component

P – Polyaromatic fraction

res – Residual

R – Resins fraction

S – Saturate fraction

CONTENT

1 INTRODUCTION

Due to the declining reserves of conventional oil, whose extraction is relatively affordable and economical, there was an increase in exploitation of heavy oil reservoirs. According to the National Petroleum Agency (ANP), in March 2016 27.8% of the oil produced in Brazil corresponded to heavy oil, which is usually rich in complex fractions such as asphaltenes. In addition, even though its use has decreased from 46% in 1973 to 31% in 2014, according to International Energy Agency, oil is still the largest source of the total primary energy supply. Besides that, the global demand growth is forecasted at 1.3 million barrels per day in 2017, with a total demand of 97.9 million barrels per day. Therefore, besides the increase in exploitation of new reservoirs, it is crucial to guarantee the operational continuity of its production.

Crude oil is a mixture of organic compounds and commonly distinguishes between four fractions: saturates, aromatics, resins and asphaltenes. This classification is known as the SARA characterization (MERINO-GARCIA and ANDERSEN, 2004; MULLINS *et al.*, 2007; OPEDAL, 2011; FOSSEN, 2007; SABETI *et al.*, 2015). Asphaltenes, polydisperse molecules of polar and heavy oil components, are often insoluble in n-alkane (n-pentane and n-heptane) and highly soluble in an aromatic solvent (benzene and toluene). Moreover, it contains a high proportion of aromatic rings, heteroatoms (C, H, N, O and S) and some metal constituents (Fe, Ni and V) (SPEIGHT. 2007).

Field operations are facing problems caused by the tendency of asphaltenes to associate and precipitate, causing several costly operational problems (VARGAS *et al.*, 2009). Deposition of asphaltenes can cause several problems in all stages of production (KORD *et al.*, 2012; GHOLAMI *et al.*, 2014), including the oil production and recovery, due the mechanisms of wettability alteration and blockage (SALAHSHOOR *et al.*, 2013), as well as in both downstream operations, where they can block pipelines and equipments, and upstream operations, since the precipitation of asphaltenes are deposited in rocks, reducing their porosity and permeability (KAZEEM *et al.*, 2012). Asphaltene deposition and flow restrictions are often observed during light oil production, with a low asphaltene content (CARDOSO *et al.*, 2014). A necessary condition for the deposition of asphaltenes on surfaces is their precipitation, described by bulk phase equilibrium thermodynamics (LI and FIROOZABADI, 2009), although in

some cases the deposition may not occur. Deposition is related to mechanisms related to the surface characteristics, to the flow field in the system and to both the amount and the properties of precipitated asphaltene (VARGAS *et al.*, 2009; LI and FIROOZABADI, 2009).

The complex structure of asphaltenes and their mechanism of precipitation and stabilization have been continuously discussed over the years. Intense research activity has been developed aiming to establish a reliable assessment of asphaltenes precipitation/deposition/fouling risks during oil production and transport. In this sense, two main models were proposed in the literature for asphaltene stabilization in crude oil: colloidal and solubility theories. The classic colloidal theory given by Pfeiffer and Saal (1940), inspired in part by Nellensteyn (1924), assumes that asphaltene and resin are polar molecules. In this model, asphaltene molecules are present in the crude oil as solid particles and are stabilized by the resins adsorbed on their surface (micelle formation). Therefore, when the resins are removed from the surface, by dilution with alkanes or any other diluent, the asphaltenes are not soluble in the resulting oil mixture, forming a separate phase. However, Czarnecki (2009) illustrated using a hydrophilic-lipophilic balance that asphaltenes are not polar and do not form micelles.

On the other hand, in the solubility model or molecular model, asphaltenes are stabilized by the oil and their precipitation can be modeled as solid-liquid or liquid-liquid equilibrium (ALHAMMADI, VARGAS and CHAPMAN, 2015; SEDGHI and GOUAL, 2014). Two pseudocomponents (asphaltene and solvent) form the crude oil and their phase behavior is determined by molecular size and Van der Waal interactions. Nowadays, the solubility model has been the focus of a number of researches. Two main types of models have emerged from this theory: (1) regular solution models that use Flory-Huggins theory, and (2) equations of state (EOS) models (LI and FIROOZABADI, 2009; PFEIFFER and SALL, 1940). The Flory-Huggins approach is able to successfully predict both the onset and the amount of asphaltene precipitate but it does not consider the asphaltene association and the compressibility effect on phase behavior that is estimated by EOS approach. Although the cubic EOS have fairly simple calculations and have been used to predict the thermodynamic behavior of fluids on reservoir conditions, they, unlike the non-cubic equations, neither precisely describe systems of phase behavior with large gaps, nor density of liquids (VARGAS *et al.*, 2009). As for the non-cubic equations, a modern equation of state based on statistical theory and all their versions give a good prediction for the phase behavior of

high-molecular-weight fluids: the statistical associating fluid theory (SAFT) model. The SAFT equation of state was developed based on statistical thermodynamics approaches proposed by Wertheim (1984a, 1984b, 1986a, 1986b). Versions of the SAFT model have been used in both colloidal and solubility models, including the PC-SAFT (Perturbed-Chain SAFT).

Although many advances have been made in previous studies, the literature still lacks investigations focused on modeling of the asphaltene precipitation from the crude oil. Most studies are focused on the description of the asphaltene precipitation from model fluids (eg. asphaltenes+heptol). Besides, very little is known when crude oils containing asphaltenes with very low molecular weights are employed, as in the case of Brazilian crude oils.

There is obviously a great interest in developing a general modeling approach able to provide proper description of the asphaltene precipitation. This task may be accomplished with the help of a thermodynamic model that adequately describes the asphaltene phase behavior. In this work, we intend to take a step further in the description of the precipitation of asphaltenes using the PC-SAFT theory.

1.1 OBJECTIVES

In this context, the objective of this work is to study PC-SAFT applications for thermodynamic analysis and modeling of Brazilian crude oil and asphaltene systems. Specific objectives include (1) present an overview of the Wertheim theory, SAFT and PC-SAFT equation of state; (2) validate asphaltene prediction density and crude oil boiling point elevation using PC-SAFT equations; (3) evaluate the precipitation curve of asphaltenes from a model oil with different n-alkanes by experimental methodology based on literature; (4) study the asphaltene precipitation from crude oil and its stability.

2 **THEORY**

2.1 PETROLEUM: GENERAL ASPECTS

Petroleum is the primary source of energy in the world due to the large amounts of energy per unit of volume contained in this mixture (MERINO-GARCIA and ANDERSEN, 2004). The Organization of the Petroleum Exporting Countries (OPEC) predicted for 2017 a world oil consumption of 97.9 million barrels per day. In large scale, the readily available hydrocarbon resources have already been drained, increasing the technical demand for exploitation of the heavy oils and bitumens, which comprise a substantial fraction of remaining hydrocarbon resources (MULLINS, 2007).

Crude oil is a product of heat, compression and bacteriological action on ancient vegetation, primarily aquatic vegetation and algae. A closed environment and the long term effect of both pressure and high temperature causes the hydrocarbons to slowly form kerogen, a solid-like hydrocarbon. Given enough time, there is the division of the kerogen into smaller hydrocarbons, which later migrate through different layers of rock until they form a reservoir (OPEDAL, 2011). This means that the petroleum composition is dependent on the local flora and fauna, which may explain some of the petroleum characteristics around the world. In addition, the age of the field and the depth of the well influence the properties of the petroleum (FOSSEN, 2007).

Petroleum is a mixture composed mainly by hydrocarbons plus organic compounds of sulfur, nitrogen and oxygen, as well as compounds containing metallic elements including vanadium, nickel and iron, which encompass a huge range of properties (MERINO-GARCIA, 2004; HAMMAMI and RATULOWSKI, 2007). Although the proportions of the elements present in the oil varies only slightly, as can be seen in TABLE 1, their physical properties may have a wide range, including an appearance from colorless to black (SPEIGHT, 2006).

A notable way to reproduce the crude oil components is the SARA classification: saturates, aromatics, resins and asphaltenes (MERINO-GARCIA and ANDERSEN, 2004; MULLINS *et al.*, 2007; OPEDAL, 2011; FOSSEN, 2007; SABETI

et al., 2015). These designations are based on operational procedures associated with solubility and adsorption.

TABLE 1 – ELEMENTAL COMPOSITION RANGES OF CRUDE OILS

Carbon	83.0-87.0%
Hydrogen	10.0-14.0%
Nitrogen	0.1-2.0%
Oxygen	0.05-1.5%
Sulfur	0.05-6.0%

Source: HAMMAMI, RATULOWSKI (2007)

Concerning to their solubility, asphaltenes are n-pentane and n-heptane insoluble and dissolve in solvents such as benzene and toluene. The portion of petroleum that is soluble in pentane or heptane is referred to as the maltenes. This fraction is subdivided by percolation through any surface-active material, such as alumina, to yield an oil fraction. The oil fraction can be further subdivided into resins, aromatics and saturates fraction by a proper solvent (SPEIGHT, 2006).

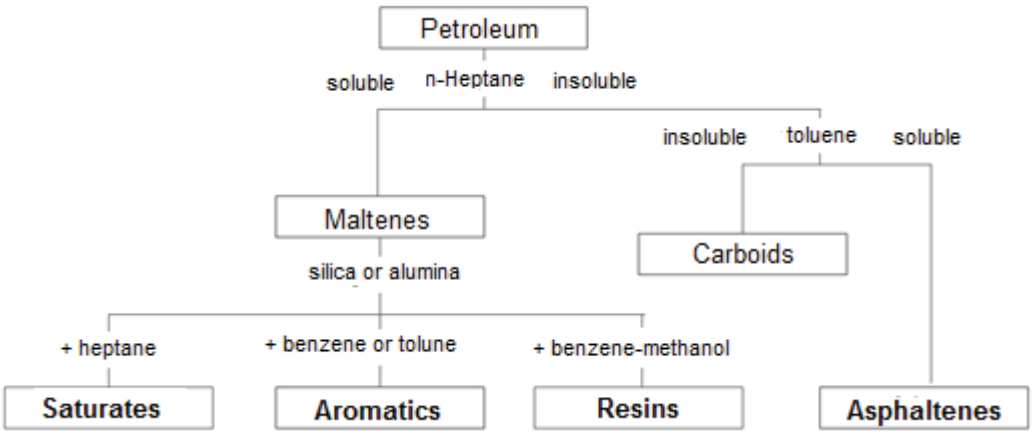

FIGURE 1 – SIMPLIFIED REPRESENTATION OF THE FRACTIONATION OF PETROLEUM
Source: MERINO-GARCIA (2004)

Saturated compounds are non-polar and consist of alkanes with normal chain, branched or cyclic (n-paraffins). Aromatic fractions are hydrocarbons chemically and physically very different from saturated compounds, because contain one or more benzene rings. Resins are composed of polar groups (heteroatoms) and non-polar paraffinic group (QUINTERO, 2009). Its molecular weight ranges between 600 and

1000 units (MERINO-GARCIA, 2004). Asphaltene molecules are similar to resins, but with a higher molecular weight and polyaromatic nuclei (HAMMAMI, RATULOWSKI, 2007).

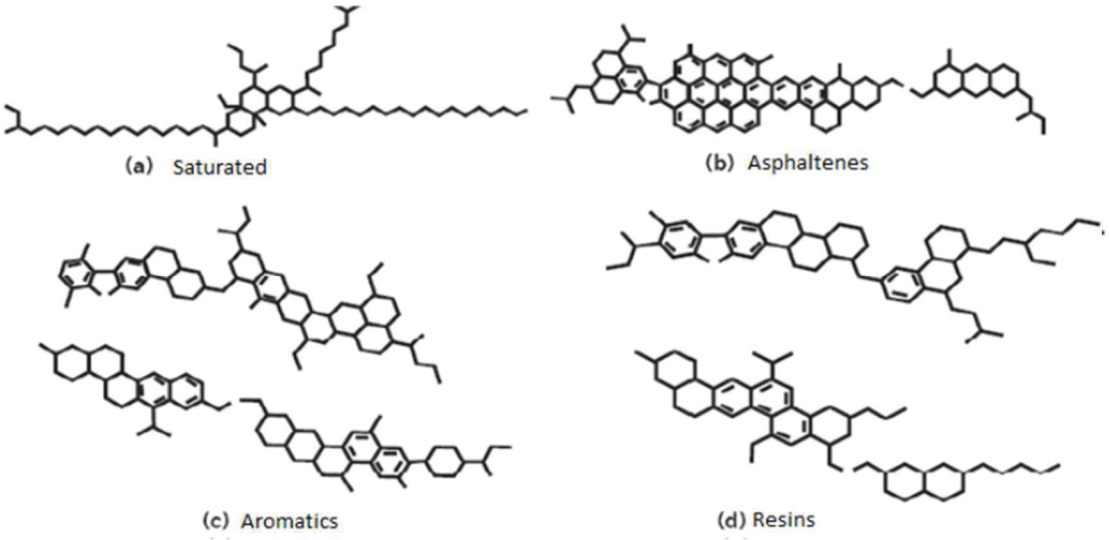

FIGURE 2 – STRUCTURES REPRESENTING SATURATED, ASPHALTENE, AROMATICS AND RESINS.
Source: Source: CHRISMAN *et al.* (2012)

2.2 ASPHALTENES

Asphaltenes are defined as the most polar fraction of crude oil (KAMINSKI *et al.*, 2000) and, consequently, they are insoluble in n-alkanes as pentane, hexane and heptane and soluble in aromatic solvents as toluene and xylene. Over the decades, it has been an intense debate with respect to its chemical composition, structure and molecular weight (QUINTERO, 2009). The number of species with very different characteristics inside the asphaltene fraction is statistically estimated to be over 100.000 (MERINO-GARCIA, 2004).

Asphaltenes are a mixture of components, generally treated as a structure with one or more aromatic rings (CALDAS, 1997) where 20 to 50 % of carbon atoms are present (YEN, 1998), with alkyl and naphthenic moieties and 1-10 wt% of heteroatom compounds, mainly composed by nitrogen (contents vary from 0.6 wt% to 3.3 wt%), oxygen (contents vary from 0.3 wt% to 4.9 wt%) and sulfur (contents vary from 0.3 wt%

to 10.3 wt%), which varies according to the crude oil. Furthermore, metals such as nickel, vanadium and iron, are concentrated in the asphaltene fraction in the ppm range (MERINO-GARCIA, 2004; SPEIGHT, 2006). The removal of metals increase the rate of dissolution or, in other words, the metal content has a direct effect on asphaltene dissolution, being important in the self-association of asphaltenes (KAMINSKI *et al.*, 2000).

The distribution of molecular weights of asphaltenes is still a matter of debate because they have a low solubility in the liquids often used for determination. Also, adsorbed resins lead to discrepancies in molecular weight determination and precipitated asphaltenes should be reprecipitated several times before this determination (SPEIGHT, 2006). Some researchers claimed the asphaltenes were arranged in a huge aromatic sheet surrounded by alkyl branches (FIGURE 3a), known as *continental* asphaltenes. Other studies showed that asphaltene molecules were more flexible, so that they could migrate along with the rest of petroleum, providing a structure of asphaltenes with some fused rings linked by alkyl branches, called *archipelago* asphaltenes (FIGURE 3b) (MERINO-GARCIA, 2004). Asphaltenes molecular weight ranges from 500 to 2000 g/mol (NASCIMENTO *et al.*, 2016) depending not only on the oil and its origin, but also depending on the nature of the solvent, the solution temperature, the preliminary treatment and the measurement method (QUINTERO, 2009).

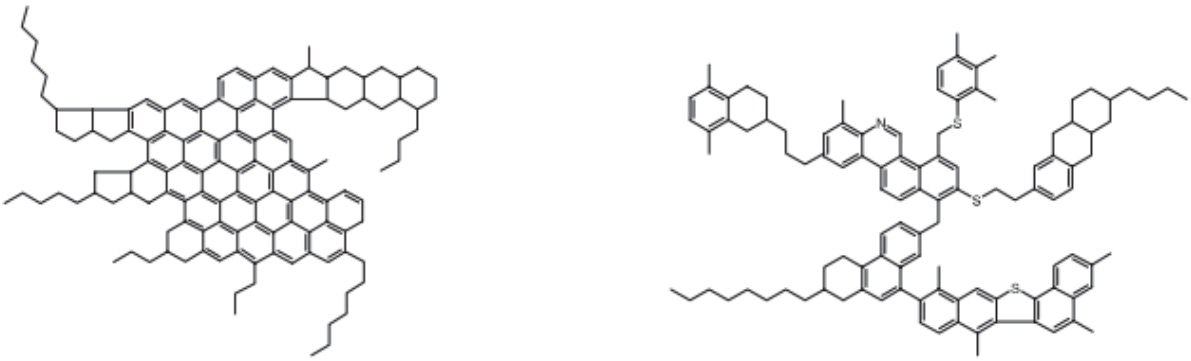

(a) (b)

FIGURE 3 – EVOLUTION OF ASPHALTENE AVERAGE MOLECULE (A) CONTINENTAL TYPE; (B) ARCHIPELAGO TYPE
Source: MERINO-GARCIA (2004)

In the initial reservoir condition, asphaltene is kept dispersed in the petroleum medium through peptizing by resin. Changes of pressure, temperature and fluid composition can cause the desorption of resin from asphaltenes and result in the phase separation and asphaltene precipitation. Hence, it can provoke undesirable impacts on the petroleum industry such as wettability alteration and clogging of transportation pipelines, as well as loss of efficiency in production facilities, heat exchangers and catalysts (GHOLAMI *et al.*, 2014).

Asphaltene precipitation or its solubilization is a consequence of pressure, temperature or composition variation. Temperature influence on asphaltene solubility is under investigation and different conclusions have been described. Thiyagarajan *et al.* (1995) claimed that as the temperature increased, the length of the aggregates decreased, while Moritis (2001) affirmed that asphaltenes have been precipitated during transportation when the temperature was decreased. According to Vargas *et al.* (2009) and Gonzalez *et al.* (2005) in systems containing molecules with large differences of molecular weights, asphaltene precipitation decreases until a certain temperature and then starts to increase, as we can see from the phase envelope in FIGURE 4. They explained that at low temperatures, the differences in interaction energies between solvent (crude oil) and asphaltene molecules make asphaltenes unstable, increasing the amount of asphaltenes precipitated. As temperature increases, the large thermal expansivity of the solvent compared to that of asphaltene ensures the solution splits and cause the precipitation of asphaltenes. Verdier *et al.* (2006) used CO_2 as a precipitant to study the effects of temperature on the stability of asphaltenes from two different crude oils and found that, for both oils, a decrease in temperature leads to an increase in the solubility of asphaltenes. The authors justified these controversial observations by simple principles of thermodynamics like Le Châtelier's principle and solubility parameters.

Influence of pressure on asphaltene precipitation is a consensus among the authors and occurs in a delimited region known as asphaltene deposition envelope (ADE) (MERINO-GARCIA and ANDERSEN, 2003; VARGAS *et al.*, 2009; SABETI *et al.*, 2015). FIGURE 5*,* adapted from Sabeti *et al.* (2015), presents the P vs. mole of solvent qualitative graphic for an oil sample at a constant temperature; the solid line are bubble points and the dotted/dashed lines are asphaltenes onset pressures. At high pressure, above the bubble point, the asphaltenes are soluble in oil and, as the pressure drops, especially for crude oils containing high fractions of saturates, the oil

expands and reduces the oil solubility parameters, becoming a poor asphaltene solvent. During the oil recovery, the system continues to depressurize until it reaches the bubble point. At this point, the light constituents (asphaltene precipitants) escape to gas phase, increasing the solubility parameters and the oil becomes a good asphaltene solvent again. Ting (2003) showed that asphaltenes are unstable below a certain solubility parameter of the oil, while Vargas *et al.* (2009) found the solubility parameter is not always constant along the asphaltenes stability boundary.

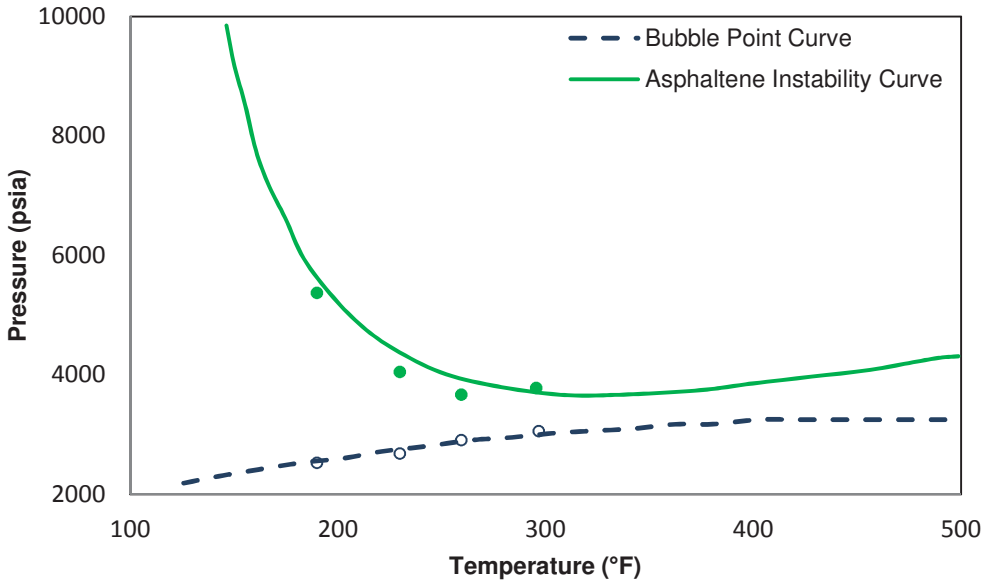

FIGURE 4 – ASPHALTENE PHASE BEHAVIOR BY PC-SAFT SIMULATIONS AND EXPERIMENTAL DATA
Source: VARGAS *et al.* (2009) – Adapted

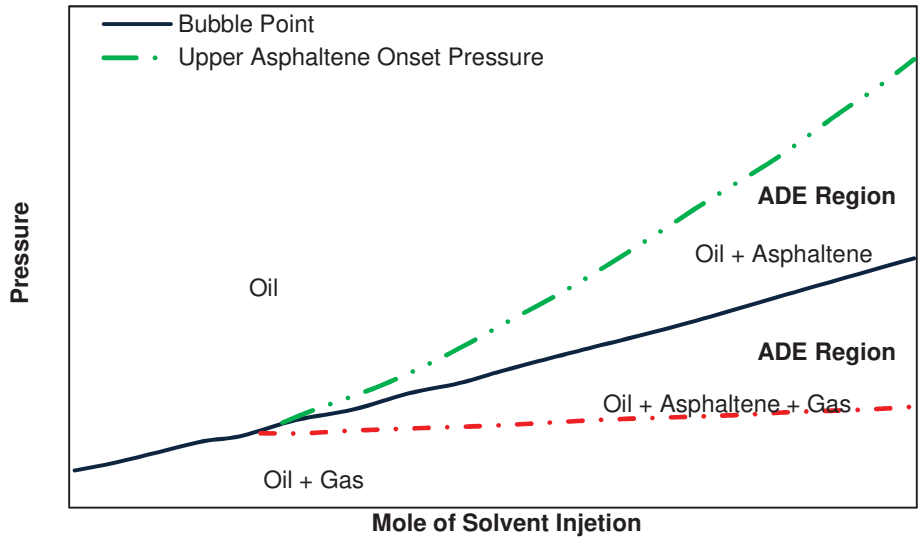

FIGURE 5 – ASPHALTENE DEPOSITION ENVELOPED REGION
Source: SABETI *et al.* (2015) - Adapted

Merino-Garcia (2004) reported that the asphaltene precipitation is more problematic because the total content of asphaltene and the accumulation of material during operation are not directly related. Some reservoirs present problems even if the amount of asphaltenes is in the order of ppm. Motivated by the significant amount of conditions that affect the characteristics of both the reservoir and the refining equipments, researches have been conducted in order to understand the asphaltene precipitation mechanism and also to develop models that can predict these problems.

Asphaltenes can be obtained from a crude oil by different precipitation techniques. Wei *et al.* (2015) conditioned the crude oil at 60 ºC for 1 h, sampled and diluted with n-hexane (4 g oil/160 mL hexane), stirred overnight and then filtrated with a 0.45 µm Millipore filter. The precipitate was washed with warm n-hexane to remove any waxes and resins and dried under a nitrogen atmosphere. The molar mass of asphaltenes was assumed to be 750 g/mol and the elemental composition of asphaltenes was determined, resulting the values as shown in TABLE 2.

TABLE 2 – ELEMENTAL COMPOSITION OF ASPHALTENE

Components	**Wei *et al.* (2015a)**	**Wei *et al.* (2015b)**
C	86.1%	85.0%
H	8.28%	8.17%
N	1.29%	1.25%
O	1.97%	1.77%
S	2.10%	
Fe		71 mg kg-1
Ni		68mgkg-1
V		220 mg kg-1

Source: WEI *et al.* (2015a and 2015b)

Asphaltenes have been shown to have some similarities with surfactants and for many years it was believed that asphaltenes in organic solutions had a well-defined CMC (Critical Micellar Concentration). However, based on ITC experiments, Merino-Garcia (2004) concluded that asphaltenes present self-association in the range of ppm in toluene solutions, which is prior to the region at which values of CMC are usually reported. The micelle concept seems to be no longer valid for asphaltenes in toluene. Besides, aggregation of asphaltenes seems to stop at a certain concentration. Deo (2002) observed that the aggregates are stable entities and keep the same structure. The formation of aggregates is not influenced by the solvent but the driving force was

found to be both the aromaticity and the polar nature of the molecules. Changes in viscosity measurements are observed when the particle aggregation occurs. However, these aggregate-aggregate interactions begin only when the concentration becomes large enough.

2.3 EQUATIONS OF STATE

Mathematical models are developed in order to predict properties or different behaviors of a system. Generally, a chemical process is a method intended to change the composition, and, consequently, the fluid properties. Therefore, a set of properties before and after the process must be known. These properties are known as properties of state or state variables, referring to any of the intensive variables of a system in equilibrium: temperature, pressure, specific volume, specific internal energy, Gibbs energy, Helmholtz energy, fugacity and other variables that are dependent on the size of the system.

The properties of a stable equilibrium state neither depend on the past history of the system nor the path to by which the equilibrium state was reached. Equations of state are mathematical models that relate the equilibrium properties of the system. The most well know equations of state are the cubic. However, with the development of applied statistical mechanics, a new model emerged, known as the equations of the SAFT family.

Equations of state for crude oil modeling:

The complex structure of crude oil and asphaltenes and theirs mechanism of precipitation and stabilization have been continuously discussed over the years. Two popular applications of colloidal and solubility models are based on statistical theory. The solubility model is correlated to PC-SAFT EOS, while the colloidal model is provided by CPA EOS (AlHammadi, Vargas and Chapman, 2015). Nowadays, the solubility model has been the focus of many researches. The Flory-Huggins approach is able to predict the onset and amount of asphaltene precipitation but it does not

consider the asphaltene association, which is estimated by EOS approach. Some studies comparing the thermodynamic models are presented in TABLE 3.

TABLE 3 – COMPARISON OF THERMODYNAMIC MODELS

AUTHORS	METHODS	MODELING
Behbahani *et al*, 2011	PC-SAFT X Flory-Huggins Model	• Tendency of asphaltenes to precipitate • PVT Properties
Panuganti *et al*, 2012	*b* X PC-SAFT	• Asphaltene phase behavior • PVT Properties
Hustad *et al*, 2014	SRK X PC-SAFT	• PVT Properties • Asphaltene onset pressures (AOP)
Yan, Varzandeh and Stenby, 2015	PC-SAFT[a] e S-BWR[a] X SRK[b] e PR[b]	• Liquid density • PVT Properties
Alhammadi, Vargas and Chapman, 2015	CPA X PC-SAFT	• Asphaltene phase behavior • Tendency of asphaltenes to precipitate

Notes: [a] Non-cubic equation of state
[b] Cubic equation of state

Source: The author (2017)

Behbahani *et al.* (2011), based on molecular models using PC-SAFT and Flory-Huggins model, compared the AOP and solvent ratios at the beginning of precipitation for different solvents and showed that PC-SAFT gives more precise results when comparing to experimental data.

Still in molecular models, cubics EOS such as SRK (Soave-Redlich-Kwong) and PR (Peng-Robinson) and non-cubics EOS such as PC-SAFT and S-BWR (Soave-Benedict-Webb-Rubin) have been compared in several studies. Although the cubic EOS have fairly simple calculations and have been used to predict the thermodynamic behavior of fluids at reservoir conditions, they, unlike the non-cubic equations, do not precisely describe either systems of phase behavior with large gaps or liquid density (PANUGANTI *et al.*, 2012; HUSTAD *et al.*, 2014; YAN, VARZANDEH and STENBY, 2015).

Zhang, Pedrosa and Moorwood (2012) applied the CPA (Cubic-Plus Association*)* and the PC-SAFT models to simulate the asphaltene stability in live oils. CPA model gives good predictions over a wide extent of pressures and temperatures. PC-SAFT model generally performed well when predicting asphaltene onset phase

boundary, but further works are still required to make it applicable to other types of crude oil. In 2015, Al Hammadi, Vargas and Chapman (2015) compared CPA and PC-SAFT models to illustrate the prediction of asphaltenes-phase behavior and the pressure-volume-temperature (PVT) properties of crude oils. Even though both EOS give acceptable predictions, the previously cited work demonstrated that PC-SAFT is superior in the projection of derivative thermodynamic properties, especially at high pressures.

Therefore, it is possible to conclude that PC-SAFT is a highly promising EOS for modeling both the densities of the fluids and the phase behavior for polydisperse systems. Furthermore, in order to elucidate the trends of deposition, PC-SAFT has been studied for modeling the asphaltene behavior

2.3.1 The Statistical Association Fluid Theory

Dolezalek (1908) was the first researcher to publish the "chemical theory" as he called, representing the relation between association systems and chemical reaction. In the 1980s, researches to develop methods that contemplate fluid association and statistical theory were led by the need to accurately model complex molecules present in chemical processes , while provide correlations that require less complex data as well as less physical mixing rules parameters..

In van der Waals equation and its variations, the repulsive interactions are represented by a hard-sphere. This approach is appropriated for nearly spherical molecules such as low-molecular-weight hydrocarbons and simple inorganic molecules. The problem is that this consideration does not suit most of the fluids, once they are highly nonspherical and associating. A good strategy to solve such problem is to consider the variables that affect the structure of the fluid, combining the chain length (molecular structure) and the molecular association. Wertheim (1984a, 1984b, 1986a, 1986b) developed a highly complex thermodynamic perturbation theory (TPT), also called association theory, in order to close such gap.

Using statistical mechanics and hard sphere systems with the hypothesis that monomers and dimers, including their possible aggregates, should be treated as distinct chemical entities (JOSLIN *et al.*, 1987), Wertheim introduced a breakup of the

pair potential into repulsive and highly directionally attractive parts into fugacity graphs, promoting association into dimers and possible higher *s*-mers. Thus, molecules are treated as different species according to the number of bonded associating sites and the fugacity is replaced by two variables: the usual single density and the density of monomers (HOLOVKO and KALYUZHNYI, 1991; ALHAMMADI, VARGAS and CHAPMAN, 2015). This theory resulted in an equation that describes the variation of residual Helmholtz free energy depending on the monomer density (GHONASGI and CHAPMAN, 1993), instead of as a function of the single density, as it was in the classical fluid theory. The advantage of the Wertheim theory not only allows any approximation made in the theory to be tested using computer simulation but also provides excellent results without requiring neither chemical reactions nor equilibrium constants in the temperature-dependent equations (MULLER and GUBBINS, 2001).

Chapman *et al.* (1988, 1989, 1990) transformed the abstract Wertheim's first-order perturbation theory into a feasible engineering equation of state (von SOLMS *et al.*, 2004) for chain molecules, known as Statistical Association Fluid Theory (SAFT). FIGURE 6 shows what occurs in processes involved in SAFT to form a molecule from individual contribution. At the beginning, it is assumed that the pure fluid is an individual hard spherical segment (a). As a dispersive potential is added, it occurs an attraction force between the spheres until a chain is formed (b). Finally, there is the chain association, due some attractive interaction (hydrogen bonding) (c). For a better understanding, Muller and Gubbins (2001) provided a cartoon presenting an alkane molecule, as shown in FIGURE 7. *m* spherical segments compose the aliphatic chain, each of them correspond to a united atom group. The rightmost sphere corresponds to an oxygen-containing segment with two associating sites, accounting for the proton and the electron pair. The perturbed theory represents the interactions of molecules into two parts: the first one is the repulsive contribution, describe by Chapman *et al.* (1988) with a hard-chain equation, and the second is the attractive contribution, further divided into dispersive and repulsive interactions. Thus, the free energy of a fluid, known as Helmholtz free energy, is calculated by the contribution of each of these steps, given by:

$$\boldsymbol{a}^{res} = \boldsymbol{a}^{seg} + \boldsymbol{a}^{chain} + \boldsymbol{a}^{assoc} \quad (1)$$

where a^{seg} is the free energy of the individual monomeric spherical "segments", a^{chain} is the change in free energy due the chain formation and a^{assoc} is the contribution from the association sites.

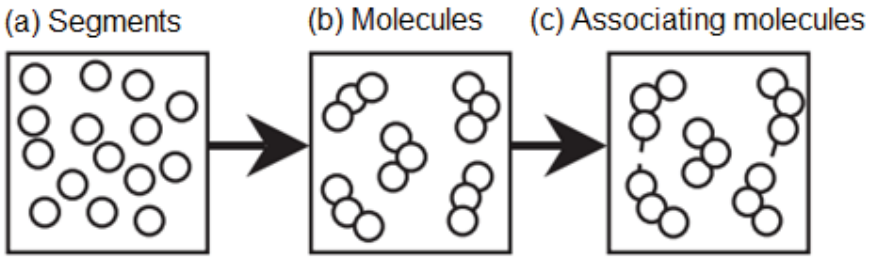

FIGURE 6 – SAFT CONTRIBUTIONS FOR AN ASSOCIATING POLYATOMIC FLUID
Source: PUNNAPALA and VARGAS (2013)

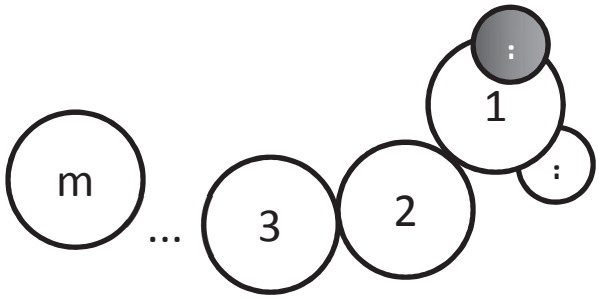

FIGURE 7 – CARTOON OF AN ALKANE MOLECULE
Source: MULLER and GUBBINS (2001) - Adapted

Due this segregation of the Helmholtz energy into three factors, it was possible to attain many SAFT variants: each term can be treated separately and modified or new contributions can be added, for example polar and electrostatic terms. As mentioned before, the first variant was the *Original SAFT* developed by Chapman *et al.* (1988, 1989, 1990) in which both the chain formation and the association terms, which make up the SAFT so original, derived from Wertheim's Thermodynamic Perturbation Theory (TPT). The first term considers segments connected in linear chains (the same as polymer molecules) and the second term takes into account the real form of associating molecules (von SOLMS, 2004). Each non-associating component requires three parameters, tangible and behaving orderly with molecular weight: σ, the molecular segment diameter (size parameter); m, the number of segments per molecule (chain length parameter), and ε/k, the segment dispersion energy - van der Waals attraction between each molecular segment (energy

parameter). For self-association molecules, two more parameters must be calculate: $\kappa^{A_iB_i}$, the volume association, and $\varepsilon^{A_iB_i}$, the energy association (von SOLMS, 2004).

The first term of Eq. 1, a^{seg}, represents segment-segment interactions:

$$a^{seg} = a_0^{seg} \sum_i X_i m_i \tag{2}$$

where a^{seg} is the residual Helmholtz energy of nonassociated spherical segments. The second term $\sum_i X_i m_i$ is a ratio of number of segments to the number of molecules in the fluid. a_0^{seg} is composed by two parts corresponding to the hard sphere interactions (a^{hs}) and to the dispersion between the molecular segments (a^{disp}) as follows:

$$a_0^{seg} = a_0^{hs} + a_0^{disp} \tag{3}$$

For a pure component the hard sphere contribution a^{hs} is calculated from:

$$\frac{a_0^{hs}}{RT} = \frac{4\eta - 3\eta^2}{(1-\eta)^2} \tag{4}$$

where T is the temperature, R is the gas constant and η is the reduced density calculated from Eq 5 for pure components or from Eq 6 for mixtures.

$$\eta = \frac{\pi N_{Av}}{6} \rho d^3 m \tag{5}$$

$$\eta = \frac{\pi N_{Av}}{6} \rho d^3 \sum_i X_i m_i \tag{6}$$

The number of segments m can be used as a measure of molecular size and is given by a mixture rule as:

$$m = \sum_i \sum_j x_i x_j \frac{1}{2} (m_i + m_j) \tag{7}$$

The dispersive contribution can be determined as a correlation of molecular simulation data for Lennard-Jones (LJ) theory-based fluids calculated by Coterman *et al.* (1986)[1] as quoted by Chapman *et al.* (1990):

$$a_0^{disp} = \frac{\epsilon R}{k}\left(a_{01}^{disp} + \frac{a_{02}^{disp}}{T_R}\right) \tag{7}$$

where $T_R = k/T\epsilon$ is the reduced temperature and:

$$a_{01}^{disp} = \rho_R[-8.5959 - 4.5424\rho_R - 2.1268{\rho_R}^2 + 10.285{\rho_R}^3] \tag{8}$$

$$a_{02}^{disp} = \rho_R[-1.9075 + 9.9724\rho_R - 22.216{\rho_R}^2 + 15.904{\rho_R}^3] \tag{9}$$

where $\rho_R = [6/(2^{0.5}\pi)]\eta$ is the reduced density.

The increment related to changes in Helmholtz energy due to covalent bonds can be determined from Eq 10, where g_{ii}, given by Eq 11, is the hard sphere pair correlation function for the interaction of two spheres i in a mixture of spheres, evaluated at the hard sphere contact.

$$\frac{a^{chain}}{RT} = \sum_i X_i(1 - m_i)ln(g_{ii}(d_{ii})^{hs}) \tag{10}$$

$$g_{ii}(d_{ii})^{hs} = \frac{1}{(1-\zeta_3)} + \left(\frac{3d_{ii}}{2}\right)\frac{\zeta_2}{(1-\zeta_3)^2} + 2\left(\frac{d_{ii}}{2}\right)^2\frac{{\zeta_2}^2}{(1-\zeta_3)^3} \tag{11}$$

where

$$\zeta_k = \frac{\pi N_{Av}}{6}\rho\sum_i X_i m_i d_{ii}^k \tag{12}$$

The association term for mixtures is an average that is linear with respect to mole fractions (Eq 13).

$$\frac{a^{assoc}}{RT} = \sum_i X_i\left[\sum_{A_i}\left[ln\, X^{A_i} - \frac{X^{A_i}}{2}\right] + \frac{1}{2}M_i\right] \tag{13}$$

[1] Cotterman, R. L.; Schwartz, B. J.; Prausnitz, J. M. Molecular Thermodynamics for Fluids at Low and High Densities. **AIChE J.**, v. 32, p. 1787-1798, 1986.

where X^{Ai} is the mole fraction of molecules i not bonded to site A and M_i is the number of association sites on molecule i.

SAFT variants:

In 1990, Huang and Radosz (1990, 1991) published the *"Original" SAFT* in which the main contribution was the regression of pure-component parameters for over 100 different fluids. It means that their EOS can be readily used for real fluids without any intermediate steps. A volume parameter ν^{00}, calculated by Eq. 14, is used instead of the size parameter σ. Moreover, the dispersion term is also different from that of Chapman *et al.* (1988, 1989, 1990).

$$\nu^{00} = \frac{\pi N_{AV}}{6\tau}\sigma^3 \tag{14}$$

Fu and Sandler (1995) proposed the *Simplified SAFT*, where the main idea was the simplification of the dispersion term given by Huang and Radosz (1990, 1991), which contains 24 constants. The *Simplified SAFT* performance is as good as the *"Original" SAFT* even though it requires re-fitting of all the pure-component parameters. Kraska and Gubbins (1996a, 1996b) proposed the *LJ-SAFT*, using Lennard-Jones (LJ) spheres for the reference term, instead of hard-spheres. The radial distribution function used in calculation of chain and association contributions is the radial distribution function for LJ. They incorporated a term to account for dipole-dipole interactions, while the other terms remained unchanged. Gil-Vilegas *et al.* (1997) developed the *SAFT-VR*, similar to the Huang and Radosz version, except for the dispersion contribution, in which was incorporated the attraction in the form of a square-well potential. As the segment is being characterized by size and energy parameters, the pure component parameter now includes the square-well width (λ) as well. Changing this new parameter λ, the range of attraction of the segment also changes (hence the name VR for "variable range"), giving greater flexibility to *SAFT-VR*.

Finally, in 2002, Gross and Sadowski (2000, 2001, 2002a, 2002b) developed the *Perturbed-Chain-SAFT* version, using the both chain term and association term as

the earlier SAFT versions. The difference between the *"Original" SAFT* and this new approach is the dispersion term, in an attempt to account the dispersion attraction between segments and also between whole chains. Due to this new term, this version focus on nonassociating components. Kontogeorgis and Voutsas (1996) used the association term outside of the SAFT context, combining it with the SRK equation to create CPA (Cubic-Plus-Association), an equation of state, which has had extraordinary success in many applications.

2.3.2 The Perturbed-Chain SAFT EOS

Applying a first-order perturbation theory, Chapman *et al.* (1990) derived an equation of state without considering the chain structure for the dispersion term of the SAFT equation. Since the dispersive forces appear by the induction of potentials in molecules, it is assumed that the behavior of these molecules is better represented if the dispersion interactions are modeled considering the structure of hard-chain. Therefore, Gross and Sadowski (2001) proposed a model referred to as *Perturbed-Chain SAFT* (PC-SAFT) using the second-order perturbation theory of Barker and Henderson[2,3], which is based on a hard-chain fluid, instead of spherical molecules as in the other SAFT versions. Gross and Sadowski introduced a new dispersion term in order to model substances that did not present association sites, but that presented a relevant molecular structure with respect to attractive interactions, as both asphaltenes and polymers molecules.

The proposed molecular model suggested that molecules are chains composed of spherical segments and the pair potential $u(r)$ for the segment of a chain is given by a modified square-well potential:

$$u(r) = \begin{cases} \infty, r < (\sigma - s_1) \\ 3\epsilon, (\sigma - s_1) \leq r \leq \sigma \\ -\epsilon, \sigma \leq r < \lambda\sigma \\ 0, r \geq \lambda\sigma \end{cases} \quad (15)$$

[2] Barker, J. A.; Henderson, D. Perturbation Theory and Equation of State for Fluids: The Squere-Well Potential. **J. Chem. Phys.**, v. 47, p. 2856, 1967.
[3] Barker, J. A.; Henderson, D. Perturbation Theory and Equation of State for Fluids II. A Successful Theory of Liquids. **J. Chem. Phys.**, v. 47, p. 4714, 1967.

where r is the radial distance between two segments, σ is the temperature-independent segment diameter, ϵ is the depth of the potential well, λ is the reduced well width and $s_1/\sigma = 0.12$. This equation proposed by Chen and Kreglewski (1977)[4] is a coarse representation of Lennard Jones potential, but much simpler to work with.

By Eq 15 it is possible to conclude that when two segments are at a distance of less than $\sigma - s_1$, the repulsive forces between them tend to infinite so there is no overlap of spheres in the system. However, when the radial distance is between $\sigma - s_1$ and σ, the repulsive interaction is maintained, but its intensity is limited. This soft repulsion is introduced because molecules have a collision diameter of σ only when they collide at an infinitely slow speed (absolute zero temperature). Increments in the temperature will result in a lower collision diameter, whereas when the distance limit ($r \geq \lambda\sigma$) is exceeded the attractive force is extinguished.

PC-SAFT focuses on non-associating components, so that there are just the three non-association parameters (σ, m and ε/k) in this equation of state, which is not a problem when it is applied in the petroleum fluid characterization (SABETI *et al.*, 2015). Before thermodynamic phase equilibrium calculations, the petroleum mixtures are characterized so as to determine the molecular weights and the PC-SAFT parameters for the pseudo-components (TING *et al.*, 2007). Tavakkoli *et al.* (2014) calculated the PC-SAFT parameters from correlations presented by Punnapala and Vargas (2013). These correlations are summarized in TABLE 4, where M_W is molar mass (g/mol) and γ is the aromaticity factor (its limit values are 0 for benzene derivatives and 1 for polynuclearomatics).

TABLE 4 – CORRELATIONS USED TO ESTIMATE PARAMETERS FOR PSEUDO-COMPONENTS

PC-SAFT PARAMETERS	CORRELATION
m	$(1-\gamma)(0.0257\,Mw + 0.8444) + \gamma(0.0101\,Mw + 1.7296)$
$\sigma\ (A)$	$(1-\gamma)(4.047 - 4.8013\ln(Mw)/Mw) + \gamma(4.6169 - 93.98/Mw)$
$\varepsilon/k\ (K)$	$(1-\gamma)(\exp(5.5769 - 9.523/Mw)) + \gamma(508 - 234100/Mw^{1.5})$

Source: TAVAKKOLI et al. (2016); ALHAMMADI, VARGAS and CHAPMAN (2015)

[4] Chen, S. S.; Kreglewski, A. Applications of the Augmented van der Waals Theory of Fluids. I. Pure Fluids. **Ber. Bunsen-Ges.**, v. 81, n. 10, p, 1048, 1977.

Equation of State: On account of there is no contribution from the association sites, the compressibility factor is given by the sum of an ideal gas contribution (Z^{id}), a hard-chain contribution (Z^{hc}) and an attractive (dispersive) contribution (Z^{disp}).

$$Z = Z^{id} + Z^{hc} + Z^{disp} \tag{16}$$

where Z is the compressibility factor with $Z^{id} = 1$ and $Z = Pv/RT$, where P is pressure, v is molar volume, R is gas constant and T is temperature.

Hard-chain Contribution: Due to the perturbation theory, Chapman *et al.* calculated the compressibility factor of hard-chain contribution by:

$$Z^{hc} = \bar{m}Z^{hs} - \sum_i x_i(m_i - 1)\dot{\rho}\frac{\partial ln g_{ij}^{hs}}{\partial \dot{\rho}} \tag{17}$$

$$\bar{m} = \sum_i x_i m_i \tag{18}$$

where the subscripti *i* is a component, the superscript *hs* is the quantities of hard-sphere system and:

x mole fraction of chains

m number of segments

$\bar{m}$ mean number of segments

$\dot{\rho}$ total number density of molecules

g_{ij}^{hs} hard-sphere radial pair distribution function for segments of component *i*.

Hard-sphere Contribution: The compressibility factor of hard-sphere (Z^{hs}), and the radial distribution function (g_{ij}^{hs}) in Eq 17 are given by Eq 19 and Eq 20, respectively:

$$Z^{hs} = \frac{\zeta_3}{(1-\zeta_3)} + \frac{3\zeta_1\zeta_2}{\zeta_0(1-\zeta_3)^2} + \frac{3{\zeta_2}^3 - \zeta_3{\zeta_2}^3}{\zeta_0(1-\zeta_3)^3} \tag{19}$$

$$g_{ij}^{hs} = \frac{1}{(1-\zeta_3)} + \left(\frac{d_i d_j}{d_i + d_j}\right)\frac{3\zeta_2}{(1-\zeta_3)} + \left(\frac{d_i d_j}{d_i + d_j}\right)^2 \frac{2{\zeta_2}^2}{(1-\zeta_3)^3} \tag{20}$$

where the packing factor (ζ_n) is represented by Eq 21 and the temperature-dependent segment diameter (d_i) by Eq 22:

$$\zeta_n = \frac{\pi}{6}\dot{\rho}\sum_i x_i m_i d_i^n \quad n \epsilon \{0,1,2,3\} \tag{21}$$

$$d_i = \sigma_i\left[1 - 0.12\, exp\left(-\frac{3\varepsilon_i}{kT}\right)\right] \tag{22}$$

in which:

ε depth of pair potential

σ segment diameter

k Boltzmann constant

T temperature

Dispersive Contribution: Finally, to complete the Eq 16, Eq 23 provides the dispersive compressibility factor:

$$Z^{disp} = -2\pi\rho\frac{\partial(\zeta_3 I_1)}{\partial\zeta_3}\overline{m^2\varepsilon\sigma^3} - \pi\rho\bar{m}\left(C_1\frac{\partial(\zeta_3 I_2)}{\partial\zeta_3} + C_2\zeta_3 I_2\right)\overline{m^2\varepsilon^2\sigma^3} \tag{23}$$

where ρ is the molar density (g/cm) and:

$$C_1 = 1 + \bar{m}\left(\frac{8\zeta_3 - 2{\zeta_3}^2}{(1-\zeta_3)^4}\right) + (1-\bar{m})\left(\frac{20\zeta_3 - 27{\zeta_3}^2 + 12{\zeta_3}^3 - 2{\zeta_3}^4}{((1-\zeta_3)(2-\zeta_3))^2}\right) \tag{24}$$

$$C_2 = -C_1^2\left(\bar{m}\frac{-4{\zeta_3}^3 + 20\zeta_3 + 8}{(1-\zeta_3)^5}\right) + (1-\bar{m})\frac{2{\zeta_3}^3 + 12{\zeta_3}^2 - 48\zeta_3 + 40}{((1-\zeta_3)(2-\zeta_3))^3} \tag{25}$$

$$\overline{m^2\varepsilon\sigma^3} = \sum_i\sum_j \mathrm{x_i y_i m_i m_j}\left(\frac{\varepsilon_{ij}}{KT}\right)\sigma_{ij}^3 \tag{26}$$

$$\overline{m^2\varepsilon^2\sigma^3} = \sum_i\sum_j x_i y_i m_i m_j\left(\frac{\varepsilon_{ij}}{KT}\right)^2\sigma_{ij}^3 \tag{27}$$

in which:

$$\sigma_{ij} = \frac{1}{2}(\sigma_i + \sigma_j) \tag{28}$$

$$\varepsilon_{ij} = \sqrt{\varepsilon_i \varepsilon_j}(1 - k_{ij}) \tag{29}$$

where k_{ij} represents the binary interaction coefficient between molecules of components *i* and *j*, and whose value is obtained adjusting experimental data.

$$I_1 = \sum_{i=0}^{6} a_i(\bar{m})\zeta_3{}^i \tag{30}$$

$$I_2 = \sum_{i=0}^{6} b_i(\bar{m})\zeta_3{}^i \tag{31}$$

The coefficients a_i and b_i are function of the chain length $\bar{m}$:

$$a_i = a_{0i} + \frac{\bar{m}-1}{\bar{m}} a_{1i} + \frac{\bar{m}-1}{\bar{m}} \frac{\bar{m}-2}{\bar{m}} a_{2i} \tag{32}$$

$$b_i = b_{0i} + \frac{\bar{m}-1}{\bar{m}} b_{1i} + \frac{\bar{m}-1}{\bar{m}} \frac{\bar{m}-2}{\bar{m}} b_{2i} \tag{33}$$

Gross and Sadowski (2000) estimated, by experimental data, the model constants $\boldsymbol{a_{0i}}$, $\boldsymbol{a_{1i}}$, $\boldsymbol{a_{2i}}$, $\boldsymbol{b_{0i}}$, $\boldsymbol{b_{1i}}$ and $\boldsymbol{b_{2i}}$ for Eq 32 and Eq 33, as presented in TABLE 5.

TABLE 5 – MODEL CONSTANTS FOR PC-SAFT

i	a_{0i}	a_{1i}	a_{2i}	b_{0i}	b_{1i}	b_{2i}
0	0.9105631445	-0.3084016918	-0.0906148351	0.7240946941	-0.5755498075	0.0976883116
1	0.6361281449	0.1860531159	0.4527842806	22.382.791.861	0.6995095521	-0.2557574982
2	26.861.347.891	-25.030.047.25	0.5962700728	-40.025.849.49	38.925.673.390	-91.558.561.53
3	-26.547.362.49	21.419.793.629	-17.241.829.13	-21.003.576.82	-17.215.471.65	20.642.075.974
4	97.759.208.784	-65.255.885.33	-41.302.112.53	26.855.641.363	19.267.226.447	-38.804.430.05
5	-15.959.154.08	83.318.680.481	13.776.631.870	20.655.133.841	-16.182.646.17	93.626.774.077
6	91.297.774.084	-33.746.922.93	-86.728.470.37	-35.560.235.61	-16.520.769.35	-29.666.905.59

Source: Gross and Sadowski (2000)

Equations for calculating density, pressure, fugacity coefficients and caloric properties are given in Appendix A.

2.3.3 Phase Equilibrium

Thermodynamic equilibrium:

To simulate and optimize any process engineering, it is necessary to understand the physical properties of fluid substances and their phase equilibrium. The equilibrium state does not present a tendency to depart spontaneously from its steady condition and the properties are independent of both time and the previous history of the system. These properties are also stable and, therefore, are not subject to big changes due to slight variations of external conditions. For a homogeneous open system, combined statements of the first and second laws of thermodynamics gives the four fundamental equations and the role of U (internal energy), H (enthalpy), A (Helmholtz energy), and G (Gibbs energy) as thermodynamic potentials:

$$dU = \left(\frac{\partial U}{\partial S}\right)_{V,n} dS + \left(\frac{\partial U}{\partial V}\right)_{S,n} dV + \sum_i \left(\frac{\partial U}{\partial n_i}\right)_{S,V,n_{j\neq i}} dn_i \quad (34a)$$

$$dH = \left(\frac{\partial H}{\partial S}\right)_{P,n} dS + \left(\frac{\partial H}{\partial P}\right)_{S,n} dP + \sum_i \left(\frac{\partial H}{\partial n_i}\right)_{S,P,n_{j\neq i}} dn_i \quad (34b)$$

$$dG = \left(\frac{\partial G}{\partial T}\right)_{P,n} dT + \left(\frac{\partial G}{\partial P}\right)_{T,n} dP + \sum_i \left(\frac{\partial G}{\partial n_i}\right)_{P,T,n_{j\neq i}} dn_i \quad (34c)$$

$$dA = \left(\frac{\partial A}{\partial V}\right)_{T,n} dV + \left(\frac{\partial A}{\partial T}\right)_{V,n} dT + \sum_i \left(\frac{\partial A}{\partial n_i}\right)_{P,T,n_{j\neq i}} dn_i \quad (34d)$$

The chemical potential μ_i is defined as:

$$\mu_i \equiv \left(\frac{\partial U}{\partial n_i}\right)_{S,V,n_j} \quad (35)$$

and the set of Eqs 34 may be rewritten in the form:

$$dU = TdS - PdV + \sum_i \mu_i dn_i \quad (36a)$$

$$dH = TdS + VdP + \sum_i \mu_i dn_i \quad (36b)$$

$$dG = VdP - SdT + \sum_i \mu_i dn_i \quad (36c)$$

$$dA = -SdT - PdV + \sum_i \mu_i dn_i \quad (36d)$$

Although any of the presented thermodynamic potentials can be used to determine an equilibrium state, it is noted that internal energy and enthalpy present entropy as an independent variable and cannot be directly measured. In contrast, the Gibbs and Helmholtz energy present (P, T and n) and (V, T and n) as independent variables, respectively, and these properties can be measured directly in a system. For this reason, it is more common to find thermodynamic equilibrium as function of these potentials.

Phase-equilibrium thermodynamics described quantitatively the distribution at equilibrium of every component among all the phases involved. Analyzing the Gibbs and Helmholtz energy in a phase-equilibrium thermodynamic for a two phases system, we obtain:

$$dG = -S^I dT + V^I dP + \sum_i \mu_i{}^I dn_i{}^I - S^{II} dT + V^{II} dP + \sum_i \mu_i{}^{II} dn_i{}^{II} = 0 \quad (37a)$$

$$dA = -S^I dT - P^I dV + \sum_i \mu_i{}^I dn_i{}^I - S^{II} dT - P^{II} dV + \sum_i \mu_i{}^{II} dn_i{}^{II} = 0 \quad (37b)$$

where superscripts I and II refers to each phase. Once the system has to be in both thermal (temperature constant and homogeneous all over the system) and mechanical (pressure constant and homogeneous all over the system) equilibria, the Eq 37 is reduced to:

$$dG = \sum_i \mu_i{}^I dn_i{}^I + \sum_i \mu_i{}^{II} dn_i{}^{II} = 0 \quad (38a)$$

$$dA = \sum_i \mu_i{}^I dn_i{}^I + \sum_i \mu_i{}^{II} dn_i{}^{II} = 0 \quad (38b)$$

For a closed system, there are no material exchange with its surroundings, what can be expressed in terms of a molar basis as $dn_i{}^I = -dn_i{}^{II}$, which means that the chemical potential for each phase should be the same:

$$\mu_i{}^I = \mu_i{}^{II} \tag{39}$$

For a pure substance i, the chemical potential is

$$d\mu_i = -s_i dT + v_i dP \tag{40}$$

where s_i is the molar entropy and v_i the molar volume. For a pure, ideal gas and integrating at constant temperature:

$$\mu_i - \mu_i{}^0 = RT\ ln\frac{P}{P^0} \tag{41}$$

To generalize the Eq 41, Lewis defined a function f called fugacity, by writing for an isothermal change and for any component in any system, solid, liquid or gas, pure or mixed, ideal or not:

$$\mu_i - \mu_i{}^0 = RT\ ln\frac{f_i}{f_i{}^0} \tag{42}$$

For phases α and β and considering the equilibrium relation in Eq 39:

$$f_i^{\alpha} = f_i^{\beta} \tag{43}$$

These equilibrium equations are valid for systems with two or more phases.

Phase stability test:

In order to analyze the thermodynamic stability and to calculate the thermodynamic properties of multi-component mixtures, many algorithms have been

designed based on the tangent plane criterion of Gibbs (BAKER *et al.*, 1982). A stability analysis determines whether a given composition is stable or instable as a single phase: if the mixture is stable, none configuration of the new phase should result in a decrease of the Gibbs free energy, while if the phase is instable, even a small amount of a second phase causes the total Gibbs free energy of the system to decrease.

Let $G_0(n)$ denote the Gibbs energy at a referenced temperature (T) and pressure (P) of a n-component mixture and since the composition (z) is not changed:

$$G_0(n) = \sum_i^{nc} n_i \mu_i^0 \tag{44}$$

where μ_i^0 is the chemical potential of component i in the mixture.

Assume that a new phase in an infinitesimal amount (θ) arises. $G_0(\theta)$ is the new Gibbs energy and the change in Gibbs energy is then

$$\Delta G = G_0(\theta) - G_0(n) = G_1(n-\theta) + G_2(\theta) - G_0(n) \tag{45}$$

where G_1 and G_2 refers to the Gibbs energy in phases 1 and 2, respectively.

Mixture stability requires that none configuration of a new phase can decrease the Gibbs energy. In this sense, a necessary criterion for stability is

$$F(y) = \sum_i y_i(\mu_i(y) - \mu_i^0) \geq 0 \tag{46}$$

for all trial compositions z.

Considering the relationship between fugacity and chemical potential, Eq 46 can be rewritten as

$$F(y) = RT \sum_i^{nc} y_i[lnf_i(y) - lnf_i(z)] \tag{47}$$

Two models are often used to calculate phase equilibrium in binary systems: the equation-of-state models ($\phi - \phi$ approach) and the activity coefficient models ($\gamma - \phi$ approach) (KLEIBER, M.; 2016). In the $\phi - \phi$ approach all phases have the same reference state and require the use of a pressure-explicit equation of state to model

both phases, meaning all phases are considered compressible. The equilibrium condition $f'(x) = f''(x)$ becomes

$$Px_i\phi'_i = Py_i\phi''_i \tag{48}$$

for each component. The $\phi - \phi$ method is applied for liquid-liquid, liquid-vapor or more generally fluid-fluid phase equilibria and for high-pressure systems.

The phase equilibria condition $f'(x) = f''(x)$ can also be elaborated using an equation of state for the vapor phase and an activity coefficient model (g^E) for the liquid phase. In this way, the liquid phase is considered incompressible and the thermodynamic model is asymmetric. This approach is applied for low pressure systems. The simplest solution for this approach is the Raoult's law:

$$x_i P_i^{sat} \gamma_i = y_i P_i \tag{49}$$

In this work, the $\phi - \phi$ method was chosen. All of the following calculations are based on this approach to model liquid-liquid phase equilibrium data, as proposed by Ferrari *et al.* (2009).

Classical thermodynamic states that the sufficient condition for fluid phase equilibrium is that the Gibbs surface tangent plane distance should be non-negative for all possible phases present in the system. Adopting the $\phi - \phi$ method, the tangent plane distance (TPD), from Eq 47, is:

$$TPD(y) = F(y) = RT \sum_i^{nc} y_i[\ln(Py_i\phi_i(\mathrm{y})) \quad - \ln(Pz_i\phi_i(\mathrm{z}))] \tag{50}$$

Rewritten:

$$\frac{TPD(y)}{RT} \equiv \frac{F(y)}{RT} = \sum_i^{nc} y_i[\ln \phi_i(\mathrm{y}) + \ln y_i - \ln \phi_i(\mathrm{z}) - \ln z_i] \tag{51}$$

for $\sum_i^{nc} y_i = 1$ and $0 \leq y_i \leq 1$, where *nc* is the number of components in the mixture, y_i is the mole fraction of component *i* in the new phase tried and ϕ_i is the fugacity coefficient of component *i*.

According to tangent plane criterion, the system is only stable if:

$$TPD(y) \geq 0 \text{ for all } y \tag{52}$$

The inequality of Eq 52 must be true for all y and at the stationary points y^* of $TPD(y)$. The stationary points of TDP must satisfy the following equation:

$$d(u) = \ln u_i + \ln \phi_i - \ln z_i + \ln \phi_i(z) = 0 \qquad (i = 1, \dots, nc) \tag{53}$$

where

$$y_i{}^* = \frac{u_i}{\sum_i^{nc} u_i} \tag{54}$$

and u denote the stationary points of TPD with $u_i \geq 0$.

Eq 53 can be solved applying the Successive Substitution Method (SSM) as follows:

$$\ln u_i{}^{(k+1)} + h_i^{(k)} - \ln \phi_i(u^{(k)}) \tag{55}$$

From the solutions found, if $\sum_i^{nc} u_i > 1$ the phase tested is unstable; otherwise, if $\sum_i^{nc} u_i \leq 1$ is stable. Two relations in the initialization of phase stability test were used:

$$y_{i,1} = kp_i z_i \tag{56a}$$

$$y_{i,2} = \frac{z_i}{kp_i} \tag{56b}$$

where $y_{i,1}$ and $y_{i,2}$ denote the mole fractions of component *i* in phases 1 and 2 and the partition coefficient kp_i used for initialization can be estimated by:

$$\ln kp_i = 5.373(1 + w_i)\left(1 - T_{C_i}/T\right) + \ln(P_{C_i}/P) \tag{57}$$

where T_{C_i} and P_{C_i} are, respectively, the critical temperature and critical pressure of component *i*.

Generally, one of the initial estimations (Eq 56a and b) will converge to the trivial solution, while the other will converge to the desired minimum, that is, for a heterogeneous composition. Another strategy was also applied using a convex interpolative strategy:

$$Y_i = \psi y_{i,2} + (1-\psi) y_{i,1} \tag{58}$$

where ψ is an interpolative parameter with values within the interval [0,1]. In the work of Ferrari *et al.*, to perform liquid-liquid stability test, the parameter ψ is iterate with step 0.1 and the value of Y_i is used as the initial condition in $\ln u_i^0 = \ln Y_i$ to solve the stability test equation (Eq 55).

The result obtained for the unstable phase is used as the initial partition coefficient for split calculation as follows:

$$If\ \psi \leq 0.5\ then\colon\ \ln kp_i = \ln \phi_i(y) - \ln \phi_i(z) \tag{59}$$

$$If\ \psi > 0.5\ then\colon\ \ln kp_i = \ln \phi_i(z) - \ln \phi_i(y) \tag{60}$$

The trivial solution in the stability test has the following stopping criteria:

$$\sum_i^{nc} (1 - kp_i)^2 < 10^{-4} \tag{61}$$

The kp_i values acquired at the end of the stability test for unstable system are used in the initialization of flash calculations. After that, one of these new phases is tested and if the result indicates an unstable phase, then the number of phases np is changed to $np + 1$ and a new split calculation phase is performed.

Multiphase flash calculation:

Ferrari *et al.* (2009) used the methodology described by Nighiem and Li (1984)[5] to perform flash calculation. Given a nonlinear system:

$$\ln Kp_{ij} + \ln \phi_{ij} - \ln \phi_{ir} = 0 \ (i = 1, \dots, n; j = 1, .. nf, r \neq j) \tag{62}$$

where Kp_{ij} is the partition coefficient of component i between the phase j and the reference phase r, defined by Eq 63. ϕ_{ij} and ϕ_{ir} are the fuggacity coefficient of component i in phase j and r, respectively.

$$Kp_{ij} = \frac{x_{ij}}{x_{ir}} \tag{63}$$

where x is the molar fraction. The mass balance of component i, considering np phases in equilibrium is:

$$g_k(\beta) = \sum_{i=1}^{nc} \frac{z_i(Kp_{ij}-1)}{\sum_{m=1}^{np} \beta_m Kp_{im}} \tag{64}$$

where z_i is the global composition of component i and β_m represents the molar fraction of phase m. The mass balance restriction should be considered:

$$\sum_{k=1}^{np} \beta_k = 1 \text{ and } \beta_{np} = 1 - \sum_{k=1}^{np-1} \beta_k \tag{65}$$

Considering $Kp_{i,np} = 1$, the derivative of Eq 61 can be given as:

$$\frac{\partial g_k}{\partial \beta_j} = -\sum_{i=1}^{nc} \frac{z_i(Kp_{ik}-1)^2}{\left[1+\sum_{m=1}^{np-1} \beta_m(Kp_{im}-1)\right]^2} \tag{66}$$

As suggest by Nighem and Li (1984), Ferrari *et al.* (2009) used the Newton-Raphson method to solve Eq 62 with:

[5] NGHIEM, Y. K.; LI, Y. K. Computation of Multiphase Equilibrium Phenomena with an Equation of State. **Fluid Phase Equilib.**, v. 17, p. 77-95, 1984.

$$x_{ij} = \frac{z_i K p_{ij}}{\sum_k^{np} \beta_k K p_{ik}} \ (1 = 1, \dots, nc; j = 1, \dots, np) \tag{67}$$

2.4 APPLICATIONS OF THE PC-SAFT MODEL

2.4.1. Modeling polymer systems

As previously discussed, for nonassociating molecules, three parameters should be settled for each pure-component. For polymers, the difficulty is to identify those pure-components. For low molecular weight components the determination of PC-SAFT parameters is made by regressing vapor pressures and liquid densities. For macromolecules, these parameters may be estimated by extrapolating the pure-component parameters of a series of low-molecular weight components, dispite, this approach do not account molecular effects like entanglement, self-interactions and shielding.

Gross and Sadowski (2002a) modeled the phase equilibrium of polymer systems, such as polypropylene, polyethylene and polystyrene, involving vapor-liquid demixing and high pressure liquid-liquid equilibria at high and low temperatures of binary and ternary systems using PC-SAFT. The results were satisfactory compared to an earlier SAFT version. To successfully settle the PC-SAFT parameter for polymer systems, Gross and Sadowski concomitantly considered liquid density data and binary phase equilibrium data. For this case, besides the three PC-SAFT parameters, the binary parameter k_{ij} should also be estimated. Vargas *et al.* (2009) modeled the mixture of polystyrene, cyclohexane and carbon dioxide, previously studied experimentally by Loos[6] and Bungert[7] (reported by Gross and Sadowski, 2002). They showed some similarities between this polymeric system and asphaltenes in crude oil. As the polystyrene, asphaltenes are stable at reservoir pressure but the depressurization causes them to become unstable, so as increases in the gas content.

Kouskoumvekaki *et al.* (2004) estimated the pure-component parameters by a new method based only on pure-polymer PVT data and extrapolation equations that relate the parameters of the monomer to those of the polymer for each homologous series. Spyriouni and Economou (2005) used SAFT and PC-SAFT to analyze the phase behavior of polymer-solvent mixtures over an ample range of temperature and

[6] de Loos, T. W. Measurements of 1994. Published in Bungert (1998)
[7] Bungert, B. Ph.D. Dissertation, Technische Universitat Berlin, Berlin, Germany, 1998.

pressure. They assure that both EOS provided reliable results and in agreement with experimental data, only requiring the careful selection of the necessary parameters.

2.4.2. Modeling ionic liquid systems

The ionic liquids have been considered good replacements for conventional volatile organic solvents because of their physical characteristics, reducing exposure of toxic and harmful chemicals to the environment (PADUSZYNSKI and DOMANKSA, 2012). These components are thermodynamically stable, being liquid over a large range of temperature and have negligible vapor pressures (CHEN, MUTELET and JOUBERT, 2012).

Paduszynski and Domanska (2012) modeled ionic liquids and their mixture with molecular compounds using the PC-SAFT to calculate the thermodynamic properties of different homologous series. They also predicted the surface tension of pure ionic liquid by the PC-SAFT EOS and the density gradient theory. Chen, Mutelet and Joubert (2012) represented the solubility of carbon dioxide (CO_2) in ionic liquid using the PC-SAFT. The binary interaction parameter k_{ij} was fitted to experimental liquid-vapor equilibrium data and, to determine the temperature-dependent parameter, they developed a correlation based on the group contribution concept.

2.4.3 Modeling crude oil systems

As already discussed, solubility models have been used to predict crude oil systems. In these models, asphaltenes and solvent phase are in thermodynamic equilibrium if the components in both phases have the same chemical potential. Two classes of solubility models are proposed, depending on how this potential is calculated: regular solution and equation of state. To accurately describe the van der Waals attraction between different pairs of molecules, the interaction energies are often modified in an equation of state by using binary interaction parameters.

Solid model is frequently used to anticipate asphaltenes phase behavior. This approach uses a cubic equation of state to predict gas and liquid fugacities while asphaltene is considered a solid phase and its fugacity is calculated using a solid model (EBRAHIMI, 2016).

Nghiem and Coombe (1997) used the solid model to predict asphaltene precipitation using vapor-liquid-solid equilibrium. The heaviest component crude oil was characterized by two pseudo-components: non-precipitating and precipitating components. The precipitating pseudo-component is considered as a pure phase composed exclusively by precipitated asphaltenes.

Using PC-SAFT equation of state to model asphaltene phase behavior, researchers such as Ting *et al.* (2007), Vargas *et al.* (2009), Panuganti *et al.* (2012) and Saajanlehto and Alopaeus (2014) used vapor-liquid equilibrium data (VLE) to fit the binary interaction parameters. Sabeti *et al.* (2015) regarded the system as a vapor-liquid-quasi-liquid equilibrium (VL-quasi-LE) where asphaltene is a quasi-liquid pure phase. Zuniga-Hinojosa *et al.* (2014), Tavakkoli *et al.* (2014) and Ebrahimi *et al.* (2016) treated asphaltene precipitation as a liquid-liquid equilibrium.

Ting *et al.* (2007) modeled the phase behavior of oil. Six pseudo-components formed were called "recombined oil". This oil is a mixture of separator gas (methane, N_2 + CO_2 and light n-alkanes) and stock tank oil (saturates, aromatics + resins and asphaltenes). Both the aromatic and resins are treated as a single pseudo-component, unlike SARA classification. They related PC-SAFT parameters of pseudo-components and molecular weight, interpolating or extrapolating values, as shown in FIGURE 8. The association term was not considered since the asphaltene phase behavior in crude oil was assumed to be dominated by molecular sizes and van der Waal interactions. For real components, PC-SAFT parameters are correlated from liquid densities and vapor pressures. Aromatics below the C_{10} cut represent 72.3 wt% of the stock tank oil and they are assumed as saturate components (all normal alkanes); 27.7 wt% are either aromatic+resins (up to C_{29} cut) or aromatics+resins and asphaltenes (in the C_{30+} cut); and 2.5 wt% are asphaltene fraction (all found in C_{30+} sub-fraction). The average molecular weight for asphaltene was settled to 1.7 g/cm^3. The binary interaction parameters for saturates were set based on vapor-liquid equilibrium data and molecular weight,. For the (aromatic+resins) pseudo-component, it is important to quantify, not only the average molecular weight but also the average aromaticity. This degree of aromaticity was defined by interpolation between parameters for polynuclear

aromatics and those for aromatic derivatives. This fraction possesses the minimum degree of aromaticity necessary to dissolve asphaltenes.

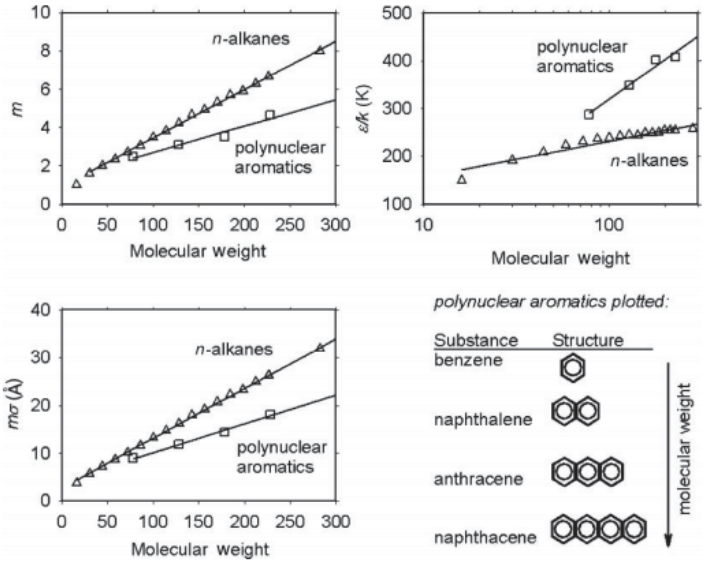

FIGURE 8 – PC-SAFT PURE COMPONENT PARAMETERS DEPENDING ON MOLECULAR WEIGHT
Source: Ting *et al.* (2007)

Based on VLE data, the optimal binary interaction parameters for toluene-dodecane and toluene-hexadecane, *kij* for saturates and aromatic+resins, were set to -0.01. Finally, they compared qualitatively the behavior of resins and the asphaltenes polydispersity on the phase behavior of asphaltenes in oil. Toluene was used as the model oil and the asphaltenes had a fixed concentration of 7.5 g asphaltenes to 100 mL of toluene. As shown in FIGURE 9 the onset of asphaltene is delayed in the presence of resins but the total amount of asphaltene precipitated does not change.

Vargas *et al.* (2009) predicted the crude oil bubble point, density and asphaltene precipitation condition. The three asphaltene PC-SAFT parameters were fitted to the precipitation data, measured at ambient pressure by titration with n-alkane precipitants or in high-pressure measurements at a given gas composition. The study intended to determine the effect of temperature, pressure and composition in asphaltene solubility. In systems with molecules with different sizes, an increase in temperature (at a fixed pressure) resulted in a decrease in oil density and in solubility parameter, precipitating the asphaltenes. At lower temperatures, asphaltene precipitates with a decrease in temperature. Adding CO_2 to the asphaltenes, at temperatures below the crossover point the CO_2 inhibits asphaltene precipitation,

whilst at higher temperatures it precipitates the asphaltenes. The effect of gas injection in asphaltene behavior has also been studied. The gas injection allows the recovery of the oil trapped in the tight pores of the rock. As Ting *et al.* (2007), Vargas also used N_2 to simulate the gas injection. For both studies, the addition of nitrogen strongly increased the asphaltene instability onset.

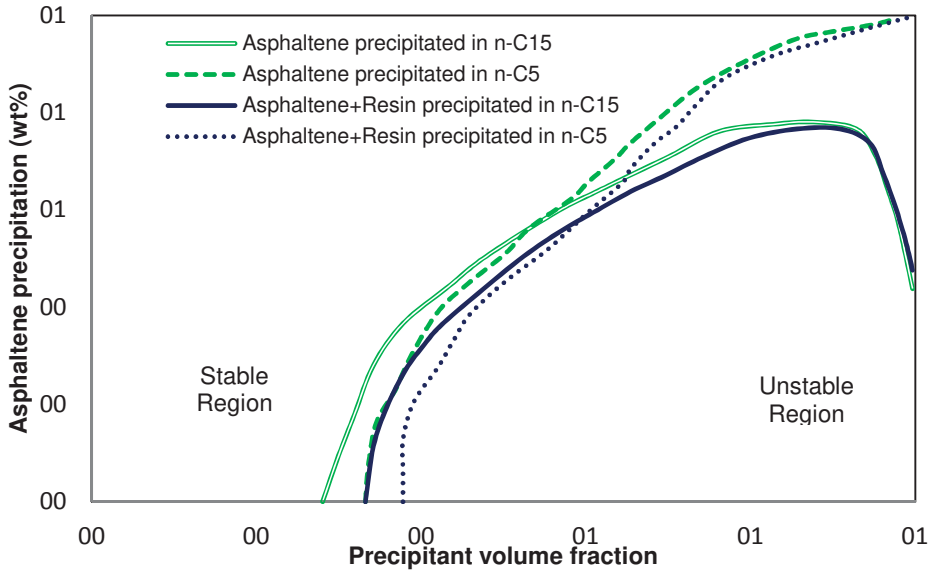

FIGURE 9 – ASPHALTENE SOLUBILITY IN MODEL OIL
Source: Ting et al. (2007) - Adapted

Saajanlehto and Alopaeus (2014) studied the phase behavior of heavy oils from Athabasca and San Joaquin Valley. The characterization was based on sorting the pseudocomponents according to the boiling points and its cuts were split into saturate, aromatic and polyaromatic fractions (SAP characterization). Assareh *et al.* assumed that each petroleum fraction contains paraffinic, naphthenic and aromatic components (PNA characterization).

To model the phase behavior of reservoir petroleum fluids Saajanlehto and Alopaeus (2014) calculated the PC-SAFT parameters - presented in Eqs 68-76 - as a function of molecular weight and aromaticity while Assareh *et al.* (2016) developed correlations that were functions of specific gravity and molecular weight – presented in Eqs. 77-79.

$$w_s = -0.00055\,(T_b - 273) + 0.41 \tag{68}$$

$$w_A = 0.0002\,(T_b - 273 + 0.53) \tag{69}$$

$$w_P = 1 - w_s - w_A \tag{70}$$

$$m_S = 0.0257Mw + 0.8444 \tag{71}$$

$$\sigma_S = 4.047 - 4.8013\ln(Mw)/Mw \tag{72}$$

$$\ln((\varepsilon/\mathrm{k})_S) = 5.5769 - 9.523/Mw \tag{73}$$

$$m_{A/P} = (1-\gamma)(0.0223Mw + 0.751) + \gamma(0.0101Mw + 1.7296) \tag{74}$$

$$\sigma_{A/P} = (1-\gamma)(4.1377 - 38.1283/Mw) + \gamma(4.6169 - 93.98/Mw) \tag{75}$$

$$(\varepsilon/\mathrm{k})_{A/P} = (1-\gamma)(0.00436Mw + 283.93) + \gamma(508 - 234100/Mw^{1.5}) \tag{76}$$

where aromaticity parameter (γ) is 0.1 for aromatic fractions and 0.6 for polyaromatic fractions, molar mass(Mw) (g.mol^{-1}) was obtained for each pseudocomponent , *w* is the mass fraction of pseudocomponent at boiling point cut and T_b the temperature of boiling point cut (K). Saajanlehto and Alopaeus (2014) treated asphaltenes as a single component, while light gas components, CO_2 and propane were treated as real components.

$$m = 33.58 + -0.08816Mw - 90.75S - 0.07727Mw.S + 61.01S^2 \tag{77}$$

$$m.\sigma^3 = -75.14 + 2.848Mw + 231.7S - 1.288Mw.S - 186.9S^2 \tag{78}$$

$$m.(\varepsilon/\mathrm{k}) = 3372 + 11.24Mw - 8955S - 5.925Mw.S + 6136 \tag{79}$$

where S is the specific gravity.

Saajanlehto and Alopaeus (2014) obtained the binary interaction parameters for propane + pseudo-components and CO_2 + propane pairs from literature, while those for CO_2 + pseudo-components were estimated from vapor-liquid equilibrium data. Assareh *et al.* (2016) considered the binary interaction coefficients as zero for all

hydrocarbon-hydrocarbon interactions, except for methane to heavier hydrocarbons, which change in function of the specific gravity.

Sabeti *et al.* (2015) established a model based on PC-SAFT theory in vapor-liquid-quasi liquid state to estimate, among other things, the amount of asphaltene precipitation. Hence, one phase was considered pure asphaltene and the other as oil and gas. Some considerations were made: 1) crude oil contains dissolved asphaltene; 2) precipitation processes are thermodynamically reversible; 3) association forces are neglected; 4) the phase rich in asphaltene is a pseudo-liquid phase and is deemed as pure; 5) interaction coefficients of asphaltene component and reference fugacity are estimated from laboratory data; and 6) the PC-SAFT parameters for each component are calculated from correlations with the average molecular weight.

The fugacities of asphaltene in oil (f_{al}) and of pure asphaltene phase (f_{as}) are evaluated and if $f_{al} < f_{as}$ the asphaltene do not precipitate or, else, if $f_{al} > f_{as}$ there is the formation of a second phase. To evaluate their model, the PC-SAFT results were compared to experimental data reported by Nikookar *et al.* (2011) (FIGURE 10). The average error for each solvent varies from 5 % to 11.8 %.

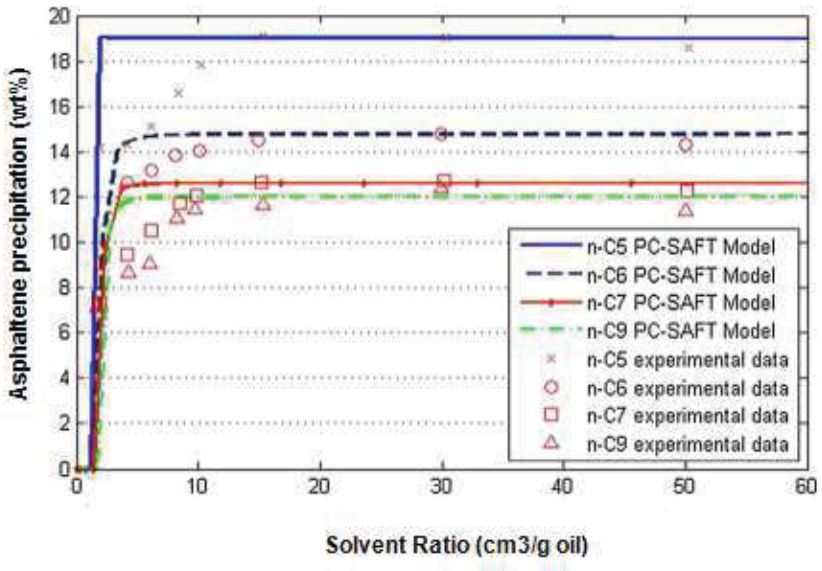

FIGURE 10 – ASPHALTENE PRECIPITATION IN FOUR DIFFERENT SOLVENTS
Source: Sabeti *et al.* (2015) - Adapted

Tavakkoli, Chen and Vargas (2015) prepared what they named modified oil, as shown in the flowchart in FIGURE 11**,** to study the asphaltene precipitation using n-C_5, n-C_6, n-C_7 and n-C_8 as the precipitants. They used the called "Indirect Method" to detect and quantify the asphaltene precipitation by measuring the absorbance of the

centrifuged fluid supernatant. FIGURE 12 summarizes this method. In the experimental data, when the absorbance values deviate from their horizontal trends, the onset of precipitation has been reached. The PC-SAFT parameters were not adjusted in the exact onset data, but in the asphaltene precipitation amount at 90 volume percent of precipitant, once the system equilibrium is reached quickly and the volume of precipitated do not changed over time.

Tavakkoli assumes that there is no influence between the association term in PC-SAFT and the asphaltene precipitation. The three PC-SAFT parameters (σ, m and ε/k) were calculated by correlations already presented in TABLE 4. Assuming that all the pseudo-components have the same nature, the aromaticity parameter was 0.35 for all the sub-fractions. To calculate the molar mass of each asphaltene sub-fraction, they used the gamma distribution function given by equations 81-83, in which the monomer molar mass ($\boldsymbol{M_m}$) was set to 1700 g/mol and the maximum value was 30.000 g/mol. The parameter $\boldsymbol{\alpha}$ that determines the shape of the distribution was adjusted to 1.1 and the average molar mass of asphaltenes $\boldsymbol{\bar{M}}$ was adjusted to 2300 g/mol in order to reproduce the asphaltene precipitation experimental data.

$$\boldsymbol{f(r) = \frac{1}{M_m \Gamma(\alpha)} \left[\frac{\alpha}{(\bar{r} - 1}\right]^{\alpha} exp \left[\frac{\alpha(1 - r)}{(\bar{r} - 1)}\right]} \tag{80}$$

where $\boldsymbol{r}$ and $\boldsymbol{\bar{r}}$ are given by $\boldsymbol{M/M_m}$ and $\boldsymbol{\bar{M}/M_m}$, respectively.

$$\boldsymbol{w_i = \frac{\int_{r_i}^{r_{i+1}} f(r) dr}{\int_{r_i}^{r_n} f(r) dr}} \tag{81}$$

$$\boldsymbol{\bar{r}_i = \frac{\int_{r_i}^{r_{i+1}} r f(r) dr}{\int_{r_i}^{r_n} r f(r) dr}} \tag{82}$$

$$\boldsymbol{M_i = \bar{r}_i M_m} \tag{83}$$

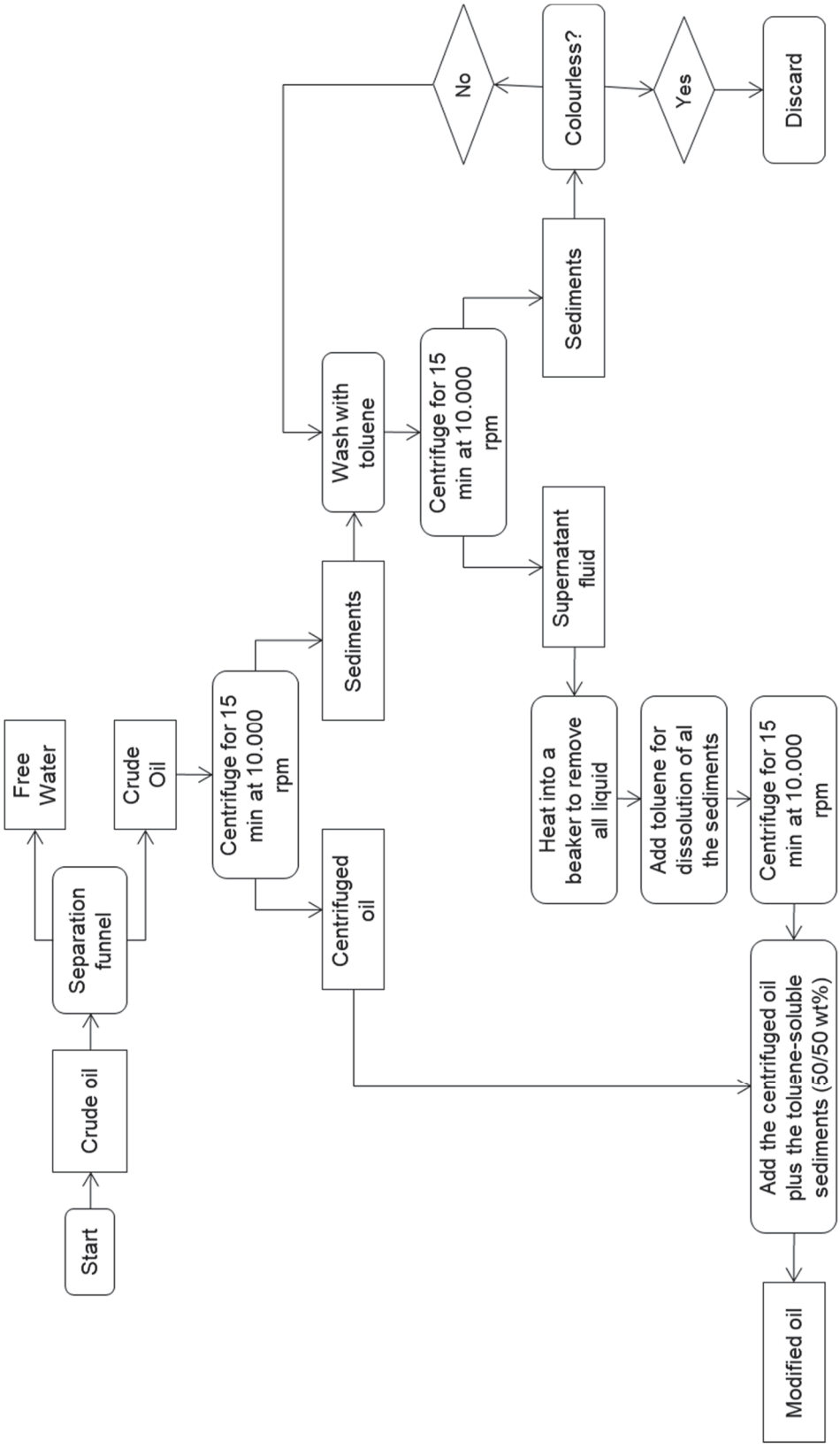

FIGURE 11 – FLOWCHART FOR PREPARE THE MODIFIED OIL
Source: Tavakkoli, Chen and Vargas (2016) – Adapted

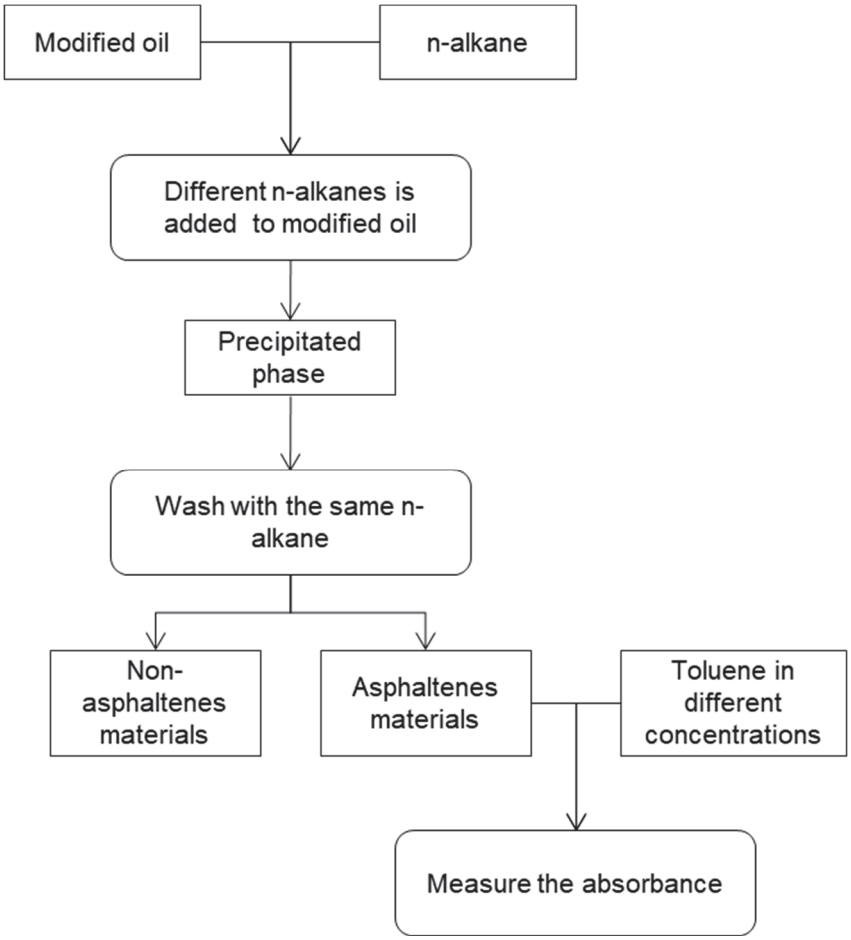

FIGURE 12 – FLOWCHART FOR "INDIRECT METHOD"
Source: Tavakkoli, Chen and Vargas (2016) - Adapted

To model the asphaltene phase behavior, a SARA analysis was made as shown in TABLE 6. Four sub-fractions were used to characterize the asphaltene pseudo-component: n-$C_{5\text{-}6}$ (n-hexane soluble and n-pentane insoluble asphaltenes), n-$C_{6\text{-}7}$ (n-heptane soluble and n-hexane insoluble asphaltenes), n-$C_{7\text{-}8}$ (n-octane soluble and n-heptane insoluble asphaltenes), n-C_{8+} (n-octane insoluble asphaltenes).

Some binary interaction parameters (k_{ij}) used were reported in the literature (underscored in TABLE **7**) and some were calculated by the linear function presented in Eq. 84. The parameters a, b and c were adjusted to obtain the best agreement for the asphaltene precipitation at 90 volume percent of the precipitant. The binary interaction parameters between the different asphaltenes' sub-fractions are zero.

$$k_{ij\,(n-alkane\,/\,saturate-asphaltene\,sub-fraction} = a - b \times M_{w(n-alkane/saturates)} + c \times M_{w(asphaltene\,sub\,fraction)} \quad (84)$$

Either fitting or calculating some parameters, they predicted the asphaltene precipitation in a range from 0 to 90 volume percent of dilution. In FIGURE 13 they compared experimental data obtained for the precipitation after one-day time with the PC-SAFT results.

TABLE 6 – TAVAKKOLI, CHEN AND VARGAS CRUDE OIL PROPERTIES AT 1 atm AND 20 ºC

Property	Value	Mw (g/mol)	γ	$\sigma\ (A)$	m	$\varepsilon/k\ (K)$
Density (g/cc)	0.826	-	-	-	-	-
Molecular weight (g/mol)	176	-	-	-	-	-
Saturates (wt%)	69.60	166.05	0	3.8992	5.11	249.52
Aromatics + Resins (wt%)	29.19	196.85	0.70	4.0808	4.14	381.70
n-C_{5-6} Asphaltenes (wt%)	0.18	1749.05	0.35	4.2143	36.55	347.51
n-C_{6-7} Asphaltenes (wt%)	0.37	1920.11	0.35	4.2170	40.02	347.74
n-C_{7-8} Asphaltenes (wt%)	0.04	2084.79	0.35	4.2192	43.35	347.92
n-C_{8+} Asphaltenes (wt%)	0.62	2701.92	0.35	4.2252	55.84	348.37

Source: Tavakkoli, Chen and Vargas (2016) - Adapted

TABLE 7 – TAVAKKOLI, CHEN AND VARGAS BINARY INTERACTION PARAMETERS

Component	n-C_5	n-C_6	n-C_7	n-C_8	Saturates	Toluene	A + R
n-C_5	0						
n-C_6	0	0					
n-C_7	0	0	0				
n-C_8	0	0	0	0			
Saturates	0	0	0	0	0		
Toluene	0.007	0.0068	0.0065	0.006	0.005	0	
A + R	0.007	0.0068	0.0065	0.006	0.007	0	0
C_{5-6} Asph	0.0149	0.0121	0.0092	0.0063	-0.0043	0	0
C_{6-7} Asph	0.170	0.0142	0.0113	0.0084	-0.0022	0	0
C_{7-8} Asph	0.0191	0.0162	0.0133	0.0104	-0.0002	0	0
C_{8+} Asph	0,0266	0.0238	0.201	0.0180	0.0074	0	0

Source: Tavakkoli, Chen and Vargas (2016) – Adapted

In one of the most recent papers about asphaltene precipitation, Ebrahimi *et al.* (2016) used PC-SAFT and solid model to predict the effect of aromatic solvents on the onset and the amount of asphaltene precipitation at reservoir conditions.

Using the same procedure as Tavakkoli, Chen and Vargas (2016), the crude oil was fractionated into the SARA classification using heptane and toluene and was

represented by three pseudo components – saturates, aromatics+resins, and asphaltenes. The asphaltene onset pressure (AOP) and the amount of asphaltene precipitation were evaluated using the original crude oil and its mixture with aromatic solvents in different concentrations: toluene (4 wt% and 7.2 wt%) and p-xylene (12 wt%). The molecular weight assumed for the asphaltene was also 1.700 g/mol.

The PC-SAFT parameters for saturates and aromatics+resins were estimated using correlations which are functions of aromaticity and molecular weight, although for asphaltenes, unlike Tavakkoli, Chen and Vargas, they were arbitrarily fitted to the experimental asphaltene instability data. Ebrahimi regarded the system as a liquid-liquid equilibrium and the binary interaction coefficients between asphaltene and saturates were adjusted.

In the solid model, the asphaltene phase behavior was predicted using a vapor-liquid-solid equilibrium. An EOS describes the fluid phases and a solid model is used to predict the fugacity of asphaltenes, similarly to Nghiem and Coombe (1997) as discussed earlier. In the end, PC-SAFT gave good predictions for all mixtures, while the accuracy of solid model decreased with the solvent concentration.

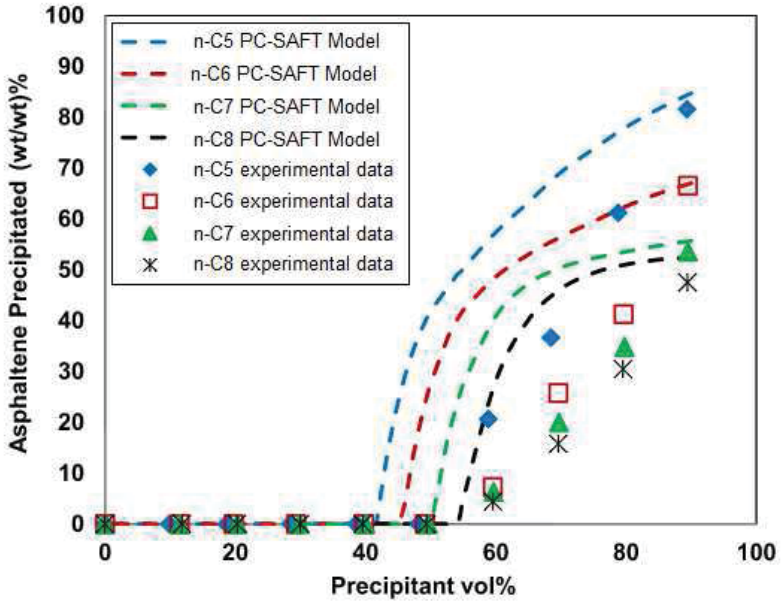

FIGURE 13 – ASPHALTENE PRECIPITATION FROM TAVAKKOLI et al. FOR THE MODIFIED OIL WITH DIFFERENT N-ALKANES
Source: Tavakkoli, Chen and Vargas (2016) - Adapted

2.4.3.1 Brazilian asphaltene

In the 90's Mohamed *et al.* (1999) were already studying asphaltene precipitation in Brazilian offshore crude oil upon addition of n-alkanes (n-pentane or n-heptane) following the same procedure as recent researches. The crude oil was fractionated into SARA classification using chromatography. The fraction insoluble in n-heptane (around 3 wt% of asphaltene in oil) was found as being smaller than the fraction insoluble in n-pentane (around 7 wt% of asphaltene in oil). The average molecular weight of asphaltene fraction with C_5 was around 3250 g/mol while that with C_7 was 5430 g/mol.

Neves *et al.* (2001) studied asphaltene solubility in heptane/toluene mixture as function of temperature. 2 wt% asphaltenes were extracted using n-heptane from a crude oil sample from the Campos Basin, RJ, presenting 19.2 °API and containing 25 wt% resins.

FIGURE 14 shows the amounts of precipitated asphaltenes from a model solution (90 g of asphaltenes/L of toluene) by adding n-heptane. By the figure, the influence of temperature over the asphaltene precipitation is obvious. From 0 °C to 20 °C the amount of precipitated decreases significantly. That is, the solubility of asphaltene in heptane increases as temperature increases. Neves and co-works showed that solutions with volumetric fractions up to 0.6 are stable, and no precipitated is form. To make sure that this influence occurs also in the precipitation of asphaltenes from crude oil, Neves *et al.* used n-decane and n-dodecane to precipitate asphaltene from crude oil. The results are shown in FIGURE 15 and it is possible to observe the same behavior. These conclusions are in agreement with what was discussed earlier in Section 2.2.

At the same Research Center, González, Sousa and Lucas (2006) have continued the work of Neves *et al.* (2001). The difference was that three Brazilian offshore crude oils were characterized, as presented in TABLE 8.

A spectrometric analysis was used to obtain the onset of asphaltene precipitation diagrams represented by FIGURE 16, in which the absorbance of asphaltenes solutions in toluene or crude oil containing different amounts of n-heptane was measured. At the beginning, the absorbance decreases as n-heptane is added because of dilution. As the asphaltenes appear, absorbance value starts to increase.

Absorbance stars to decrease again due to new dilutions and sedimentation of asphaltenes. As it is possible to see from the color-faded points of the figure, the onset values for asphaltene precipitation are: 2.8 mL of C_7/g of oil (crude oil A), 1.1 mL of C_7/g of oil (crude oil B) and 0.7 mL of C_7/g of oil (crude oil C).

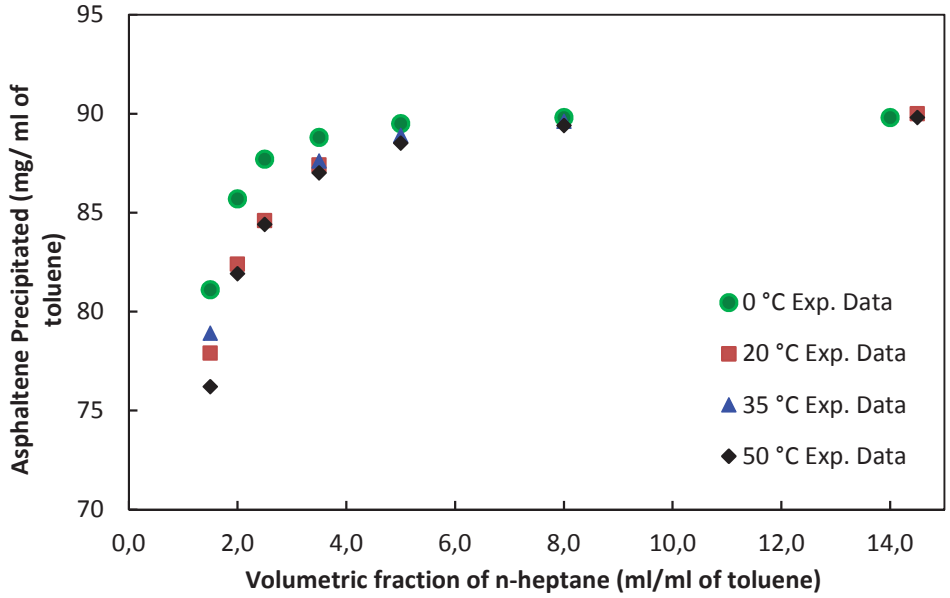

FIGURE 14 – ASPHALTENE PRECIPITATION FROM NEVES et al. FROM MODEL SOLUTION WITH N-HEPTANE AT DIFFERENT TEMPERATURES
Source: Neves *et al.* (2001) – Adapted

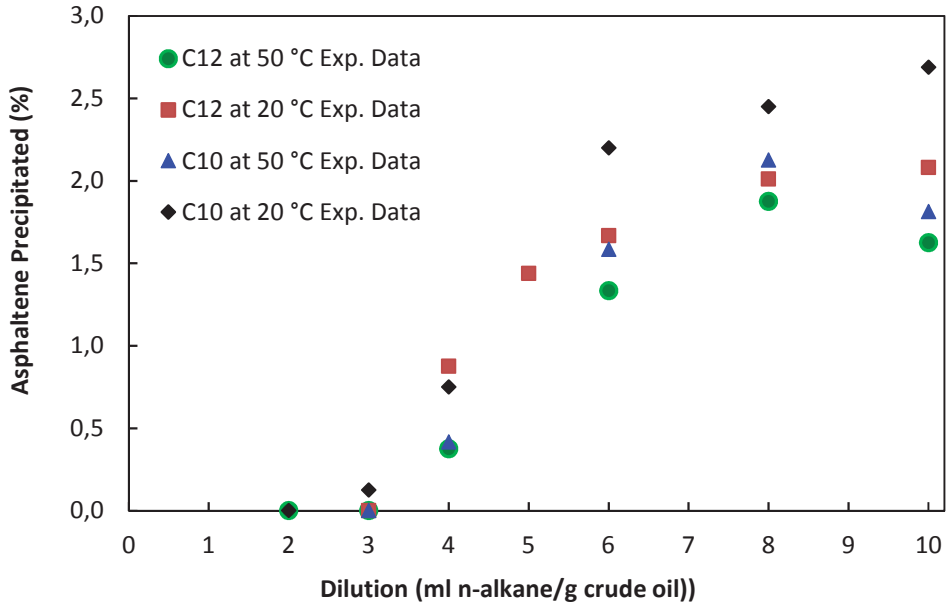

FIGURE 15 – ASPHALTENE PRECIPITATION FROM NEVES et al. FROM CRUDE OIL WITH N-DECANE AND N-DODECANE AT DIFFERENT TEMPERATURES
Source: Neves *et al.* (2001) – Adapted

TABLE 8 – BRAZILIAN CRUDE OIL PROPERTIES FROM GONZÁLEZ, SOUZA and LUCAS (2006).

	Sample A	Sample B	Sample C
API degree	19.2	28.9	39.6
Relative density, 20/4 °C	0.934	0.879	0.823
Viscosity at 30 °C cSt	357.7	22.4	4.4
Asphaltenes (wt%)	2.3	2.3	0.4
Resins (wt%)	20-25		8.0

Source: GONZÁLEZ, SOUZA and LUCAS (2006) – Adapted.

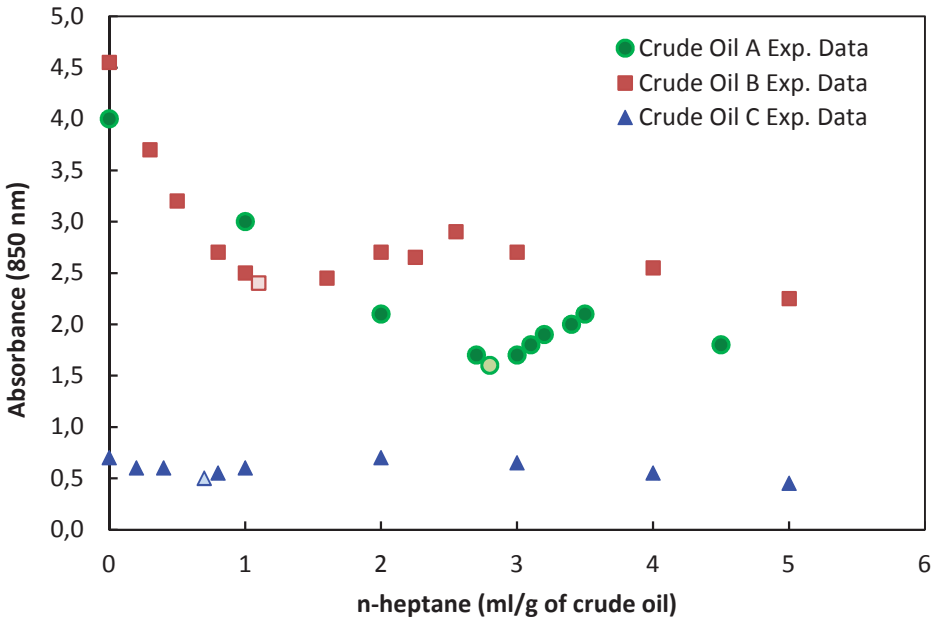

FIGURE 16 – ABSORBANCE DIAGRAM FROM GONZÁLEZ *et al.*
Source: González *et al.* (2006) – Adapted

Gonzáles, Souza and Lucas (2006) observed a decrease in asphaltenes precipitation onset as n-alkene molecular weight increased, including for n-alkanes with 10 carbon and more. In other words, as the number of carbon increases, it is necessary a larger volume of n-alkane to precipitate the same amount of asphaltene. Although, as they quoted, Wang and Buckley[8] and Wiehe *et al.*[9] reported results

[8] Wang, J. X.; Buckley, J. S. An Experimental Approach to Prediction of Asphaltene Flocculation. SPE Paper 64994. Presented at the SPEInternation Symposium on Oilfield Chemistry, Houston, February 13-16, 2001.
[9] Wiehe, L. A.; Yarranton, K.; Akbarzadeh, K.; Rahini, P.;Teclemarian, A. The Maximum Volume with Carbon Number of N-Paraffins at the Onset of Asphaltene Precipitation. In Proceedings of the 5th Internation Conference on Phase Bahavior and Fouling, Banff, Canada, June 13-17 2004.

indicating that the volume of n-alkane required do reach the precipitation onset goes through a maximum at a carbon number of 8-10.

Cardoso *et al.* (2014) studied the effect of both CO_2 injection and temperature on the asphaltene phase envelope (APE) of a Brazilian crude oil sample with a quartz crystal resonator technique. In this technique, resonance frequency and bandwidth of a quartz crystal resonator immersed into the sample is monitored. Temperature influences the stability of asphaltene in two different ways: in the range from 35 to 80 °C, temperature leads to an increase in the asphaltene stability, while from 87 to 147 °C, temperature decreases the asphaltene stability. The effect of the depressurization rate of the fluid during the crude oil production was also monitored. Higher asphaltene onset values were found when depressurization rate is slower and thus the asphaltene precipitation is time dependent.

Loureiro, Palermo and Spinelli (2015) studied the influence of n-heptane and CO_2 on asphaltene phase behavior, monitored by ultraviolet visible (UV-Vis) spectrometry. Asphaltenes were extracted from Brazilian asphaltic residue by adding n-C_5 and toluene and the precipitation test was induced by n-C_7 at room temperature or CO_2. Asphaltene precipitation onset from model system (asphaltene + toluene) occurred at n-heptane:toluene ratio of 70 % (vol/vol). Adding DDBSA to the mixture, more n-heptane needs to be added to start the asphaltene precipitation, meaning that DDBSA is very effective to prevent asphaltenes flocculation during oil production. Analyzing the precipitation of asphaltene by the CO_2 addition at different pressures, they did not observe significant changes.

Santos *et al.* (2017) used near-infrared spectroscopy to analyze asphaltene stability at the desalting process conditions, in an attempt to determine the influences of pressure, temperature and composition variation. Three Brazilian asphaltenes provided by Petrobras were analyzed. SARA analysis showed a percentage of asphaltenes ranging from 1 to 11 wt% for crude oil with °API of 25 to 22. Santos and co-workers, unlike Cardoso *et al.* (2014), found that the asphaltene precipitation onset was not significantly influenced by T, P and the rate of precipitant agent added to the oil.

Asphaltenes have been one of the main subjects of researches involving Brazilian crude oil in the last thirty years. However, both the molecular structure and the deposition mechanism of this compound are not clearly understood. In addition, PC-SAFT has not yet been applied to Brazilian crude oil.

3 MATERIAL AND METHODS

3.1 EXPERIMENTAL PROCEDURE

3.1.1 Chemicals

The study of asphaltene precipitation in Brazilian light crude oil was performed using the following chemicals: n-hexane (95.0% Neon), n-heptane (Quimica Nova, PA) and toluene (Merck, PA). All of these materials were used as received.

3.1.2 Reference thermodynamic data

The equipment must be validated before conducting an unprecedented thermodynamic data measurement, which consists in the verification of the quality of experimental data obtained for a fluid whose thermodynamic behavior is widely known. The reference values for pure substances are available in the National Institute of Standards and Technology (NIST) database. NIST is a measurement standards laboratory and an agency of the United States Department of Commerce, covering a broad range of chemical and physical property data. In this work, thermodynamic properties of toluene were obtained from NIST database, such as density data and saturation pressure data of pure compounds as function of temperature over all range of liquid-vapor equilibrium. Moreover, reference data for the vapor-liquid equilibrium of the binary mixtures toluene-hexane and toluene-heptane were obtained from DECHEMA Vapor-Liquid Equilibrium Data Collection. DECHEMA is an organization based in Frankfurt, Germany, member of the European Federation of Chemical Engineering.

3.1.3 Asphaltene extraction

In order to study asphaltene precipitation, Brazilian light crude oil was chosen and the SARA fractionation was applied to reproduce the crude oil components. Maltenes were separated from asphaltenes using two different solvents (n-hexane and n-heptane), following a procedure described by Hannisdal, Hemmingsen and Sjöblom (2015) and also used by Nascimento *et al.* (2016). FIGURE 17 shows the scheme for asphaltene extraction from crude oil.

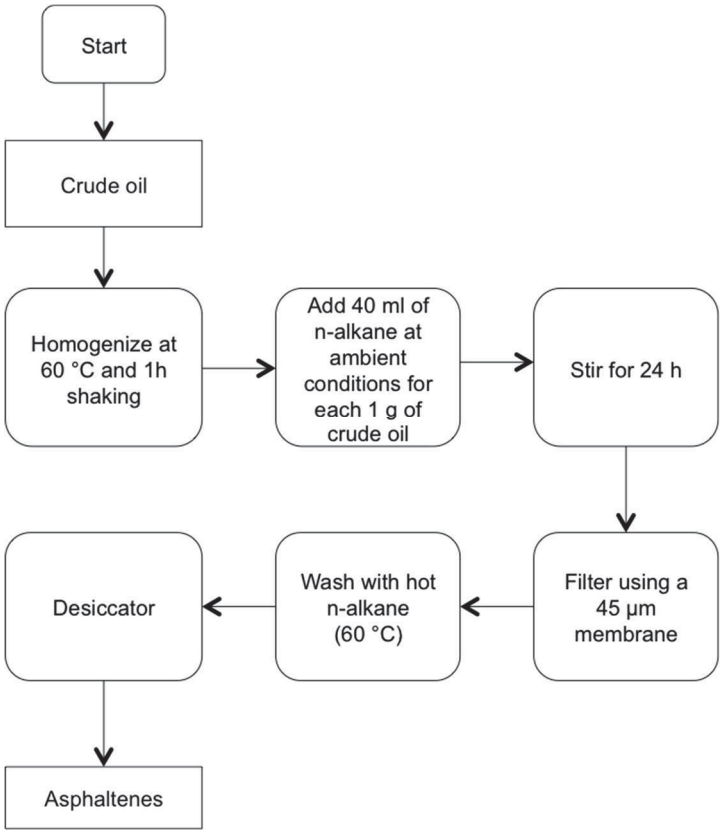

FIGURE 17 – ASPHALTENE EXTRACTION SCHEME
Source: The Author, 2017

The oil sample was heated to 60 °C and then shaken for at least one hour to obtain a homogeneous solution. The n-alkane was added to the oil sample at ambient conditions and stirred for 24 h to allow the sample to reach the equilibrium. The precipitated material was filtered using a vacuum system with a previously weighed 45 µm membrane (Sartorius Stedium), and later washed with hot n-alkane (60 °C) to separate asphaltene materials from any material also precipitated. Once the n-alkane was evaporated in a desiccator and the asphaltenes were dried, the membrane was

weighted and reported. The maltene (de-asphalted oil) fraction was previously separated into saturates, aromatics and resins and the SARA analysis of the Brazilian crude oil was performed at Petrobras R&D Center, as reported by Nascimento *et al.* (2016).

To study the asphaltene precipitation, two different n-alkanes were mixed to the crude oil, n-hexane and n-heptane, at n-alkane-to-oil ratios of 20, 30, 40, 60, 80 and 90 ml/g, using the same procedure previously described.

To prepare the “Model Oil”, a n-alkane-to-oil ratio of 40 ml/g was selected, as it has been shown in literature that this ratio provides more accurate results. The asphaltene precipitation from the “Model Oil” follows the same procedure as that from crude oil: the model mixture was precipitated with the corresponding n-alkane in different concentrations. The samples were shaken for one day to ensure the equilibrium is reached and finally filtered, enabling the separation of the asphaltene precipitated. The asphaltenes obtained after the precipitation and drying were then dissolved using different concentrations of toluene (FIGURE 18). The mixture containing asphaltenes from crude oil plus toluene was called “Model Oil”.

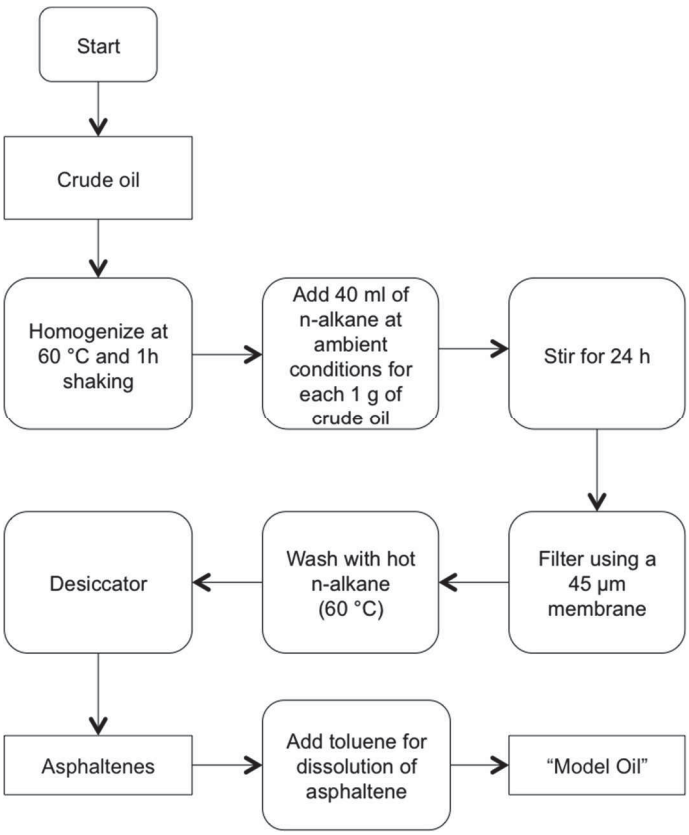

FIGURE 18 – “MODEL OIL” PREPARATION SCHEME
Source: The Author, 2017

3.1.4 Density

Density of asphaltenes was measured using an Anton Paar DMA 5000 high-precision vibrating tube density meter, represented in FIGURE 19, with an accuracy of ± 1.10^{-6} g/cm^3, which was calibrated with ultrapure water and dry air. This equipment provides a high temperature accuracy (± 0.001 °C), whereas the value is controlled traceable to national standards by two integrated Pt 100 platinum thermometers. The equipment detects filling errors caused by gas bubbles present in the sample and exhibits live images that allow the operator to check whether the oscillating U-tube is completely filled so that accurate measurements could be carried out. After the thermostat is set to the desired temperature, approximately 1 mL is injected to the equipment, the temperature equilibrium is reached and then the display gives the density value. Densities were measured in a temperature range from 30 °C to 80 °C at atmospheric pressure.

FIGURE 19 – ANTON PAAR DMA 5000 HIGH-PRECISION DENSIMETER
Source: ANTON PAAR, 2017

Before conducting the asphaltene density measurement, the density meter was also validated through the comparison between toluene densities measured using the equipment and data available in the literature. I

The procedure to determine the density of asphaltenes was as follows: dried asphaltene precipitated from crude oil was dissolved in toluene, here used as

displacement fluid, in four different concentrations. Trapped air bubbles were eliminated by ultra sonication. It is also good to remember that asphaltenes used in this experiments were precipitated using n-hexane.

3.1.5 Boiling point elevation

The boiling point of a pure solvent can be changed though the obtainment of a solution, with the addition of another component. Boiling point elevation (BPE) methods are, in general, a fast and accurate method to define boiling temperature but when applied to the higher molecular weight fractions of crude oil this precision tends to decrease (SPEIGHT, 2006). To avoid this, Brazilian crude oil was dissolved in toluene.

The experimental tests were carried out using the apparatus represented in FIGURE 20, as proposed by Hoerning *et al.* (2016), to build a boiling point elevation curve. A 250 ml three neck flask was filled with 100 to 200 ml of solution. Small pieces of porcelain were added to the flask before heating. Since when the liquid boils it releases energy as bubbles, the pieces of porcelain are necessary to provide extra surface area for the bubbles to form, allowing the gradual release of energy and thus avoiding bumping of liquid when the temperature rises. One neck of the flask was closed with a rubber cork wrapped with aluminum foil. To the second neck was attached another cork with a bore to introduce a thermistor (standard uncertainty of 0.1 K) connected to a temperature indicator (Novus, model N480D) used for temperature measurement. The measuring junction of the thermistor was kept at about 1-2 cm below the surface of the liquid. The mixture was heated by a heating mantle and specific pressures were set with a Solab Cientifica vacuum pump, model SL60. The pressure of the system was monitored with a digital vacuumeter (Greisinger Eletronic GmbH, model GDH12AN, with standard uncertainty of 0.1 kPa) and controlled using a needle valve, which was connected between the ebulliometer system and the pump. A condenser was connected to the central opening of the flash to assure that no vapor was lost during the boiling.

Since the controlled variable was the pressure, the strategy to collect the experimental data was to start with the minimum value and perform increases up to the atmospheric pressure. At a constant pressure, the solution was continuing heated until the temperature became constant. The system was considered to be at equilibrium when the temperature of the liquid phase remained constant for at least 5 min. After that, the temperature was measured every minute, five times, and the average of these measurements was considered. After six pressure steps had been measured, until the atmospheric pressure, the heating was switched off.

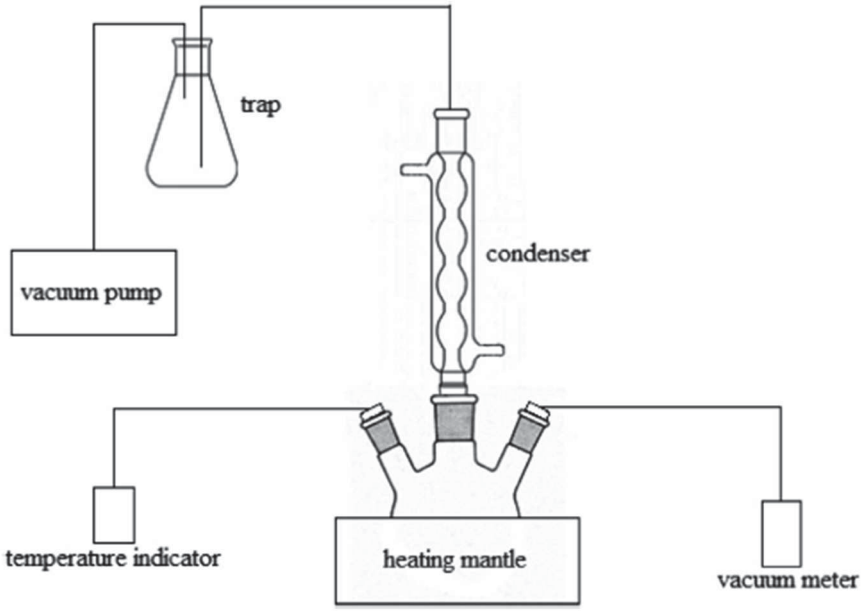

FIGURE 20 – BOILING POINT ELEVATION APPARATUS
Source: Hoerning *et al.* (2016)

Before conducting the crude oil boiling point measurement, the experimental methodology was validated. Temperatures of toluene and distilled water were measured over a certain pressure range and compared to the values within the NIST database. Boiling temperatures were obtained for solutions at different values of mass fraction of crude oil (8, 11, 50 and 70 wt%) and pressures (5.7 to 91.1 kPa).

3.2 MODELING PROCEDURE

Crude oil and asphaltene thermodynamic properties, as well as asphaltene precipitation using PC-SAFT Equation of State (PC-SAFT EoS) were simulated with a set of sub routines in Fortran 95 language, developed by and available in the Laboratory of Catalysis and Applied Thermodynamics (LACTA). The PC-SAFT subroutines for the fugacity coefficients were kindly provided by Prof. Walter Chapman Group (Rice University, Houston, Texas, USA). The PC-SAFT methodology was summarized in section 2.3.2 and is described in details in the literature (PANUGANTI *et al.*, 2012).

3.2.1 PC-SAFT parameter estimation

For each non-associating component, there are just three PC-SAFT parameters (σ, m and ε/k). As reported by other researchers (Sabeti *et al.*, 2015 and Tavakkoli *et al.*, 2016) the association term in PC-SAFT can be set to zero in petroleum fluid characterization, since there are no association between the nonpolar hydrocarbon molecules.

As an example of its applications and in order to validate the experimental density apparatus, PC-SAFT EoS is used to obtain T vs. ρ diagrams of pure toluene at ambient pressure. PC-SAFT parameters for toluene were adopted from Gross and Sadowski (strategy 1) and also adjusted to obtain the best agreement for toluene density (strategy 2).

Correlations for the three PC-SAFT parameters have been reported by Tavakkoli *et al.* (2016) and Al Hammadi, Vargas and Chapman (2015) as functions of molecular weight as presented in TABLE 4. However, to ensure a good density modeling, different strategies were used to fit the PC-SAFT parameters for an asphaltene component: (i) using the correlations in TABLE 4 and adjusting the asphaltene aromaticity value to 0.35 (strategy 1A) as reported by Tavakkoli *et al.* (2016); (ii) considering asphaltene aromaticity parameter as being 0.06 (strategy 1B) as found by Nascimento *et al.* for a Brazilian asphaltene; and (iii) adjusting the parameters in order to obtain the best fitting for apparent density data obtained experimentally (strategy 2).

Apparent density data was obtained based on toluene-asphaltene mixtures. Four different concentrations of asphaltene in toluene were prepared, as reported in section 3.1.4. A temperature-density diagram was obtained for each concentration. For each temperature measured, a correlation was estimated between density and system composition. By extrapolating curves density-concentration of asphaltene, pure densities of asphaltene were estimated for each temperature. Therefore, to proceed strategy 2, PC-SAFT parameters were adjusted using density-temperature diagram for pure asphaltene.

The estimation of binary interaction parameters from thermodynamics models is an important step in phase equilibrium modeling. Different strategies have been used to perform the binary parameter estimation, for example, by using a regression of either isothermal equilibrium data or critical point data (Corazza *et al.*, 2004). In this work, the binary interaction parameters were adjusted to obtain the best agreement with experimental data.

3.2.2 Boiling point elevation

Michelsen (1985) presented a method for the calculation of saturation temperatures or pressures for multicomponent mixtures with interaction in only a single variable. This method is summarized in Appendix B. An algorithm is presented in FIGURE 21 for solving the bubble-point temperature problem using the Michelsen method and PC-SAFT equation of state to find the fugacity coefficient of components. Temperature, pressure and global composition are the input arguments. The method uses Newton-Raphson method to perform iterations to correct T using the equations B.6-B.9 and find equilibrium phase compositions.

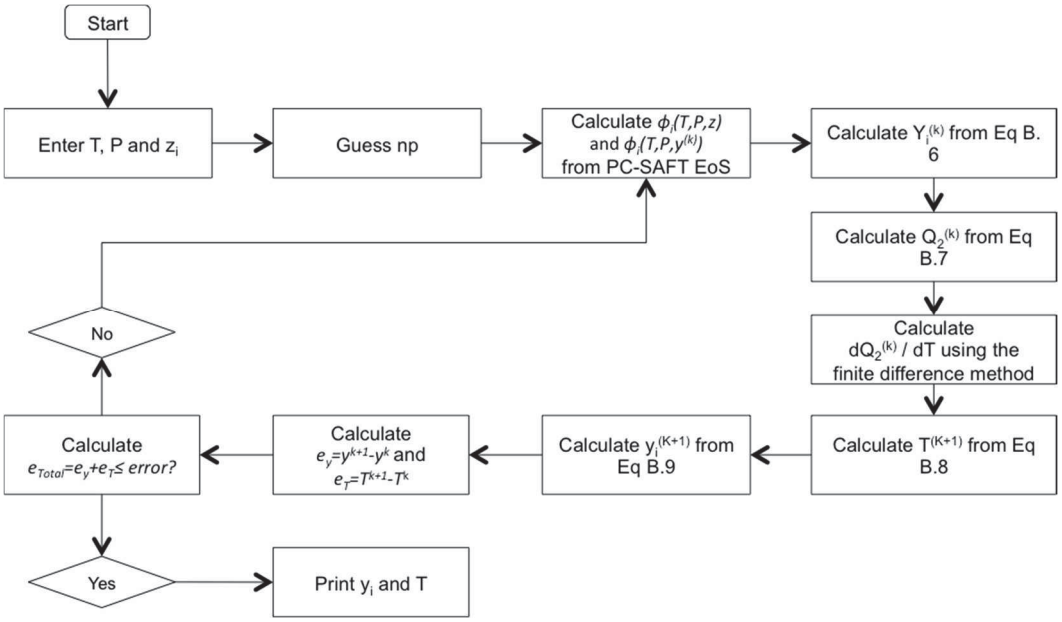

FIGURE 21 – ALGORITHM FOR SOLVING THE BUBBLE-POINT TEMPERATURE PROBLEM USING THE MICHELSEN METHOD AND PC-SAFT EQUATION OF STATE
Source: The Author (2017)

3.2.4. Asphaltene precipitation modeling

To perform the modeling for the precipitation of asphaltenes, it was considered that asphaltenes are dissolved in crude oil and, as already mentioned before, the association term is neglected. The precipitation process from the model oil (asphaltene+toluene) is treated as the traditional liquid-liquid phase separation. For the crude oil, it is considered that one liquid-phase is composed by pure asphaltene and the other liquid-phase is characterized in terms of two pseudo-components: saturates and (aromatics+resins). Using the same principle as Li and Firoozabadi (2010), aromatics and resins were considered as a pseudo-component, since both of them have polar-polar interaction with asphaltenes.

The following algorithm of multiphase flash calculation was used in this work to estimate asphaltene precipitation:

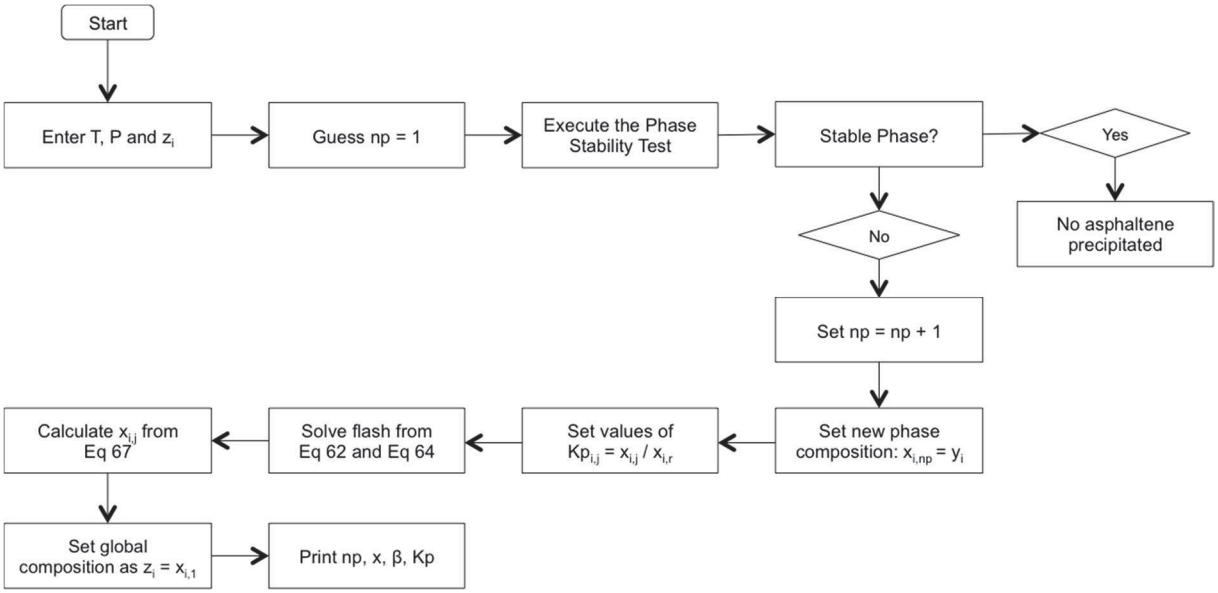

FIGURE 22 – ALGORITHM FOR SOLVING PHASE EQUILIBRIUM PROBLEM CONSIDERING A LIQUID-LIQUID EQUILIBRIUM AND USING THE PC-SAFT EQUATION OF STATE.
Source: The Author

Given the global composition (z), temperature (T) and pressure (P) and for one phase system ($np = 1$) the phase stability is executed as describe in section 2.3.3. As the phase is unstable, meaning that there is asphaltene precipitation, the number of phases is assumed to be equal to $np + 1$ and a split calculation (with $np + 1$ phases) is performed.

The binary interaction parameters were fitted in order to match with the experimental data. Once the k_{ij} value is already known for toluene-asphaltene from section 3.2.3, the following pairs were fitted to predict the asphaltene precipitation from crude oil: toluene-saturates, toluene-(aromatics+resins), saturates-(aromatics+resins), saturates-asphaltenes, asphaltenes-(aromatics+resins). The binary pairs asphaltene-n-alkanes were assigned to reproduce experimental results from asphaltene precipitation using the “Model Oil”. k_{ij} values for toluene-n-alkanes were fitted based on experimental data of vapor-liquid equilibrium.

4 RESULTS AND DISCUSSIONS

4.1 PREVIOULSY CRUDE OIL PROPERTIES

For the SARA analysis of Brazilian crude oil, Petrobras R&D Center developed a standard chromatographic procedure obtaining the following weight fraction: 61.8 wt% of saturates, 35.7 wt% of aromatics plus resins and 2.5 wt% of asphaltenes. Nascimento *et al.* (2016) used the Fourier Transform Ion Cyclotron Resonance Mass Spectrometry equipped with an atmospheric pressure photoionization (APPI(+)–FT-ICR MS) to determine the average molar mass distribution (M_W) for the asphaltene fraction. The M_W for asphaltenes precipitated from n-hexane centered at approximately *m/z* 466. TABLE 9 presents the Brazilian crude oil properties.

TABLE 9 – BRAZILIAN CRUDE OIL PROPERTIES

Density[1]	° API[1]	Viscosity at 60 °C[1]		SARA Classification		
				Saturates	Aromatics + Resins	Asphaltenes
0.8899 g/cm^3	27.5	21.26 mPa.s	wt (%)	61.8[1]	35.7[1]	2.5[1]
			Mw	117[1]	189[1]	466[2]

Source: Petrobras R&D Center[1] and Nascimento *et al.* (2016)[2]

4.2 BINARY INTERACTION PARAMETERS

Binary interaction parameters used in this work are reported in TABLE 10. k_{ij} value for the binary system asphaltenes-toluene was fitted based on the temperature-density diagram presented in Section 4.5. For the binary systems toluene-saturate and toluene-(A+R), k_{ij} values were fitted based on boiling point elevation data presented in Section 4.6. Vapor-liquid equilibrium helps to define k_{ij} value for n-alkanes-toluene, presented in Section 4.7. The study of asphaltene precipitation from model oil was used to predicted interaction parameters for n-hexane-asphaltene and n-heptane-

asphaltene, presented in Section 4.7. The binary interaction parameters for the system n-alkanes-crude oil (represented as three pseudo-components: saturates, (aromatics+resins) and asphaltenes) are analyzed in order to obtain the best match for asphaltene precipitation from crude oil, through the comparison of PC-SAFT modeling results with experimental data, showed in Section 4.8.

TABLE 10 – BINARY INTERACTION PARAMETERS USED FOR PC-SAFT MODELING.

Component	n-C_6	n-C_7	Toluene	Saturates	A + R	Asphaltenes
n-C_6	0					
n-C_7	0	0				
Toluene	0.0082	0.0065	0			
Saturates	0.2000	0.3000	0	0		
A + R	-0.0050	-0.0050	0	0	0	
Asphaltenes	0.0500	0.0550	0.0320	0.0350	0.0050	0

Source: The Author (2017)

4.3 TEMPERATURE-DENSITY DIAGRAM OF PURE TOLUENE

Before conducting the asphaltene density measurement, the equipment was validated, checking if density values of toluene obtained experimentally coincide with the reference values (NIST). As indicated by TABLE 11, experimental data obtained in this work are in good agreement with literature data, at ambient pressure and temperatures from 30 °C up to 80 °C. It can also be noted that as the temperature increases, the relative error (Eq. 78) also increases. However, the low value of MRE (mean relative errors, 0.003 %) combined to a R^2 near to 1 (R-square, 0.997) allow the evaluation that the experimental data are acceptable. These two statistical resources are calculated by the following equations, remembering that low MRE value and high R^2 value indicate that the estimation is adequate.

.

$$\boldsymbol{Relative\ error}\ (\%) = \left|(\boldsymbol{Y_i} - \widehat{\boldsymbol{Y}}_{\boldsymbol{i}})\right| / \boldsymbol{Y_i} \times \mathbf{100} \tag{78}$$

$$\boldsymbol{MRE} = \frac{\sum\left|(\boldsymbol{Y_i} - \widehat{\boldsymbol{Y}}_{\boldsymbol{i}})\right| / \boldsymbol{Y_i} \times \mathbf{100}}{\boldsymbol{n}} \tag{79}$$

$$R^2 = \frac{\sum(\hat{Y}_i - \bar{Y})^2}{\sum(Y_i - \bar{Y})^2} = 1 - \frac{\sum(Y_i - \hat{Y}_i)^2}{\sum(Y_i - \bar{Y})^2} \quad (80)$$

where Y_i is the actual value of n predictions and $\hat{Y}_i$ is the predicted or estimated value. The $\bar{Y}$ is the average of the original Y_i-values. In this case, Y_i is the experimental values and $\hat{Y}_i$ is the value obtained from NIST.

TABLE 11 – STATISTICAL EVALUATION BETWEEN LITERATURE AND EXPERIMENTAL DATA FOR LIQUID DENSITY OF PURE TOLUENE

P = 680 mmHg			
Temperature °C	Exp. density g/cm^3	Lit.density g/cm^3	Relative Error (%)
30.00	0.857573	0.857560	0.001516
39.99	0.848193	0.848190	0.000354
49.99	0.838736	0.838750	0.001669
59.99	0.829189	0.829220	0.003738
69.99	0.819543	0.819600	0.006955
79.99	0.809811	0.809850	0.004816
MRE		0.003175	
R^2		0.997274	

Source: The Author (2017)

PC-SAFT EoS was used to obtain temperature-density diagrams of pure toluene at ambient pressure. PC-SAFT parameters of toluene were taken from Gross and Sadowski (2001) (strategy 1) and re-estimated to obtain the best match for toluene density (strategy 2). TABLE 12 presents the EoS parameters used on both strategies

TABLE 12 – PC-SAFT PARAMETERS FOR TOLUENE FROM GROSS AND SADOWSKI (2001) (STRATEGY 1) AND FITTED BASED ON EXPERIMENTAL DATA (STRATEGY 2)

Toluene parameters	m	σ (A)	ε/k (K)
Strategy 1	2.8149	3.7169	285.69
Strategy 2	2.7616	3.7316	289.22

Source: The Author (2017)

Considering the data in TABLE 13 and FIGURE 23 it can be concluded that the PC-SAFT EoS was able to find a good prediction for toluene density using strategy

2. In this scenario, the best set of PC-SAFT parameters were: m = 2.7616, σ = 3.7316 A and ε/k = 289.22 K. It can be noticed that there is an increase in the relative error as the temperature also increases, which is the same observation made by Sabeti *et al.* (2015). Nevertheless, the absolute error for vapor pressure is 0.10 %, for the saturate liquid density is 0.85 % and for sub-cooled liquid density is 0.17 %.

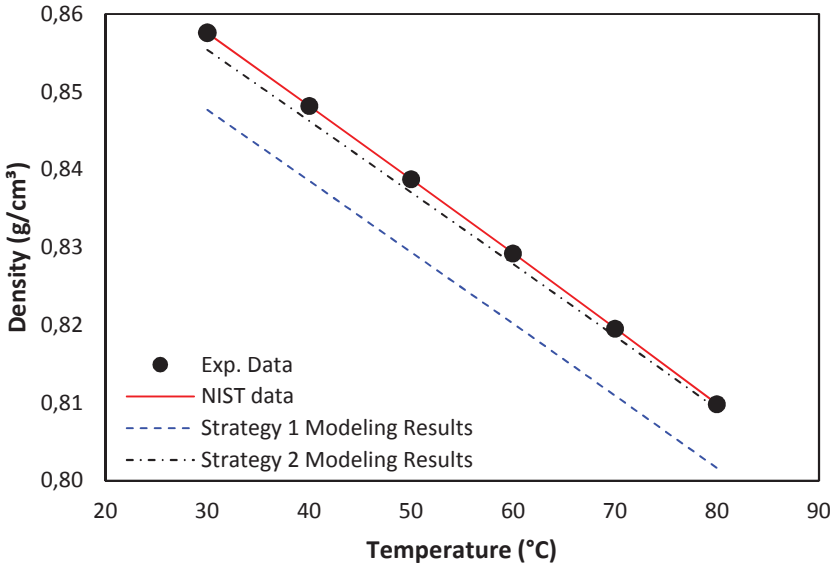

FIGURE 23 – COMPARISON OF PC-SAFT PREDICTED LIQUID DENSITIES VERSUS EXPERIMENTAL DATA FOR PURE TOLUENE AT AMBIENT PRESSURE. MODEL PARAMETERS: GROSS AND SADOWSKI (2001) (STRATEGY 1) AND FITTED BASED ON EXPERIMENTAL DATA (STRATEGY 2)
Source: The Author (2017)

TABLE 13 – STATISTICAL EVALUATION CALCULATED LIQUID DENSITY OF PURE TOLUENE WITH RESPECT TO EXPERIMENTAL DATA

P = 680 mmHg

Temperature (°C)	Strategy 1		Strategy 2	
	Density g/cm^3	Relative error (%)	Density g/cm^3	Relative error (%)
30.0	0.864573	1.155022	0.847668	0.254237
40.0	0.855393	1.139807	0.838525	0.231794
50.0	0.846227	1.116513	0.829371	0.200774
60.0	0.837052	1.086226	0.820182	0.162195
70.0	0.827844	1.050598	0.810933	0.117645
80.0	0.818579	1.014119	0.801599	0.071569
MRE		1.093714		0.173036
R^2		0.746989		0.990332

Source: The Author (2017)

4.4 TEMPERATURE-DENSITY DIAGRAM FOR ASPHALTENE-TOLUENE MIXTURE AND APPARENT DENSITY DATA

Asphaltenes precipitated from crude oil using n-hexane were mixed with toluene in four different concentrations. TABLE 14 and

FIGURE 24 present the experimental data.

TABLE 14 – EXPERIMENTAL DENSITY FOR ASPHALTENE-TOLUENE MIXTURE WITH DIFFERENT CONCENTRATIONS OF ASPHALTENE: 0.35 wt%, 0.45 wt%, 2.08 wt% AND 4.85 wt%

P = 680 mmHg

Temperature °C	0.35 wt%	0.45 wt%	2.08 wt%	4.85 wt%
	Density g/cm^3	Density g/cm^3	Density g/cm^3	Density g/cm^3
30.0	0.858135	0.858049	0.861810	0.868980
40.0	0.848733	0.848679	0.852320	0.859614
50.0	0.839328	0.839241	0.842971	0.850102
60.0	0.829793	0.829709	0.833431	0.840561
70.0	0.820152	0.820078	0.823820	0.830996
80.0	0.810396	0.810328	0.814102	0.821356

Source: The Author (2017)

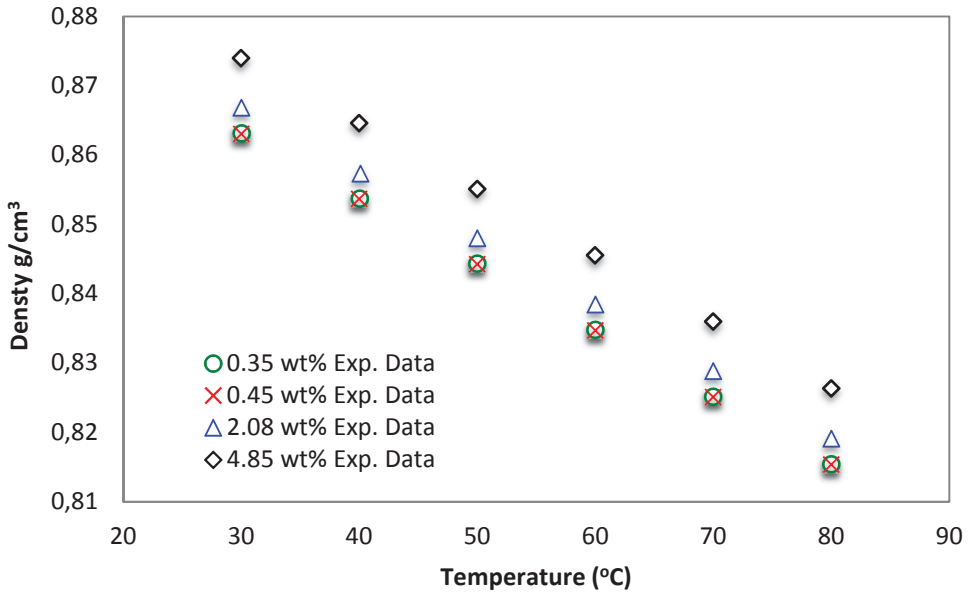

FIGURE 24 – TEMPERATURE-DENSITY DIAGRAM FOR ASPHALTENE-TOLUENE MIXTURE IN DIFFERENT CONCENTRATIONS
Source: The Author (2017)

In order to obtain apparent density data, a correlation between density and the system composition was estimated for each temperature measure, as it can be seen in FIGURE 25.

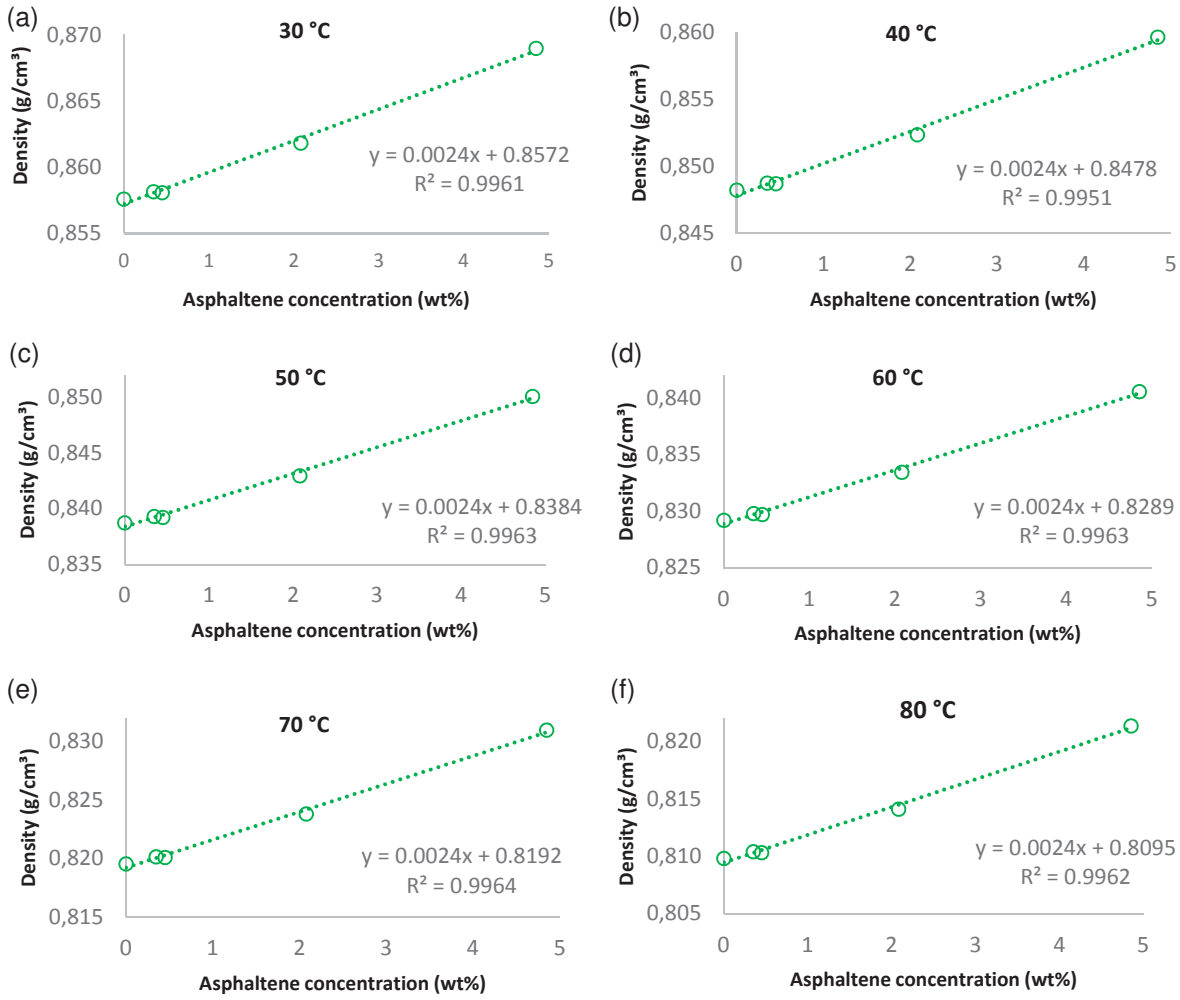

FIGURE 25 – DENSITY VERSUS ASPHALTENE CONCENTRATIONS AT (a) 30 °C, (b) 40 °C, (c) 50 °C, (d) 60 °C, (e) 70 °C, (f) 80 °C
Source: The Author (2017)

By extrapolating density-concentration of asphaltene curves, it was possible to estimate the densities of pure asphaltene at each temperature. TABLE 15 shows the densities of pure asphaltene based on pseudo-experimental results. Pseudo-experimental asphaltene density at 50 °C is 1.08 g/cm^3. Generally, the density of asphaltenes at 50 °C stands between 1.13 and 1.20 g/cm^3 (Akbarzadeh *et al.*, 2004). Rogel and Carbognani (2003) found experimental density for different asphaltenes in a range from 1.17 to 1.52 g/cm^3 at 25 °C. Moreover, Barreta, Ortiz and Yarranton (2013) measured a very similar density for the asphaltene from four oil samples, with

an average density of 1.176 g/ cm^3, using an Anton Paar DMA 46 density meter at 20 °C.

TABLE 15 – PSEUDO-EXPERIMENTAL DENSITY OF PURE ASPHALTENE

P = 680 mmHg	
Temperature °C	Density g/cm^3
30.0	1.0972
40.0	1.0878
50.0	1.0784
60.0	1.0689
70.0	1.0592
80.0	1.0495

Source: The Author (2017)

4.5 ASPHALTENE'S PARAMETER ESTIMATION

TABLE 16 shows de PC-SAFT parameters for asphaltene, achieved using different strategies. The molecular weight of asphaltene is 466 g/mol, according to Nascimento *et al.* (2016). Strategy 1 used the equations presented in TABLE 4 with aromaticity of 0.3500 (1A) and 0.0063 (1B) for the estimation of PC-SAFT parameters while strategy 2 is based on pseudo-experimental results of pure asphaltene densities presented in TABLE 15.

TABLE 16 – PC-SAFT PARAMETER FOR ASPHALTENE (STRATEGY 1A) WITH AROMATICITY OF 0.35 FROM TAVAKKOLI *et al.* (2016), (STRATEGY 1B) WITH AROMATICITY OF 0.063 FROM NASCIMENTO *et al.* (2016), (STRATEGY 2) FITTED BASED ON EXPERIMENTAL DATA

Asphaltene parameters	γ	m	σ (A)	ε/k (K)
Strategy 1A	0.3500	10.5861	4.1347	337.94
Stratedy 1B	0.0063	12.4184	4.0109	273.13
Strategy 2	0,3500	11.5076	3.7967	305.11

Source: The Author (2017)

The pseudo-experimental data shown in FIGURE 26 is resulted from the extrapolation of asphaltene concentration curves. The figure also shows the PC-SAFT

modeling results obtained using each strategy, whose values are presented in TABLE 17. Based on that, it is noteworthy that strategy 2, in which the parameters were obtained so as to provide the best experimental fit, ensured a smaller deviation from the pseudo-experimental density data.

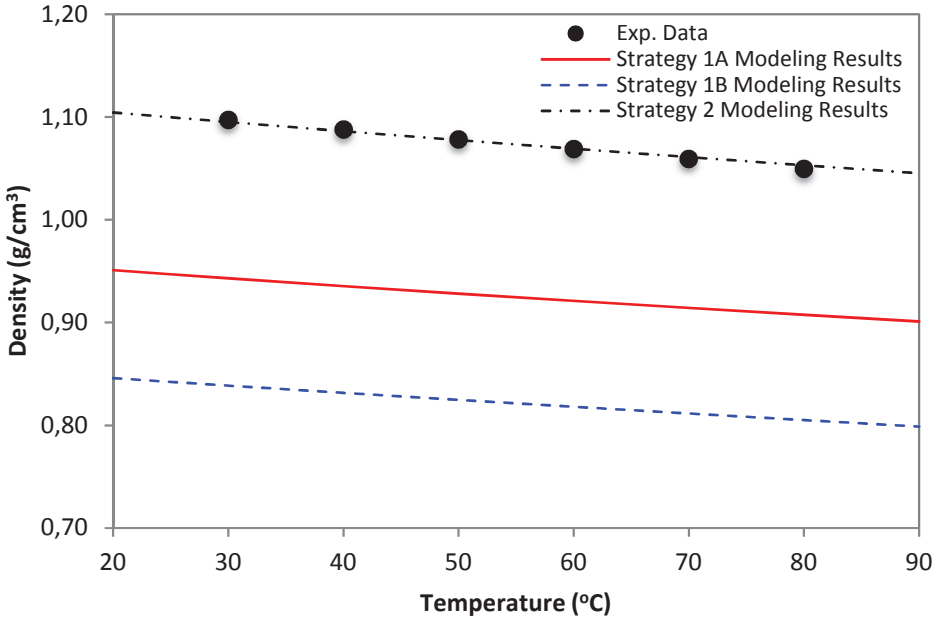

FIGURE 26 – COMPARISON OF PC-SAFT PREDICTED LIQUID DENSITIES VERSUS PSEUDO-EXPERIMENTAL DATA FOR PURE ASPHALTENE AT AMBIENT PRESSURE. MODEL PARAMETERS: (STRATEGY 1A) WITH AROMATICITY 0.35 FROM TAVAKKOLI *et al.* (2016), (STRATEGY 1B) WITH AROMATICITY 0.063 FROM NASCIMENTO *et al.* (2016), (STRATEGY 2) FITTED BASED ON EXPERIMENTAL DATA
Source: The Author (2017)

TABLE 17 – STATISTICAL EVALUATION CALCULATED LIQUID DENSITY OF PURE ASPHALTENE WITH RESPECT TO PSEUDO-EXPERIMENTAL DATA

P = 680 mmHg

Temperature °C	Strategy 1A		Strategy 1B		Strategy 2	
	Density g/cm³	Relative error (%)	Density g/cm³	Relative error (%)	Density g/cm³	Relative error (%)
30.0	0.943086	14.046092	0.838703	23.559710	1.095168	0.185244
40.0	0.935481	14.002514	0.831659	23.546657	1.086228	0.144558
50.0	0.928157	13.932041	0.824807	23.515709	1.077579	0.076168
60.0	0.921084	13.828777	0.818121	23.461443	1.069188	0.026953
70.0	0.914236	13.686174	0.811581	23.377961	1.061027	0.172526
80.0	0.907589	13.521760	0.805168	23.280821	1.053071	0.340238
MRE		13.836226		23.457050		0.157615

Source: The Author (2017)

The pure asphaltene density data are referred to values extrapolated from the density diagram of a binary mixture containing toluene and asphaltenes in low concentrations. According to Barrera, Ortiz and Yarranton (2013), the density distributions for asphaltene has an abrupt rise, due to the little or no self-associative nature of this component, followed by a much slower increase due to cuts showing self-association. Barrera and co-workers believe that asphaltene which do not self-associate are essentially found in the most soluble fraction of asphaltenes.

Based on the aforementioned claims, it is necessary to guarantee that this extrapolation is valid for Brazilian asphaltenes. In this sense, PC-SAFT parameters already estimated were applied for modeling temperature-density diagram of the mixture containing 4.85 wt% of asphaltene.

As can be seen in FIGURE 27, the resulting diagram of the PC-SAFT solution is not in good agreement with experimental data when strategy 2 is used. The lowest relative errors in TABLE 18 indicate that the best match is obtained using the first strategy, in which the asphaltene aromaticity is 0.35, adopted by Tavakkoli *et al.* (2016).

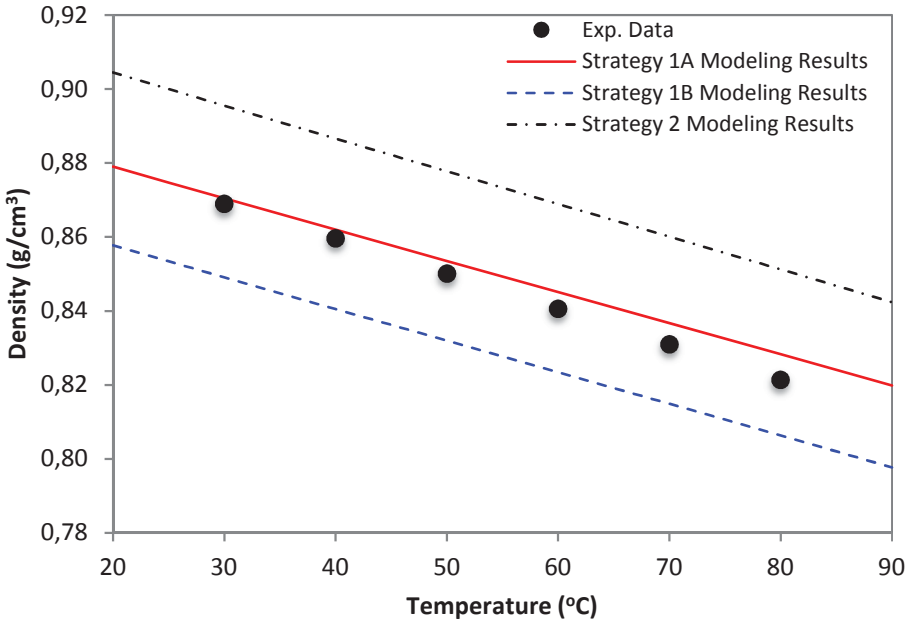

FIGURE 27 – COMPARISON OF PC-SAFT PREDICTED LIQUID DENSITIES VERSUS EXPERIMENTAL DATA FOR 4.85 wt% ASPHALTENE-TOLUENE MIXTURE AT AMBIENT PRESSURE. MODEL PARAMETERS: (STRATEGY 1A) WITH AROMATICITY 0.35 FROM TAVAKKOLI *et al.* (2016), (STRATEGY 1B) WITH AROMATICITY 0.063 FROM NASCIMENTO *et al.* (2016), (STRATEGY 2) FITTED BASED ON EXPERIMENTAL DATA
Source: The Author (2017)

TABLE 18 – STATISTICAL EVALUATION CALCULATED LIQUID DENSITY OF 4.85 wt% ASPHALTENE-TOLUENE MIXTURE WITH RESPECT TO EXPERIMENTAL DATA

P = 680 mmHg

Temperature °C	Strategy 1A		Strategy 1B		Strategy 2	
	Density g/cm^3	Relative error (%)	Density g/cm^3	Relative error (%)	Density g/cm^3	Relative error (%)
30.0	0.870422	0.165953	0.849090	2.288932	0.895502	3.052088
40.0	0.861935	0.270060	0.840510	2.222406	0.886602	3.139546
50.0	0.853500	0.399665	0.831965	2.133535	0.877747	3.251940
60.0	0.845095	0.539362	0.823433	2.037668	0.868915	3.373246
70.0	0.836702	0.686588	0.814894	1.937650	0.860086	3.500640
80.0	0.828301	0.845558	0.806327	1.829747	0.851239	3.638259
MRE		0.343605		1.770032		2.719577

Source: The Author (2017)

At this point, the PC-SAFT parameters that obtained the best results were from strategy 1A: m = 10.5861, σ = 4.1347 A and ε/k = 337.94 K. The asphaltene aromaticity value was set to 0.35 and the binary interaction parameter (k_{ij} value) for asphaltene-toluene was considered zero. The next step is to study the influence of k_{12} value for the binary asphaltene (1) – toluene (2).

FIGURE 28 compares the PC-SAFT predicted density curve using different k_{12} values. The importance of adjusting binary interaction parameter is obvious. The best match was obtained using k_{12} = 0.032. TABLE 19 shows the low value of MRE and R^2 value between 0.80 and 0.90 for modeling results if k_{12} = 0.032.

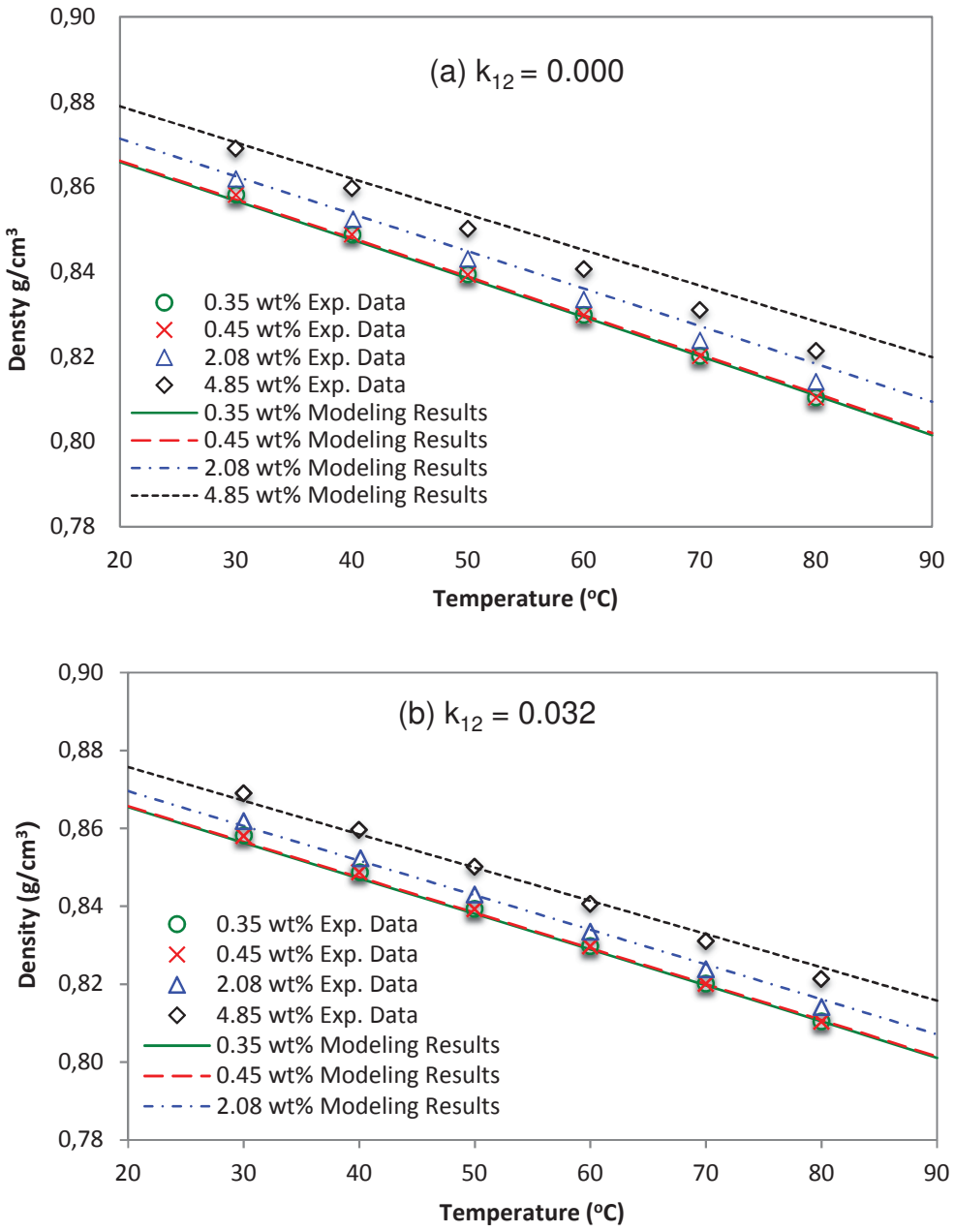

FIGURE 28 – COMPARISON OF PC-SAFT PREDICTED LIQUID DENSITIES VERSUS EXPERIMENTAL DATA FOR ASPHALTENE DILUTED WITH TOLUENE AT DIFFERENT CONCENTRATION AT AMBIENT PRESSURE. MODEL PARAMETERS: AROMATICITY 0.35 AND BINARY INTERACTIHON PARAMETERS (a) 0.000, (b) 0.032
Source: The Author (2017)

TABLE 19 – STATISTICAL EVALUATION FOR CALCULATED LIQUID DENSITY OF ASPHALTENE-TOLUENE MIXTURE WITH RESPECT TO EXPERIMENTAL DATA

P = 680 mmHg

Temperature (°C)	0.35 wt%		0.45 wt%	
	Density (g/cm^3)	Relative error (%)	Density (g/cm^3)	Relative error (%)
30.0	0.856294	0.214445	0.856550	0.174663
40.0	0.847178	0.183138	0.847448	0.145040
50.0	0.838058	0.151337	0.838343	0.107005
60.0	0.828910	0.106392	0.829212	0.059951
70.0	0.819710	0.053832	0.820030	0.005824
80.0	0.810434	0.004808	0.810775	0.055134
MRE		0.118992		0.091269
R^2		0.926624		0.921175
Temperature (°C)	2.08 wt%		4.85 wt%	
	Density (g/cm^3)	Relative error (%)	Density (g/cm^3)	Relative error (%)
30.0	0.860622	0.137834	0.867083	0.218343
40.0	0.851729	0.069334	0.858481	0.131817
50.0	0.842853	0.013942	0.849925	0.020842
60.0	0.833974	0.065092	0.841394	0.099136
70.0	0.825067	0.151401	0.832870	0.225458
80.0	0.816113	0.246986	0.824331	0.362197
MRE		0.114098		0.176299
R^2		0.871855		0.805022

Source: The Author (2017)

4.6 BOILING POINT ELEVATION OF CRUDE OIL

In order to check the reliability of the boiling point elevation measurement apparatus, the vapor pressure of pure toluene was measured. The mean relative error (MRE) between the experimental data and those published in literature (NIST) was of 2.40 %. These results are presented in TABLE 20 and confirm that the apparatus is reliable and applicable for experimental measurements. This experiment was repeated using water, presenting a MRE of 3.47 %. All sequences and results are shown as Appendix C.

TABLE 20 – STATISTICAL EVALUATION OF SATURATED VAPOR PRESSURE OF PURE TOLUENE WITH RESPECT TO THOSE PUBLISHED IN LITERATURE (NIST)

Pressure (kPa)	Experimental temperature (°C)	Literature temperature (°C)	Relative error (%)
5.68	37.7	37.43	0.72
13.50	54.7	50.49	8.33
23.86	68.0	64.76	5.01
43.71	84.0	84.15	0.17
64.17	95.8	96.22	0.44
79.27	102.8	102.13	0.66
91.00	107.6	106.04	1.47
MRE			2.40

Source: The Author (2017)

Crude oil was diluted in different concentrations with toluene: 8.0 wt%, 11 wt%, 50 wt% and 70 wt%. PC-SAFT parameters for toluene and asphaltenes were the same fitted in Section 4.3 and 4.5, respectively. PC-SAFT parameters for saturates and (aromatics+resins) were adjusted using two different strategies, resumed in TABLE 21: (1) using PC-SAFT parameters and molecular weight from Tavakkoli *et al.* (2016) and (2) using PC-SAFT parameters calculated by equations presented in TABLE 4, and the molecular weight presented in TABLE 9, provided by Petrobras.

The aromaticity value of saturates is 0.0 and for aromatics+resins it was adjusted to 0.70, as suggested by Tavakkoli *et al.* (2016) after they compared experimental and modeling results for densities of crude oil. Aromaticity value of asphaltene was adjusted to 0.35 as previously justified in Section 4.5.

The binary interaction parameters for the system toluene (1) – crude oil (represented as three pseudo-components: saturates (2), aromatics+resins (3) and asphaltenes (4)) were analyzed in order to get the best match for boiling point elevation, comparing PC-SAFT modeling results with experimental data, except for toluene-asphaltene as defined before (k_{14} = 0.032). FIGURE 29(a) presents a diagram based on strategy 1 and FIGURE 29(b) the modeling results from strategy 2.

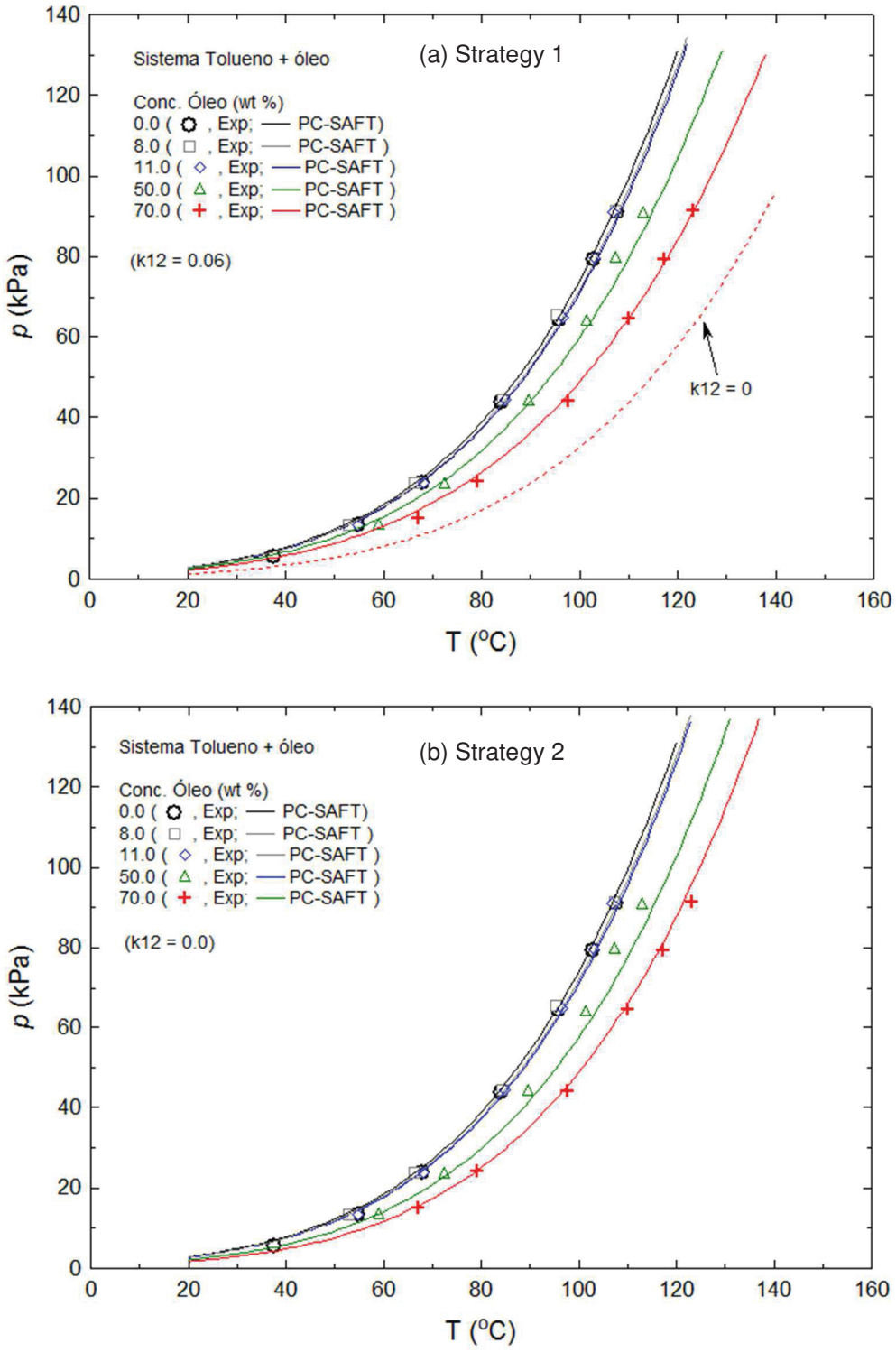

FIGURE 29 – COMPARISON OF PC-SAFT PREDICTED PRESSURE-TEMPERATURE DIAGRAM VERSUS EXPERIMENTAL DATA FOR CRUDE OIL DILUTED WITH TOLUENE (1) AT DIFFERENT CONCENTRATION AND AT AMBIENT PRESSURE. CRUDE OIL REPRESENTED BY (2) SATURATES, (3) AROMATICS + RESINS AND (4) ASPHALTENES. PC-SAFT PARAMETERS AND MOLECULAR WEIGHT (a: STRATEGY 1) FROM TAVAKKOLI *et al.* (2016) AND (b: STRATEGY 2) CALCULATE USING PETROBRAS ANALYSIS (TABLE **9**)
Source: The Author (2017)

TABLE 21 – PC-SAFT PARAMETER FOR SATURATES AND AROMATICS + RESINS WITH PC-SAFT PARAMETERS AND MOLECULAR WEIGHT (STRATEGY 1) FROM TAVAKKOLI *et al.* (2016) AND (STRATEGY 2) CALCULATE USING PETROBRAS ANALYSIS (TABLE 9)

	Component	γ	Mw (g/mol)	m	σ (A)	ε/k (K)
Strategy 1[a]	Saturates	0.0	166.05	5.1100	3.8992	249.52
	A + R	0.7	196.85	4.1400	4.0808	381.70
Strategy 2[b]	Saturates	0.0	117.00	3.8513	3.8516	243,59
	A + R	0.7	188.58	4.2513	4.0571	367.69

Source: Tavakkoli et al. (2016)[a] and The Author (2017)[b]

Both strategies furnish good predictions of pressure-temperature diagram. For a better match with experimental results by strategy 1, it is necessary to adjust the k_{ij} value for toluene-saturates ($k_{12} = 0.060$). On the other hand, strategy 2 predicts the vapor-liquid behavior of toluene-crude oil mixture without having to adjust any other binary parameter. Therefore, strategy 2 was chosen to calculate the precipitation of asphaltenes from crude oil, as will be discussed in Section 4.8.

4.7 ASPHALTENE PRECIPITATION FROM MODEL OIL

Asphaltene extracted from crude oil using the methodology presented in Section 3.1.3 was dissolved in different amounts of toluene forming what was called “Model Oil”. Two n-alkanes were used to precipitate asphaltene from this Model Oil: n-hexane and n-heptane. TABLE 22 presents the percentage of asphaltene precipitated at different mass fractions of added n-alkane at ambient condition.

As widely explored in literature (Tavakkoli *et al.*, 2016, 2014; Sabeti *et al.*, 2015, Mohamed *et al.*, 1999), the amount of precipitated asphaltene should increase with the decrease in the n-alkane carbon chain length. However, FIGURE 30 shows an inverse behavior, as n-C_7 is precipitating more asphaltenes than n-C_6. Nascimento (2016) also observed this behavior using the same Brazilian crude oil.

Possibly, the different behaviors observed are due to the purity of the precipitants used in procedure. N-hexane used is this work has 95% of purity while n-heptane (PA) has a high purity grade.

TABLE 22 – EXPERIMENTAL DATA FOR ASPHALTENE PRECIPITATION OF THE MODEL OIL FROM THE ADDITION OF TWO DIFFERENT SOLVENTS WITH IT

n-hexane		n-heptane	
n-C_6 Mass fraction (asphaltene free basis)	Asphaltene precipitated (%)	n-C_7 Mass fraction (asphaltene free basis)	Asphaltene precipitated (%)
0.0000	0.00	0.0000	0.00
0.2347	0.00	0.2459	0.00
0.3878	0.00	0.3799	14.35
0.4898	0.00	0.5898	54.92
0.5918	17.15	0.6742	62.50
0.6939	38.22	0.7802	77.46
0.7959	57.33	0.8638	86.25
0.8469	74.52	0.9099	82.20
		0.9179	82.60

Source: The Author (2017)

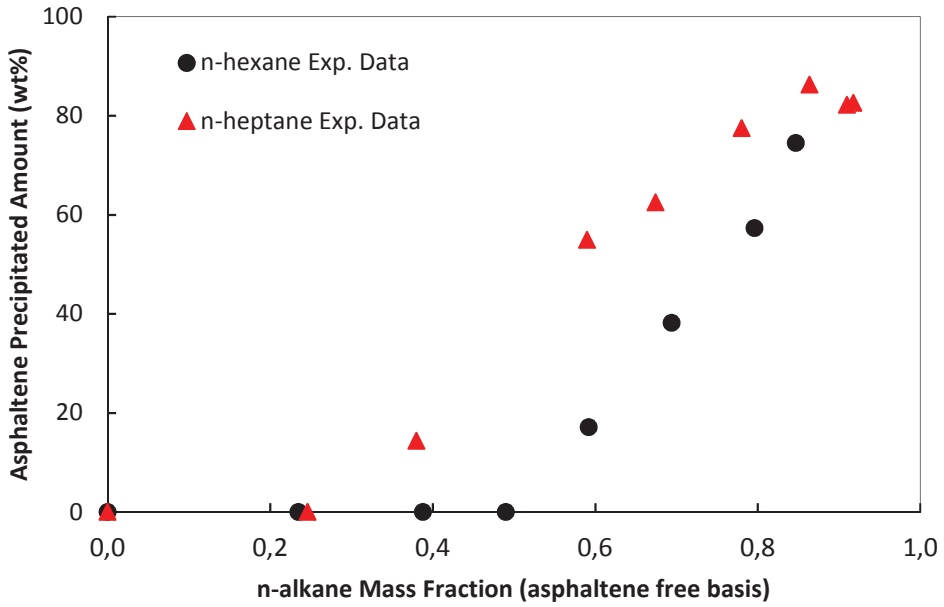

FIGURE 30 – EXPERIMENTAL DATA FOR ASPHALTENE PRECIPITATED AMOUNT OF THE MODEL OIL FROM THE ADDITION OF TWO DIFFERENT SOLVENTS WITH IT
Souce: The Author (2017)

The binary interaction parameters for the systems toluene-n-hexane and toluene-n-heptane are analyzed in order to get the best fit for vapor-liquid equilibrium, comparing PC-SAFT modeling results with literature data (Dechema). FIGURE 31 shows the influence of k_{ij} value for modeling the VLE for the system toluene (1) – n-hexane (2). This relatively simple system is better predicted using $k_{12} = 0.0082$, rather than using $k_{12} = 0.00$. FIGURE 32 shows the k_{ij} value for the system toluene (1) – n-

heptane (2). The prediction presents a better agreement with experimental data using $k_{12} = 0.0065$, rather than using $k_{12} = 0.00$.

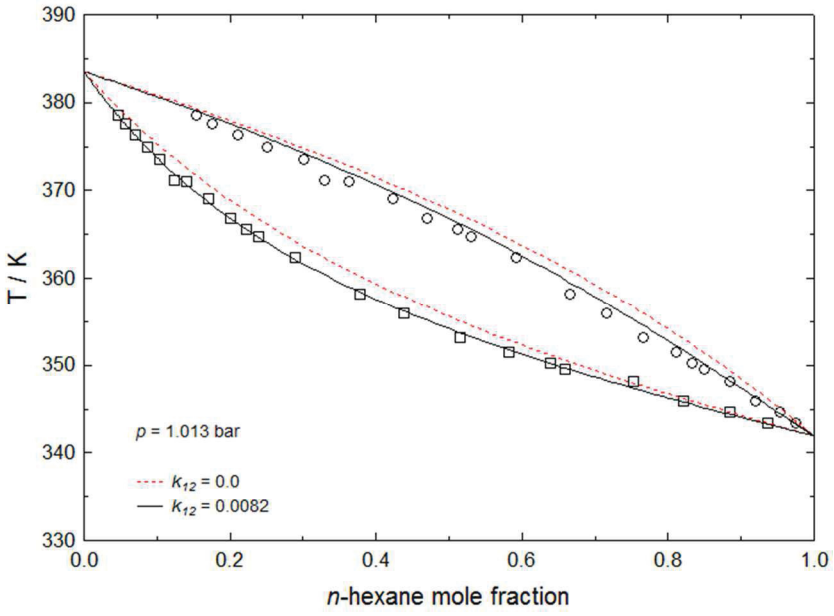

FIGURE 31 – COMPARISON OF PC-SAFT PREDICTED VAPOR-LIQUID EQUILIBRA VERSUS LITERATURE DATA (DECHEMA) FOR TOLUENE (1) – n-HEXANE (2) WITH k_{12} = 0.0 (DASHED LINE) AND k_{12} = 0.0082 (CONTINUOUS LINE) AT 1.1013 bar
Source: The Author (2017)

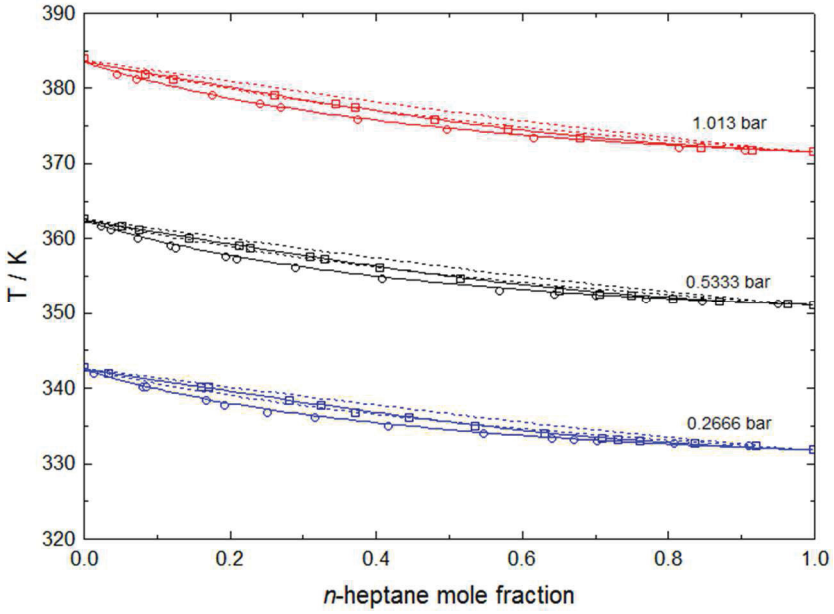

FIGURE 32 – COMPARISON OF PC-SAFT PREDICTED VAPOR-LIQUID EQUILIBRA VERSUS LITERATURE DATA (DECHEMA) FOR TOLUENE (1) – n-HEPTANE (2) WITH k_{12} = 0.0 (DASHED LINE) AND k_{12} = 0.0065 AT 0.2666 bar, 0.533 bar AND 1.1013 bar
Source: The Author (2017)

TABLE 24 provides PC-SAFT parameters for non-associating compounds first presented by Gross and Sadowski (2001). For n-hexane, m = 3.0576, σ = 3.7983 A

and ε/k = 236.40 K. For n-heptane, m = 3.4831, σ = 3.8049 A and ε/k = 238.40 K. Binary interaction parameters for toluene (1) - asphaltene (3) and toluene (1) - n-alkanes (2) have already been discussed. However, the influence of the k_{23} parameter (asphaltene – n-alkane) still remains to be analyzed. Both FIGURE 33 and FIGURE 34 compare modeling results for different k_{23} values in the asphaltene precipitation by addition of n-C_6 and n-C_7, respectively, showing a very good match for both cases.

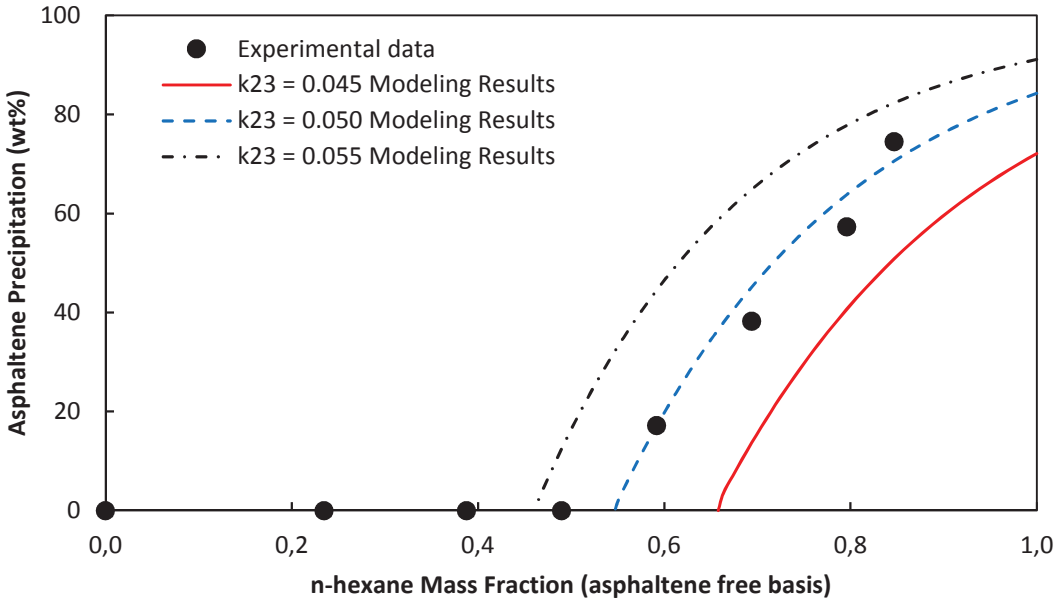

FIGURE 33 – COMPARISON OF PC-SAFT PREDICTED PRECIPITATION CURVE VERSUS EXPERIMENTAL DATA FOR MODEL OIL [TOLUENE (1) + ASPHALTENE (3)] DILUTED WITH N-HEXANE (2). k_{12} = 0.0082 AND k_{13} = 0.032
Source: The Author (2017)

In summary, the best set of PC-SAFT parameters adjusted for asphaltenes, with asphaltene aromatic value of 0.35, are: m = 10.5861, σ = 4.1347 A, ε/k = 337.94 K. The binary interaction parameters used are: n-hexane-toluene (0.0082), n-heptane-toluene (0.0065), asphaltene-toluene (0.032), n-hexane-asphaltene (0.050) and n-heptane-asphaltene (0.055).

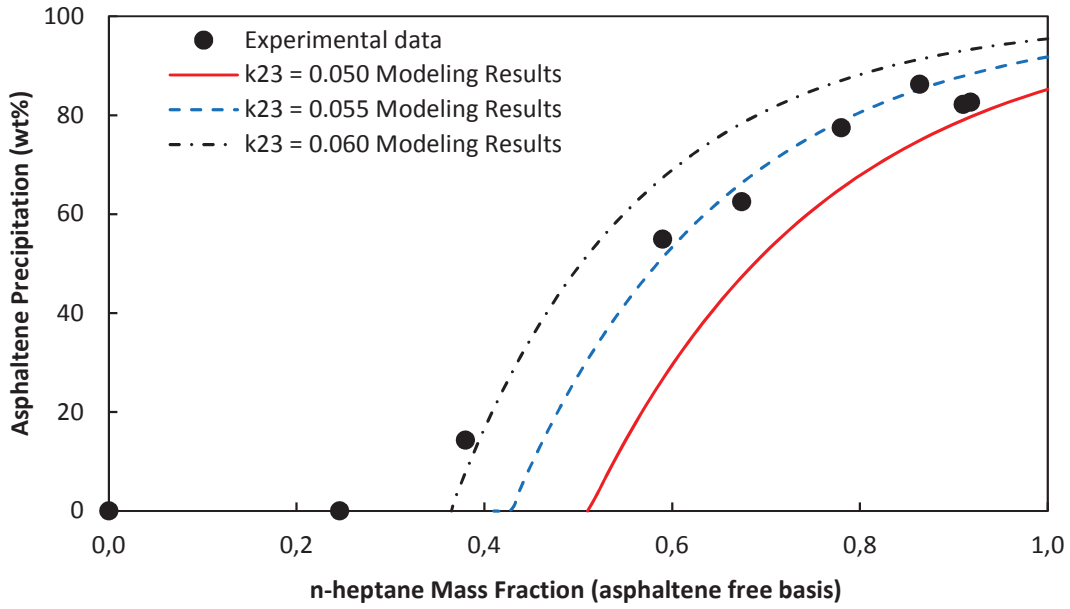

FIGURE 34 – COMPARISON OF PC-SAFT PREDICTED PRECIPITATION CURVE VERSUS EXPERIMENTAL DATA FOR MODEL OIL [TOLUENE (1) + ASPHALTENE (3)] DILUTED WITH N-HEPTANE (2). k_{12} = 0.0065 AND k_{13} = 0.032
Source: The Author (2017)

4.8 ASPHALTENE PRECIPITATION FROM CRUDE OIL

Binary interaction parameters used to model asphaltene precipitation from crude oil by addition of n-hexane and n-heptane are reported in TABLE 10. The k_{ij} values for the binary systems n-hexane-asphaltene (0.050) and n-heptane-asphaltene (0.055) were fixed according to values found in the study of precipitation from model oil, as presented earlier in Section 4.7. The following binary parameters were adjusted in order to obtain the best match with experimental data: n-hexane-saturates (0.200), n-heptane-saturates (0.300), n-hexane-(A+R) (-0.005), n-heptane-(A+R) (-0.005), saturates-A+R (0.000), saturates-asphatenes (0.035) and asphaltenes-(A+R) (0.005). Aromaticity values for saturates, A+R and asphaltenes were already discussed in Section 4.6. TABLE 23 summarizes crude oil components and mass fraction used in this work and their respective model parameters.

FIGURE 35 shows the asphaltene precipitation weight percentage as function of solvent ratio under ambient conditions. It is evident that the carbon number of the n-alkane influences the amount of asphaltene precipitated. The molecular structure of n-alkanes have a strong effect over both the yield and the physicochemical properties of

precipitated asphaltene. It is noticed that as the carbon number increases, the weight percentage of precipitated asphaltene decreases, as previously reported in the literature (Tavakkoli *et al.*, 2016, Sabeti *et al.*, 2015 and Behbahani *et al.*, 2011, Mohamed *et al.*, 1999). For this reason and also due to the fact that n-C_7 is denser and more viscous than n-C_6, which also affects the aggregation rate, it is possible to guarantee that n- C_6 precipitates more asphaltenes than n- C_7. To improve the results and to be able to predict the exact asphaltene onset point, experiments using low solvent ratio should be made, as reported by Zang, Pedrosa and Moorwood (2011).

TABLE 23 – MODELED CRUDE OIL COMPOSITON AND PC-SAFT PARAMETERS

Component	Mw (g/mol)	wt (%) in crude oil	γ	m	σ (A)	ε/k (K)
n-Hexane	86	-	0	3.0576	3.7983	236.77
n-Heptane	100	-	0	3.4831	3.8049	238.40
Toluene	92	-	0	2.7616	3.7316	289.22
Saturates	117	61.8	0	3.8513	3.8516	243.59
A + R	188	35.7	0.70	4.2513	4.0571	367.69
Asphaltenes	466	2.5	0.35	10.5861	4.1347	337.94

Source: The Author (2017)

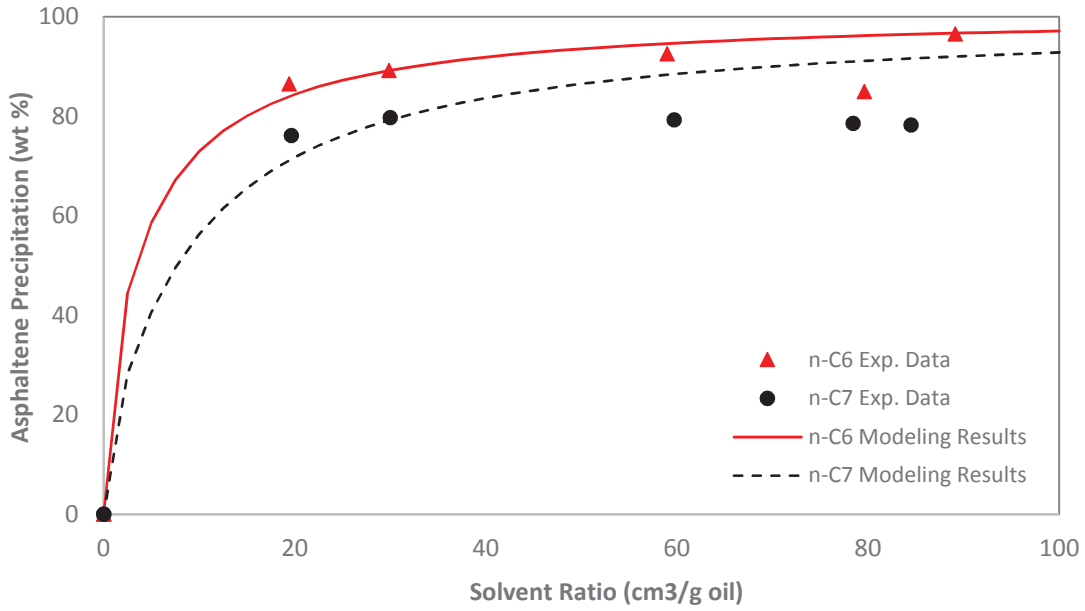

FIGURE 35 – COMPARISON OF PC-SAFT PREDICTED PRECIPITATION CURVE VERSUS EXPERIMENTAL DATA FOR CRUDE OIL DILUTED WITH N-HEXANE AND N-HEPTANE.
Source: The Author (2017)

FIGURE 35 exhibits the good agreement between experimental results and PC-SAFT modeling. Comparing the amount of precipitated asphaltene calculated by PC-SAFT model with experimental results, mean relative errors of 3.75 % and 10.25 % are obtained for n-hexane and n-heptane solvents, respectively, as presented in TABLE 24. Ignoring the association term of PC-SAFT can be the motive of such errors. The modeling results show a better agreement for the n-C_6 experimental data, when compared to the heavier n-alkane. Tavakkoli *et al.* (2016) observed the same difference and justified it by the higher aggregation rate between precipitated asphaltenes when lighter n-alkanes were used.

TABLE 24 – EXPERIMENTAL DATA FOR ASPHALTENE PRECIPITATION OF THE CRUDE OIL FROM THE ADDITION OF TWO DIFFERENT SOLVENTS WITH IT

n-hexane			
Solvent ratio (n-C_6 cm^3/g of oil)	wt% Asph. precipitated (Exp. Data)	wt% Asph. precipitated (Modeling Results)	Relative error (%)
19.42	0.8649	0.8396	2.92
29.85	0.8918	0.8918	0.01
58.97	0.9254	0.9463	2.26
79.60	0.8491	0.9621	13.31
89.11	0.9650	0.9674	0.25
MRE			3.75
n-heptane			
Solvent ratio (n-C_7 cm^3/g of oil)	wt% Asph. precipitated (Exp. Data)	wt% Asph. precipitated (Modeling Results)	Relative error (%)
19.66	0.7610	0.7140	6.17
30.00	0.7970	0.7927	0.54
59.70	0.7928	0.8848	11.60
78.43	0.7855	0.9101	15.86
84.51	0.7825	0.9161	17.07
MRE			10.25

Source: The Author (2017)

León *et al.* (2000) determined the stability of different crude oils by means of the flocculation points and concluded that a crude oil becomes more stable when more n-alkane is added to begin the precipitation. In this regard FIGURE 36 allows to reach the conclusion that Brazilian asphaltenes are almost as stable as the asphaltenes from Middle East, studied by Tavakkoli *et al.* (2016) even if there is a big difference between the molecular weight of these asphaltenes. Molecular weight of Brazilian asphaltenes is 466 g/mol while of those from Middle East is 2300 g/mol. This result raises doubts

about the influence of the molecular weight of the asphaltenes on the precipitation of these compounds.

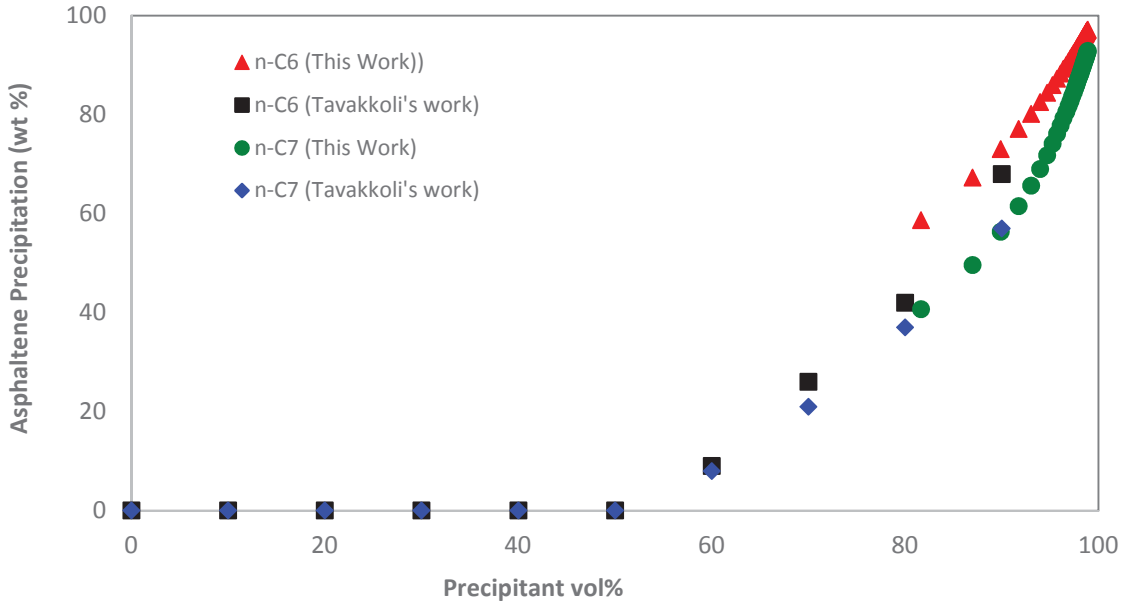

FIGURE 36 – COMPARISON OF EXPERIMENTAL DATA FOR ASPHALTENE PRECIPITATION FROM THIS WORK (Mw_{asph} = 466 g/mol) VERSUS FROM TAVAKKOLI et al. (2016) (Mw_{asph} = 2300 g/mol)

5 CONCLUSIONS

In this work, PC-SAFT algorithms were presented in details. First of all, temperature-density diagram of pure toluene were experimentally obtained in order to check the applicability of PC-SAFT equation of state to model liquid densities. The average relative error for sub-cooled liquid density was 0.17 %. The average relative error interval for asphaltene density ranges from 0.09 % to 0.18 %, and the pseudo-experimental asphaltene density obtained at 50 °C is 1.08 g/cm^3.

Boiling point elevation apparatus was validated collecting toluene experimental data and showed good agreement with vapor-liquid equilibrium data from literature. Modeling results for crude oil boiling point elevation were similar to experimental data.

Asphaltenes were extracted from Brazilian crude oil based on solubility theory using n-C_6 and n-C_7 as precipitants and, as expected, the amount of asphaltene precipitated by the addition of n-C_6 was higher. The system were considered in a liquid-liquid state were one phase consists of asphaltenes while saturates and (resins+aromatics) constitutes another. Furthermore, mean relative errors of 3.75 % and 10.25 % are obtained for n-C_6 and n-C_7 solvents, respectively.

5.1 PROPOSED FUTURE WORKS

SARA characterization is one of the most important inputs for PC-SAFT modeling procedure. Different techniques from different laboratories can result in large differences. Therefore, it would be interesting if this analysis were redone, confirming the results provide by Petrobras.

Although the association term of PC-SAFT has been neglected for the most researchers in the study of asphaltene precipitation to reduce the number of adjustable parameters, this influence could be analyzed for Brazilian asphaltenes using the CPA modeling for example.

There are few studies related to precipitation and deposition of asphaltenes from Brazilian crude oil. In addition, the use of SAFT and its variants for this purpose is recent and there are still a number of analyzes to be done using Brazilian asphaltenes,

for example: influence of both temperature and pressure in asphaltene precipitation, effect of gas injection on asphaltene stability and effect of polydispersity on asphaltene phase behavior. In addition, the influence of the molecular weight on precipitation of asphaltenes is still questionable and should be further investigated.

So far, it was study the amount of precipitated asphaltene. However, asphaltene deposition does not necessarily occurs when they precipitate. Since the asphaltene deposition influences both the properties of the precipitate and the fluid flow in the production process, there should be further research concerning to this matter.

6 REFERENCES

AGÊNCIA NACIONAL DO PETRÓELO (ANP). **Notas à imprensa 2016**, em: <http://www.anp.gov.br/?pg=80729&m=%F3leo%20pesado&t1=&t2=%F3leo%20pesado&t3=&t4=&ar=0&ps=1&1462930107160>. Acesso: 10 mai. 2016.

AKBARZADEH, K.; DHILLON, A.; SVRCEK, W. Y.; YARRANTON, H. W. Methodology for the Characterization and Modeling of Asphaltene Precipitation from Heavy Oils Diluted with n-Alkanes. **Energy & Fuels**, v. 18, p. 1434-1441, 2004.

ALHAMMADI, A. A.; VARGAS, F. M.; CHAPMAN, W. G. Comparison of Cubic-Plus-Association and Perturbed-Chain Statistical Associating Fluid Theory Methods for Modeling Asphaltene Phase Behavior and Pressure-Volume-Temperature Properties. **Energy & Fuels**, v. 29, p. 2864-2875, 2015

ANTAN-PAAR. Available in: < http://www.anton-paar.com>. Access in: April 22th, 2017.

ASSAREH, M.; GHHOTBI, C.; TAVAKKOLI, M.; BASHIRI, G. PC-SAFT Modeling of Petroleum Reservoir Fluid Phase Behavior Using New Correlations for Petroleum Cut and Plus Fractions. **Fluid Phase Equilibria**, v. 408, p. 273-283, 2016.

BARKER, J. A.; HENDERSON, D. Perturbation Theory and Equation of State for Fluids: The Square-Well Potential **J. Chem. Phys**, v. 47, p. 2856-2861, 1967.

BARRERA, D. M.; ORTIZ, D. P.; YARRANTON, H. W. Molecular Weight and Density Distributions of Asphaltenes from Crude Oils. **Energy & Fuels**, v. 27, p. 2474-2487, 2013.

BEHBAHANI, T. J.; GHOTBI, C.; TAGHIKHANI, V.; SHAHRABADI, A. Experimental Investigation and Thermodynamic Modeling of Asphaltene Precipitation. **Scientia Iranica**, v. 18, n. 6, p. 1384-1390, 2011.

CALDAS, J. N. **Estudo Experimental e Modelagem Termodinâmica da Floculação dos Asfaltenos.** Thesis (Doctor Degree in Chemical Engineering) - COPPE, Federal University of Rio de Janeiro, Rio de Janeiro, 1997.

CARDOSO, F. M. R.; CARRIER, H.; DARIDON, J. –L.; PAULY, J.; ROSA, P. T. V. CO2 and Temperature Effects on the Asphaltene Phase Envelope as Determined by a Quartz Crystal Resonator. **Energy & Fuels**, v. 28, n. 11, p. 6780-6787, 2014.

CASIMIRO, M. H.; LEAL, J. P.; GIL, M. H.; CASTRO, C. A. N. de. Análise Calorimétrica aplicada a Polímeros Biológicos - Parte I: Fundamentos Teóricos. **Boletim da Sociedade Portuguesa de Química**, série II, n. 98, p 29-36, 2005.

CHAPMAN, W. G.; JACKSON, G.; GUBBINS, K. E. Phase Equilibria of Associating Fluids: Chain Molecules with Multiple Bonding Sites. **Mol. Phys.**, v. 65, n. 5, p.1057-1079, 1988.

CHAPMAN, W. G.; GUBBINS, K. E.; JACKSON, G.; RADOSZ, M. SAFT: Equation-of-state Solution Model for Associating Fluids. **Fluid Phase Equilibria**, v. 52, p. 31-38, 1989.

CHAPMAN, W. G.; GUBBINS, K. E.; JACKSON, G.; RADOSZ, M. New Reference Equation of State for Associating Liquids. **Ind. Eng. Chem. Res.**, v. 29, n. 8, p. 1709-1721, 1990.

CHEN, Y.; MUTELET, F.; JOUBERT, J. Modeling the Solubility of Carbon Dioxide in Imidazolium-Based Ionic Liquids with the PC-SAFT Equation of State. **J. Phys. Chem. B**, v. 116, p. 14375-14388, 2012.

CHRISMAN, E.; LIMA, V.; MENECHINI, P. Asphaltenes - Problems and Solutions in E&P of Brazilian Crude Oils. In: ABDEL-RAOUF, M. El-S. **Crude Oil Emulsions - Composition Stability and Characterization**, Croatia: InTech, 2012. p. 3-26.

CORAZZA, M. L.; FILHO, L. C.; OLIVEIRA, J. V.; DARIVA, C. A robust strategy for SVL equilibrium calculation at high pressures. **Fluid Phase Equilibria**, v. 221, p. 113-126, 2004.

CZARNECKI, J. Proceedings of the 10th International Conference on Petroleum Phase Behavior and Fouling; Rio de Janeiro, Brazil, June 14-18, 2009.

DEO, M.D. Examination of Asphaltene Precipitation and Self-Aggregation. In: Proceedings of the 2002 Heavy Oil Deposition Conference, Puerto Vallarta, Mexico, Nov 17-21; C. Lira-Galeana, Ed. 2002.

DOLEZALEK, F. Zur Theorie der Binaren Gemische und Konzentrierten Loungen, **Z. Phys. Chem.**, v. 64, p. 727-747, 1908.

EBRAHIMI, M.; MOUSAVI-DEHGHANI, S. A.; DABIR, B.; SHAHRABADI, A. The Effect of Aromatic Solvents on the Onset and Amount of Asphaltene Precipitation at Reservoir Conditions: Experimental and Modeling Studies. **Journal of Molecular Liquids**, v. 223, p. 119-127, 2016.

FERRARI, J. C.; NAGATANI, G.; CORAZZA, F. C.; OLIVEIRA, J. V.; CORAZZA, M. L. Application of Stochastic Algorithms for Parameter Estimation in the Liquid-Liquid Phase Equilibrium Modeling. **Fluid Phase Equilibria**, v. 280, p. 110-119, 2009.

FOSSEN, M. **Aggregation, Interfacial Properties and Structural Characteristics of Asphaltene Solubility Fractions**. Thesis (Doctor Degree in Chemical Engineering) - Norwegian University of Science Technology, Trondheim, 2007.

FU, Y.-H.; SANDLER, S. I. A Simplified SAFT Equation of State for Associating Compounds and Mixtures. **Ind. Eng. Chem. Res.**, v. 34, p. 1897-1909, 1995.

GHOLAMI, A.; MORADI, S.; ASOODEH, M.; BAGHERIPOUR, P.; VAEZZADEH-ASADI, M. Asphaltene precipitation modeling through ACE reaping of scaling equations. **Science China Chemistry**, v. 57, n. 12, p. 1774-1780, 2014.

GIL-VILLEGAS, A.; GALINDO, A.; WHITEHEAD, P. J.; MILLS, S. J.; JACKSON, G.; BURGESS, A. N. Statistical Associating Fluid Theory for Chain Molecules with Attractive Potentials of Variable Range. **J. Chem. Phys.**,v. 106, p. 4168-4186, 1997.

GHONASGI, D.; CHAPMAN, W. G. Theory and Simulation for Associating Fluids with Four Bonding Sites. **Molecular Physics**, v. 79, p. 291-311, 1993.

GONZALEZ, D. L.; TING, P. D.; HIRASAKI, G. J.; CHAPMAN, W. G. Precipitation of Asphaltene Instability under Gas Injection with the PC-SAFT Equation of State. **Energy & Fuels**, v. 19, p. 1230-1234, 2005.

GONZÁLEZ, G.; SOUSA, M. A.; LUCAS, E. F. Asphaltenes Precipitation from Crude Oil and Hydrocarbon Media. **Energy & Fuels**, v. 20, p. 2544-2551, 2006.

GROSS, J.; SADOWSKI, G. Application of Perturbation Theory to a Hard-Chain Reference Fluid: an Equation of State for Square-Well Chains. **Fluid Phase Equilibria**, v. 168, p. 183-199, 2000.

GROSS, J.; SADOWSKI, G. Perturbed-Chain SAFT: An Equation of State Based on a Perturbation Theory for Chain Molecules. **Industrial & Engineering Chemistry Research**, v. 40, p.1244-1260, 2001.

GROSS, J.; SADOWSKI, G. Modeling Polymer Systems Using the Perturbed-Chain Statistical Associating Fluid Theory Equation of State. **Industrial & Engineering Chemistry Research**, v. 41, p.1084-1093, 2002a.

GROSS, J.; SADOWSKI, G. Application of the Perturbed-Chain SAFT Equation of State to Associating Systems. **Industrial & Engineering Chemistry Research**, v. 41, p. 5510-5515, 2002b.

HAMMAMI, A.; RATULOWSKI, J. Precipitation and Deposition of Asphaltenes in Production Systems: A Flow Assurance Overview. In: MULLINS, O. C.; SHEU, E. Y.; HAMMAMI, A.; MARSHALL, A. G. **Asphaltenes, Heavy Oils, and Petroleomics**. New York: Springer, p. 617-660, 2007.

HANNISDAL, A.; HEMMINGSEN, P. V.; SJÖBLOM, J. Group-Type Analysis of Heavy Crude Oils Using Vibrational Spectroscopy in Combination with Mutivariate Analysis. **Ind. Eng. Chem. Res.,** v. 44, p. 1349-1357, 2005.

HOERNING, A.; RIBEIRO, F. R. G.; FILHO, L. C.; LUCIANO, M. L.; CORAZZA, M. L.; VOLL, F. A. P. Boiling Point Elevation of Aqueous Solution of Ionic Liquid from Diethanolamine Base and Carboxylic Acids. J**. Chem. Thermodynamics**, v. 98, p. 1-8, 2016.

HOLAVKO, M. F.; KALYUZHNYI, Y. V. On the Effects of Association in the Statistical Theory of Ionic Systems. Analytic Solution of the PY-MSA version of the Wertheim Theory, **Molecular Physics**, v. 73, n. 5, p. 1145-1157, 1991.

HUANG, S. H.; RADOSZ, M. Equation of State for Small, Large, Polydisperse and Associating Molecules. **Ind. Eng. Chem. Res.,** v. 29, n. 11, p. 2284-2294, 1990.

HUANG, S. H.; RADOSZ, M. Equation of State for Small, Large, Polydisperse and Associating Molecules: Extension to Fluid Mixtures. **Ind. Eng. Chem. Res.,** v. 30, n. 8, p. 1994-2005, 1991.

JOSLIN, C. G.; GRAY, C. G.; CHAPMAN, W. G.; GUBBINS, K. E. Theory and Simulation of Associating Liquid Mixtures: Part II. **Molecular Physics**, v. 62, p. 843-860, 1987.

KAMINSKI, T. J.; FOGLER, H. S.; WOLF, N.; WATTANA, P.; MAIRAL, A. Classification of Asphaltenes via Fractionation and the Effect of Heteroatom Content on Dissolution Kinetics. **Energy & Fuels**, v. 14, p. 25-30, 2000.

KARAKATSANI, E. K.; SPYRIOUNI, T.; ECONOMOU, I. G. Extended Statistical Associating Fluid Theory (SAFT) Equation of State for Dipolar Fluids, **AIChE J.**, v. 51, p. 2328-2342, 2005.

KAZEEM, A. L.; CRAWSHAW, J. P.; BOEK, E. S.; VESOVIC, V. Experimental Investigation of Asphaltene Deposition in Capillary Flow. **Energy & Fuels**, v. 26, p. 2145-2153, 2012.

KLEIBER, M. **Process Engineering: Addressing the Gap between Studies and Chemical Industry**. Berlin: De Gruyter, 2016.

KONTOGEORGIS, G. M.; VOUTSAS E. C. An Equation of State for Associating Fluids. **Ind. Eng. Chem. Res**., v. 35, p. 4310-4318, 1996.

KORD, S.; MIRI, R.; AYATOLLAHI, S.; ESCROCHI, M. Asphaltene Deposition in Carbonate Rocks: Experimental Investigation and Numerical Simulation. **Energy & Fuels**, v. 26, p. 6186-6199, 2012.

KOUSKOUMVEKAKI, I. A.; von SOLMS, N.; LINDVIG, T. MICHELSEN, M. L.; KONTOGEORGIS, G. M. Novel Method for Estimating Pure-Component Parameters for Polymers: Application to the PC-SAFT Equation of State. **Ind. Eng. Chem. Res**., v. 43, p. 2830-2838, 2004.

KRASKA, T.; GUBBINS, K. E. Phase Equilibria Calculations with a Modified SAFT Equation of State. 1. Pure Alkanes, Alkanols and Water. **Ind. Eng. Chem. Res**., v. 35, n. 12, p. 4727-4737, 1996a.

KRASKA, T.; GUBBINS, K. E. Phase Equilibria Calculations with a Modified SAFT Equation of State. 2. Binary Mixtures of n-Alkanes, 1-Alkanols and Water. **Ind. Eng. Chem. Res**., v. 35, n. 12, p. 4738-4746, 1996b.
LAWAL, K. A.; CRAWSHAW, J. P.; BOEK, E. S.; VESOVIC, V. Experimental Investigation of Asphaltene Deposition in Capillary Flow. **Energy & Fuels**, v. 26, n. 4, p. 2145-2153, 2012.

LEON, O.; ROGEL, E.; ESPIDEL, J. Asphaltenes: Structural Characterization, Self Association and Stability Behavior. **Energy & Fuels**, v. 14, p. 6-10, 2000.

LI, Z.; FIROOZABADI, A. Cubic-Plus Association Equation of State for Water-Containing Mixtures: Is “Cross Association”Necessary? **AIChE Journal**, v. 55, n. 7, p. 1803-1813, 2009.

LOUREIRO, T. S.; PALERMO, L. C. M.; SPINELLI, L. S. Influence of Precipitation Conditions (n-Heptane or Carbon Dioxide Gas) on the Performance of Asphaltene Stabilizers. **Journal of Petroleum Science and Engineering**, v. 127, p. 109-114, 2015.

MALVERN. **Calorimetria de titulação isotérmica**, em: <http://www.malvern.com/br/products/technology/isothermal-titration-calorimetry/>. Acesso: 13 mai. 2016.

McQUARRIE, D. A. Statistical Mechanics, Harper Collins, New York (1976).

MELO, F. A. de**. Interações moleculares no mecanismo de ação de clorocatecol 1,2-dioxigenase e da tirosina quinase FGFR2.** Thesis (Doctor Degree in Science)- Instituto de física de São Carlos, Universidade de São Paulo, São Carlos, 2010.

MERINO-GARCIA, D. **Calorimetric investigations of asphaltene self-association and interaction with resins**. Thesis (Doctor Degree in Chemical Engineering) - Center for Phase Equilibria and Separation Processes, Technical University of Denmark, Copenhague, 2004.

MERINO-GARCIA, D.; ANDERSEN, S. I. Isothermal Titration Calorimetry and Fluorescence Spectroscopy Study of Asphaltene Self-Association in Toluene and Interaction with a Model Resin. **Petroleum Science and Technology**, v. 21, p. 507-525, 2003.

MERINO-GARCIA, D.; ANDERSEN, S. I. Thermodynamic Characterization of Asphaltene-Resin Interaction by Microcalorimetry. **Langmuir**, v. 20, p. 4559-4565, 2004.

MERINO-GARCIA, D.; ANDERSEN, S. I. Application of Isothermal Titration Calorimetry in the Investigation of Asphaltene Association. . In: MULLINS, O. C.; SHEU, E. Y.; HAMMAMI, A.; MARSHALL, A. G. **Asphaltenes, Heavy Oils, and Petroleomics**. New York: Springer, p. 329-352, 2007.

MICHELSEN, M. L. Saturation Point Calculations. **Fluid Phase Equilibria**, v. 23, p. 181-192, 1985.

MICHELSEN, M. L.; HENDRICKS, E. Physical Properties from Associating Models, **Fluid Phase Equilibria**, v. 180, p. 165-174, 2001.

MITRA-KIRTLEY, S.; MULLINS, O. C. Sulfur Chemical Moieties in Carbonaceous Materials. In: MULLINS, O. C.; SHEU, E. Y.; HAMMAMI, A.; MARSHALL, A. G. **Asphaltenes, Heavy Oils, and Petroleomics**. New York: Springer, 2007. p. 157-188.

MOHAMED, R. S.; RAMOS, A. C. S. Aggregation Behavior of Two Asphaltenic Fractions in Aromatic Solvent. **Energy & Fuels**, v. 13, p. 323-327, 1999.

MORITIS, G. Flow Assurance Challenges Production from Deeper Water. **Oil & Gas Journal**, v. 99, p. 66-67, 2001.

MULLER, E. A.; GUBBINS, K. E. Molecular-Based Equations of State for Associating Fluids: A Review of SAFT and Related Approaches. **Ind. Eng. Chem. Res.**, v. 40, n. 10, p. 2193-2211, 2001

MULLINS, O. C. Petroleomics and Structure-Function Relations of Crude Oils and Asphaltene. In: MULLINS, O. C.; SHEU, E. Y.; HAMMAMI, A.; MARSHALL, A. G. **Asphaltenes, Heavy Oils, and Petroleomics**. New York: Springer, 2007. p. 1-16.

MULLINS, O. C; SABBAH, H.; EYSSAUTIER, J.; POMERANTZ, A. E.; BARRE, L.; ANDREWS, A. B. *et al*. Advances in asphaltene science and the Yen-Mullins model. **Energy & Fuels**, v. 26, n. 5, p. 3986-4003, 2012.

NASCIMENTO, P. T. H.; SANTOS, A. F.; YAMAMOTO, C. I.; TOSE, L. V.; BARROS, E. V.; GONÇALVES, G. R.; FREITAS, J. C. C.; VAZ, B. G., ROMÃO W.; SCHEER, A. P. Fractionation of Asphaltene by Adsorption onto Silica and Cemical Characterization by Atmospheric Pressure Mass Spectrometry, Fourier Transform Infrared Spectroscopy Coupled to Attenuated Total Reflectance and Proton Nuclear Magnetic Resonance. **Energy & Fuels**, v. 30, p. 5439-5448, 2016b.

NASCIMENTO, P. T. H. **Estudo do Fracionamento de Asfaltenos por Adsorção em Partículas de Sílica**. Thesis (Master Degree in Chemical Engineering) – Technology Sector, Federal University of Paraná, Curitiba, 2016.

NEVES, G. B. M.; SOUSA, M. A.; TRAVALLONI-LOUVISSE, A. M.; LUCAS, E. F. GONZÁLEZ, G. Characterization of Asphaltene Particles by Light Scattering and Electrophoresis. **Petroleum Science and Technology**, v. 19:1-2, p. 35-43, 2001.

NELLENSTEYN, F. The constitution of asphalt. **J. Inst. Pet. Technol.**, v. 10, p. 311-325, 1924.

NGHIEM, L. X.; COOMBE, D. A. Modeling Asphaltene Precipitation During Primary Depletion. **SPE Journal**, v. 2, p. 170-176, 1997.

PADUSZYNSKI, K.; DOMANSKA, U. Thermodynamic Modeling of Ionic Liquid Systems: Development and Detailed Overview of Novel Methodology Based on the PC-SAFT. **J. Phys. Chem. B**, v. 116, p. 5002-5018, 2012.

PANUGANTI S. R.; VARGAS, F. M.; GOZALEZ, D. L.; KURUP, A.S.; CHAPMAN, W. G. PC-SAFT Characterization of Crude Oils and Modeling of Asphaltene Phase Behavior. **Fuel**, v. 93, p. 658-669, 2012.

PFEIFFER, J. P.; SAAL, R. N. J. Asphaltic Bitume as Colloid System. **J. Phys. Chem.**, v. 44, n. 2, p. 139-149, 1940.

PUNNAPALA, S.; VARGAS, F. M. Revisiting the PC-SAFT Characterization Procedure for an Improved Asphaltene Precipitation Prediction. **Fuel**, v. 108, p. 417-429, 2013.

Organization of the Petroleum Exporting Countries (OPEC), **Monthly Oil Market Report**, em: <http://www.opec.org/opec_web/static_files_project/media/downloads/publications/MOMR%20April%202016.pdf>. Acesso: 10 mai. 2016.

OPEDAL, N. T. **NMR as a tool to follow destabilization of water-in-oil emulsions.** Thesis (Doctor Degree in Science) – Norwegian University of Science Technology, Trondheim, 2011.

QUINTERO, L. C. N. **Fracionamento e análise de asfaltenos extraídos de petróleo brasileiro**. Thesis (Doctor Degree in Science), Federal University of Rio de Janeiro, Rio de Janeiro, 2009.

ROGEL, E.; CARBOGNANI, L. Density Estimation of Asphaltene Using Molecular Dynamics Simulations. **Energy & Fuels**, v. 17, p. 378-386, 2003.

SAAJANLEHTO, M.; ALOPAEUS, V. Heavy oil characterization method for PC-SAFT. **Fuel**, v. 133, p. 216-223, 2014.

SABETI, M.; RAHIMBAKHSH, A.; NIKOOKAR, M.; MOHAMMADI, A. H. Estimation of asphaltene precipitation and equilibrium properties of hydrocarbon fluid phases using the PC-SAFT equation of state. **Journal of Molecular Liquids**, v. 209, p. 447-460, 2015.

SALAHSHOOR, K.; ZAKERI, S.; MAHDAVI, S.; KHARRAT, R.; KHALIFEH, M. Asphaltene Deposition Prediction Using Adaptive Neuro-Fuzzy Models Based on Laboratory Measurements. **Fluid Phase Equilibria**, v. 337, p. 89-99, 2013.

SANTOS, D.; FILHO, E.; DOURADO, R.; AMARAL, M.; FILIPAKIS, S. D.; OLIVEIRA, L. M. S. L.; GUIMARÃES, R. C. L.; SANTOS, A. F.; BORGES, G. R.; FRANCESCHI, E.; DARIVA, C. Study of Asphaltene Precipitation in Crude Oils at Desalter Conditions by Near-infrared Spectroscopy. **Energy & Fuels**, Just Accepted Manuscript, 19 Apr, 2017.

SEDGHI, M.; GOUAL, L. PC-SAFT Modeling of Asphaltene Phase Behavior in the Presence of Nonionic Dispersants. **Fluid Phase Equilibria**, v. 369, p. 86-94, 2014.

SOUSA, M. A.; OLIVEIRA, G. E.; LUCAS, E. F.; GONZÁLEZ, G. The onset of precipitation of asphaltenes in solvents of different solubility parameters. In: Surface and Colloid Science. Progress in Colloid and Polymer Science, vol 128. Springer, Berlin, 2004.

SPEIGHT, J. G. **The Chemistry and Technology of Petroleum**. 4. ed. Taylor and Francis Group, 2006.

SUBRAMANIAN, S.; SIMON, S.; SJOBLOM, J. Comparison of Asphaltene Fractions Separated by Adsorption and Bulk Precipitation. Study presented at the JIP Asphaltene Meeting, Prague, 2015.

TAVAKKOLI, M.; PANUGANTI, S. R; TAGHIKHANI, V.; PISHVAIE, M. R.; CHAPMAN, W. G. Understanding the polydisperse behavior of asphaltenes during precipitation. **Fuel**, v. 117, p. 206-217, 2014.

TAVAKKOLI, M.; CHEN, A.; VARGAS, F. M. Rethinking the Modeling Approach for Asphaltene Precipitation Using the PC-SAFT Equation of State. **Fluid Phase Equilibria**, v. 416, p. 120-129, 2016.

THIYAGARAJAN, P. Temperature-Dependent Structural Changes of Asphaltenes in 1-Methylnaphthalene. **Energy & Fuels**, v. 9, p. 829-833, 1995.

TING, P. D.; HIRASAKI, G. J.; CHAPMAN, W. G. Modeling of Asphaltene Phase Behavior with the SAFT Equation of State. **Petroleum Science and Technology**, v. 21, n. 3 & 4, p. 647-661, 2003.

TING, P. D.; GONZALEZ, D. L.; HIRASAKI, G. J.; CHAPMAN, W. G. Application of the PC-SAFT Equation of State to Asphaltene Phase Behavior. In: MULLINS, O. C.; SHEU, E. Y.; HAMMAMI, A.; MARSHALL, A. G. **Asphaltenes, Heavy Oils, and Petroleomics**. New York: Springer, 2007. p. 301-327.

VARGAS, F. M.; GONZALEZ, D. L.; HIRASAKI, G. J.; CHAPMAN, W. G. Modeling Asphaltene Phase Behavior in Crude Oil Systems Using the Perturbed Chain Form of the Statistical Associating Fluid Theory (PC-SAFT) Equation of State. **Energy & Fuels**, v. 23, p. 1140-1146, 2009.

VERDIER, S.; CARRIER, H.; ANDERSEN, S. I.; DARIDON, J.-L. Study of Pressure and Temperature Effects on Asphaltene Stability in Presence of CO_2. **Energy & Fuels**, v. 20, p. 1584-1590, 2006.

von SOLMS, N. **Short Course on PC-SAFT**. Internal Report of Center for Phase Equilibria and Separation Processes, Department of Chemical and Biochemical Engineering, Technical University of Denmark, Denmark, 2003.

VON SOLMS, NICOLAS; KOUSKOUMVEKAKI, EIRINI; LINDVIG, THOMAS; MICHELSEN, MICHAEL LOCHT; KONTOGEORGIS, GEORGIOS. **A novel approach to liquid-liquid equilibrium in polymer solutions with application to simplified PC-SAFT. Fluid Phase Equilibria**, v. 222, p. 87-93, 2004.

WEI, D.; ORLANDI, E.; SIMON, S.; SJOBLOM, J.; SUURKUUSK, M. Interactions between asphaltenes and alkylbenzene-derived inhibitors investigated by isothermal titration calorimetry. **Journal of Thermal Analysis and Calorimetry**, v. 120, n. 3, p. 1835-1846, 2015a.

WEI, D.; ORLANDI, E.; BARRIET, M.; SIMON, S.; SJOBLOM, J. Aggregation of tetrameric acid in xylene and its interaction with asphaltenes by isothermal titration calorimetry. **Journal of Thermal Analysis and Calorimetry**, v. 122, n. 1, p. 463-471, 2015b.

WERTHEIM, M. S. Fluids with Highly Directional Attractive Forces. I. Statistical Thermodynamics. **J. Stat. Phys.**, v. 35, n. 1/2, p. 19-34, 1984a.

WERTHEIM, M. S. Fluids with Highly Directional Attractive Forces. II. Thermodynamic Perturbation Theory and Integral Equations. **J. Stat. Phys.**, v. 35, n. 1, p. 35-47, 1984b.

WERTHEIM, M. S. Fluids with Highly Directional Attractive Forces. III. Multiple Attraction Sites. **J. Stat. Phys.**, v. 42, n. 3/4, p. 459-476, 1986a.

WERTHEIM, M. S. Fluids with Highly Directional Attractive Forces. IV. Equilibrium Polymerization. **J. Stat. Phys.**, v. 42, n. 3/4, p. 477-492, 1986b.

ZHANG, X.; PEDROSA, N.; MOORWOOD, T. Modeling Asphaltene Phase Behavior: Comparison of Methods for Flow Assurance Studies. **Energy & Fuels**, v. 26, p. 2611-2620, 2012.

ZUNIGA-HINOJOSA, M. A.; JUSTO-GARCÍA, D. N.; AQUINO-OLIVOS, M. A; ROMÁN-RAMÍREZ, L. A.; GARCÍA-SÁNCHEZ, F. Modeling of Asphaltene Precipitation from n-Alkane Diluted Heavy Oils and Bitumens Using the PC-SAFT Equation of State. **Fluid Phase Equilibria**, v. 376, p. 210-224, 2014.

VARZANDEH, F.; STENBY, E. H.; Yan, W. General Approach to Characterizing Reservoir Fluids for EoS Models Using a Large PVT Database. **Fluid Phase Equilibria**, V. 433, P. 97-111, 2017.

APPENDIX A – SUMMARY OF EQUATIONS FOR CALCULATING DENSITY, PRESSURE, FUGACITY COEFFICIENTS AND CALORIC PROPERTIES

This section provides a summary of equation for calculating thermophysical properties using PC-SAFT.

Density: The total number density of molecules has the following form:

$$\dot{\rho} = \frac{6\zeta_3}{\pi}\left(\sum_i x_i m_i d_i^3\right)^{-1} \tag{A.1}$$

Pressure: The pressure (P) is function of compressibility factor (Z) given by Eq 16 and total number density of molecules ($\dot{\rho}$) given by Eq A.1:

$$P = ZkT\dot{\rho}\left(10^{10}\frac{\dot{A}}{m}\right)^3 \tag{A.2}$$

Helmholtz Free Energy: Back to Helmholtz free energy, the Eq 1 is rewritten for reduced quantities (Eq A.3). Moreover, this equation, as said before, is reduced to hard-chain reference contribution and the dispersive contribution (Eq A.4).

$$\tilde{a}^{res} = \frac{A^{res}}{NkT} \tag{A.3}$$

where N is the total number of molecules, k the Boltzmann constant and T the temperature.

$$\tilde{a}^{res} = \tilde{a}^{hc} + \tilde{a}^{disp} \tag{A.4}$$

Eq A.5 gives the hard-chain contribution:

$$\tilde{a}^{hc} = \bar{m}\tilde{a}^{hs} - \sum_i x_i(m_i - 1)\, ln g_{ii}^{hs}(\sigma_{ii}) \tag{A.5}$$

where the reduced Helmholtz free energy of the hard-sphere fluid ($\tilde{a}^{hs}$) is:

$$\tilde{a}^{hs} = \frac{1}{\zeta_0}\left[\frac{3\zeta_1\zeta_2}{(1-\zeta_3} + \frac{\zeta_2^3}{\zeta_3(1-\zeta_3)^2} + \left(\frac{\zeta_2^3}{\zeta_3^2} - \zeta_0\right)\ln(1-\zeta_3)\right] \quad \text{(A.6)}$$

The dispersive contribution is given by:

$$\tilde{a}^{disp} = -2\pi\rho I_1\overline{m^2\varepsilon\sigma^3} - \pi\rho\bar{m}C_1 I_2\overline{m^2\varepsilon^2\sigma^3} \quad \text{(A.7)}$$

Fugacity Coefficient: As will be explained in the next section, the fugacity of each component *i* in the phase *p* is function of the fugacity coefficient (ϕ_k) that is calculated by Eq A.8. The residual chemical potential (μ_k^{res}) is obtained from Eq A.9.

$$ln\phi_k = \frac{\mu_k^{res}(T,v)}{kT} - \ln Z \quad \text{(A.8)}$$

$$\frac{\mu_k^{res}(T,v)}{kT} = \tilde{a}^{res} + (Z-1) + \left(\frac{\partial\tilde{a}^{res}}{\partial x_k}\right)_{T,v,x_{i\neq k}} - \sum_{j=1}^{N}\left[x_j\left(\frac{\partial\tilde{a}^{res}}{\partial x_j}\right)_{T,y,x_{i\neq j}}\right] \quad \text{(A.9)}$$

The derivatives relative to mole fractions are calculated by the following equations.

$$\left(\frac{\partial\tilde{a}^{hc}}{\partial x_k}\right)_{T,\rho,x_{i\neq k}} = m_k\tilde{a}^{hs} + \bar{m}\left(\frac{\partial\tilde{a}^{hs}}{\partial x_k}\right)_{T,\rho,x_{j\neq k}} - \sum_i x_i(m_i-1)(g_{ii}^{hs})^{-1}\left(\frac{\partial g_{ii}^{hs}}{\partial x_k}\right)_{T,\rho,x_{j\neq k}} \quad \text{(A.10)}$$

$$\left(\frac{\partial \tilde{a}^{hs}}{\partial x_k}\right)_{T,\rho,x_{j\neq k}} = -\frac{\zeta_{0,xk}}{\zeta_0}\tilde{a}^{hs} + \frac{1}{\zeta_0}\left[\frac{3(\zeta_{1,xk}\zeta_2+\zeta_1\zeta_{2,xk})}{(1-\zeta_3)} + \frac{3\zeta_1\zeta_2\zeta_{3,xk}}{(1-\zeta_3)^2} + \frac{3{\zeta_2}^2\zeta_{2,xk}}{\zeta_3(1-\zeta_3)^2} + \frac{{\zeta_2}^3\zeta_{3,xk}(3\zeta_3-1)}{{\zeta_3}^2(1-\zeta_3)^3} + \left(\frac{3{\zeta_2}^2\zeta_{2,xk}\zeta_3 - 2{\zeta_2}^2\zeta_{3,xk}}{{\zeta_3}^3} - \zeta_{0,xk}\right)\ln(1-\zeta_3) + \left(\zeta_0 - \frac{{\zeta_2}^3}{{\zeta_3}^2}\right)\frac{\zeta_{3,xk}}{(1-\zeta_3)}\right] \tag{A.11}$$

$$\left(\frac{\partial g_{ij}^{hs}}{\partial x_k}\right)_{T,\rho,x_{j\neq k}} = \frac{\zeta_{,xk}}{(1-\zeta_3)^2} + \left(\frac{d_i d_j}{d_i+d_j}\right)\left(\frac{3\zeta_{2,xk}}{(1-\zeta_3)^2} + \frac{6\zeta_2\zeta_{3,xk}}{(1-\zeta_3)^3}\right) + \left(\frac{d_i d_j}{d_i+d_j}\right)^2\left(\frac{4\zeta_2\zeta_{2,xk}}{(1-\zeta_3)^3} + \frac{6{\zeta_2}^2\zeta_{3,xk}}{(1-\zeta_3)^4}\right) \tag{A.12}$$

$$\left(\frac{\partial \tilde{a}^{disp}}{\partial x_k}\right)_{T,\rho,x_{j\neq k}} = -2\pi\rho\left[I_{1,xk}\overline{m^2\varepsilon\sigma^3} + I_1\overline{(m^2\varepsilon\sigma^3)}_{xk}\right] - \pi\rho\left\{\left[m_k C_1 I_2 + \bar{m}C_{1xk}I_2, + \bar{m}C_1 I_{2,xk}\right]\overline{m^2\varepsilon^2\sigma^3} + \bar{m}C_1 I_2\overline{(m^2\varepsilon^2\sigma^3)}_{xk}\right\} \tag{A.13}$$

$$\overline{(m^2\varepsilon\sigma^3)}_{xk} = 2m_k\sum_j x_j m_j\left(\frac{\varepsilon_{kj}}{kT}\right){\sigma_{kj}}^3 \tag{A.14}$$

$$\overline{(m^2\varepsilon^2\sigma^3)}_{xk} = 2m_k\sum_j x_j m_j\left(\frac{\varepsilon_{kj}}{kT}\right)^2{\sigma_{kj}}^3 \tag{A.15}$$

$$C_{1,xk} = C_2\zeta_{3,xk} - {C_1}^2\left\{m_k\frac{8\zeta_3-2{\zeta_3}^2}{(1-\zeta_3)^4} - m_k\frac{20\zeta_3-27{\zeta_3}^2+12{\zeta_3}^3-2{\zeta_3}^4}{[(1-\zeta_3)(2-\zeta_3)]^2}\right\} \tag{A.16}$$

$$I_{1,xk} = \sum_{i=0}^{6}\left[a_i(\bar{m})i\zeta_{3,xk}\zeta_3^{i-1} + a_{i,xk}\zeta_3^i\right] \tag{A.17}$$

$$I_{2,xk} = \sum_{i=0}^{6}\left[b_i(\bar{m})i\zeta_{3,xk}\zeta_3^{i-1} + b_{i,xk}\zeta_3^i\right] \tag{A.18}$$

$$a_{i,xk} = \frac{m_k}{\bar{m}^2} a_{1i} + \frac{m_k}{\bar{m}^2}\left(3 - \frac{4}{\bar{m}}\right) a_{2i} \tag{A.19}$$

$$b_{i,xk} = \frac{m_k}{\bar{m}^2} b_{1i} + \frac{m_k}{\bar{m}^2}\left(3 - \frac{4}{\bar{m}}\right) b_{2i} \tag{A.20}$$

Enthalpy and Entropy: The derivative of Helmholtz free energy with respect to temperature gives the molar enthalpy ($\hat{h}^{res}$):

$$\frac{\hat{h}^{res}}{RT} = -T\left(\frac{\partial \tilde{a}^{res}}{\partial T}\right)_{\rho, X_i} + (Z-1) \tag{A.21}$$

The residual entropy $\hat{s}^{res}(P,T)$ is a function of pressure and temperature and can be written as:

$$\frac{\hat{s}^{res}(P,T)}{R} = -T\left[\left(\frac{\partial \tilde{a}^{res}}{\partial T}\right)_{\rho, X_i} + \frac{\tilde{a}^{res}}{T}\right] + ln(Z) \tag{A.22}$$

The residual molar Gibbs free energy $\hat{g}^{res}(P,T)$ is:

$$\frac{\hat{g}^{res}}{RT} = \frac{\hat{h}^{res}}{RT} - \frac{\hat{s}^{res}(P,T)}{R} \tag{A.23}$$

or else

$$\frac{\hat{g}^{res}}{RT} = \tilde{a}^{res} + (Z-1) - ln(Z) \tag{A.24}$$

APPENDIX B – SATURATION POINT CALCULATIONS

The following method was developed by Michelsen (1984) for the calculation of saturation temperatures or pressures for multicomponent mixtures.

As discussed earlier in section 2.3.3, the condition for phase equilibrium is based on the equality of chemical potentials of components present in the equilibrium phases (Eq 39) or can be determined from the condition of equal fugacity in both phases for all components (Eq 43). Therefore, for a n-component mixture, there are n unknown variables:

$$f_i = \ln y_i + \ln \phi_i(y) - \ln z_i - \ln \phi_i(z) = 0 \quad (i = 1, \dots, nc) \tag{B.1}$$

It is convenient to treat the mole fractions y_i as independent, thus requiring another condition:

$$f_{N+1} = 1 - \sum_i y_i = 0 \tag{B.2}$$

An equivalent equation can be obtained by a linear combination of Eq B.1 and B.2:

$$Q_1 = 1 - \sum_i y_i + \sum_i y_i \{\ln y_i + \ln \phi_i(y) - \ln z_i - \ln \phi_i(z)\} = 0 \tag{B.3}$$

Solving the equations at $P = P_{spec}$ wherein $y = y^*$ and $T = T^*$. An approximation to y^* is $\hat{y}$. Substituting this approximation in Eq B.3 and solving for the corresponding temperature T, an approximate saturation temperature is obtained, which is more accurate than the approximation $\hat{y}$. However, the point (T, P_{spec}) satisfying $Q_1(T, P_{spec}, y) = 0$ can not be located in the sigle-phase region for the mixture of composition z. This implies in negative values for the tangent plane distance and consequently the mixture is unstable.

An alternative form is obtained isolating y_i from Eq B.1 and substituting into Eq B.3:

$$Q_2(y,\ T) = 1 - \sum_i z_i \phi_i(z)/\phi_i(y) \tag{B.4}$$

At the equilibrium point between the phases with composition z and y, the Eq B.1 is satisfied:

$$\frac{z_i \phi_i(T,P,z)}{\phi_i(T,P,y^*)} = Y_i \tag{B.5}$$

Using the Newton-Raphson method to correct T through an iterative calculation, Eq B.4 can be combined by direct substitution with Eq B.5, for revising y values:

$$Y_i^{(k)} = \frac{z_i \phi_i(T,P,z)}{\phi_i(T,P,y^{(k)})} \tag{B.6}$$

$$Q_2^{(k)} = 1 - \sum_i Y_i^{(k)} \tag{B.7}$$

$$T^{(k+1)} = T^{(k)} - Q_2^{(k)} / \frac{\partial}{\partial T}(Q_2^{(k)}) \tag{B.8}$$

$$y_i^{(k+1)} = Y_i / \sum_j Y_j \tag{B.9}$$

where Y is the auxiliary vector, z is the feed composition and y is the equilibrium phase composition and Q is the saturation point function. The procedure described by Eq B.6-B.9 is repeated until the convergence: $e_y = \|y^{k+1} - y^k\|$, $e_T = \|T^{k+1} - T^k\|$ and $e_{Total} = e_y + e_T \leq \varepsilon$, where ε is the maximum allowed error.

APPENDIX C – COMPARISON OF EXPERIMENTAL AND LITERATURE RESULTS OF BOILING POINT ELEVATION

The manufacturer of the pressure gauge used in this equipment provides the following correlation to correct the measure pressure:

$$P_{real} = 1.0101857 \times P_{measured} + 38.0716577$$

Using data of saturation temperature and pressure from NIST, presented in TABLE 25, it is possible to add a trend line to correlate THE temperature as function of pressure, as shown in FIGURE 37 for (a) water and (b) toluene.

TABLE 25 – LITERATURE DATA FOR SATURATION TEMPERATURE AND PRESSURE FOR WATER AND TOLUENE

Water			Toluene		
Temperature (°C)	Pressure (bar)	Pressure (kPa)	Temperature (°C)	Pressure (bar)	Pressure (kPa)
30.0	0.042	4.25	34.2	0.06	6.00
35.0	0.056	5.63	47.4	0.110	11.00
40.0	0.074	7.38	56.3	0.160	16.00
45.0	0.096	9.60	63.2	0.210	21.00
50.0	0.124	12.35	68.8	0.260	26.00
55.0	0.158	15.76	73.6	0.310	31.00
60.0	0.199	19.95	77.8	0.360	36.00
65.0	0.250	25.04	81.6	0.410	41.00
70.0	0.312	31.20	85.0	0.460	46.00
75.0	0.386	38.60	88.1	0.510	51.00
80.0	0.474	47.41	91.0	0.560	56.00
85.0	0.579	57.87	93.6	0.610	61.00
90.0	0.702	70.18	96.2	0.660	66.00
95.0	0.846	84.61	98.5	0.710	71.00
100.0	1.014	101.42	100.8	0.760	76.00
105.0	1.209	120.90	102.9	0.810	81.00
			104.9	0.860	86.00
			106.9	0.910	91.00
			112.2	1.060	106.00
			113.8	1.110	111.00
			115.4	1.160	116.00
			117.0	1.210	121.00

Source: NIST

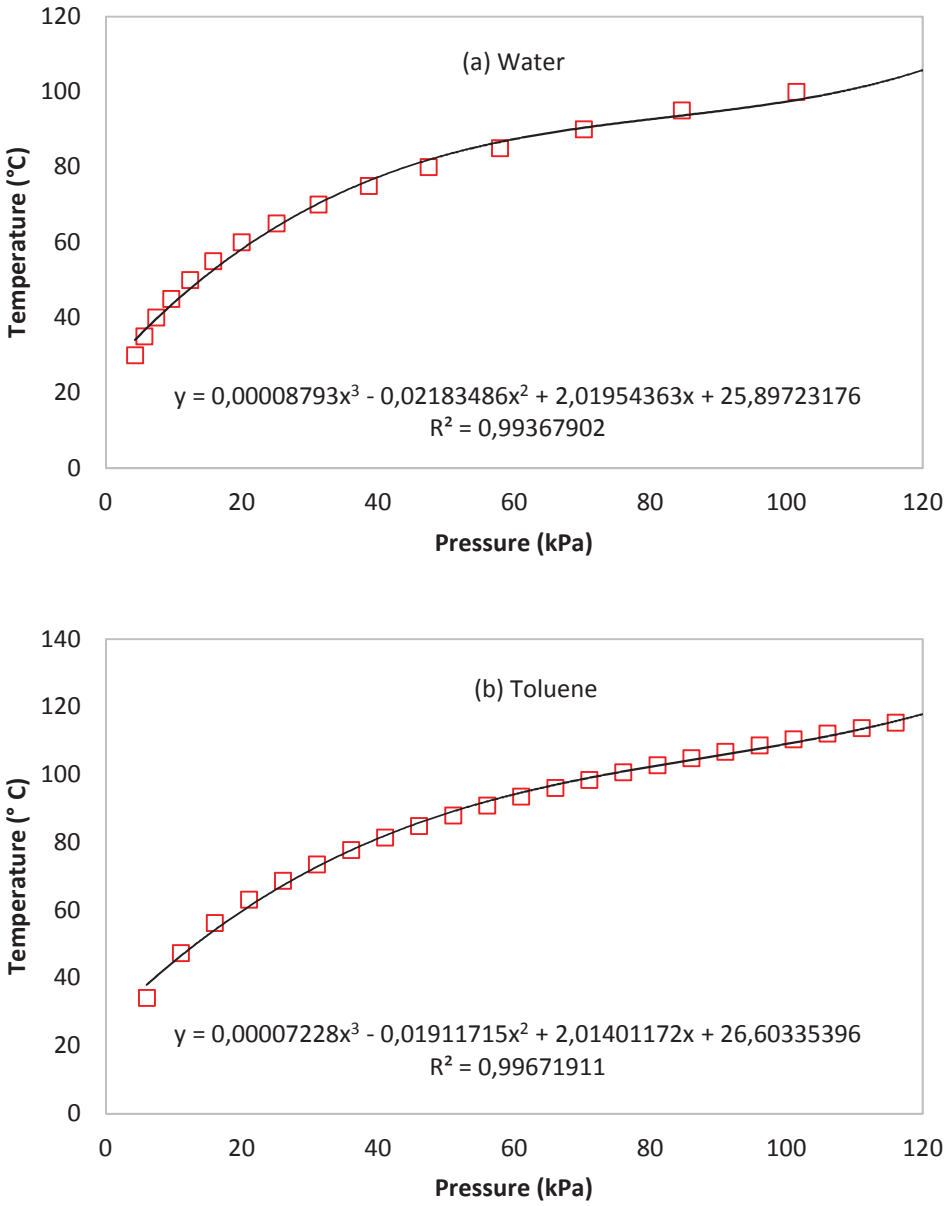

FIGURE 37 – LITERATURE DATA AND TREND LINE FOR SATURATION TEMPERATURE AS A FUNCTION OF PRESSURE FOR (a) WATER AND (b) TOLUENE
Source: The Author (2017)

From these correlations, for each experimentally measured pressure, the corresponding literature saturation temperature was estimated. Both temperatures (from literature and experimental) are presented in TABLE 26, that also presents relative errors, as calculated by Equation 78. FIGURE 38 presents both literature data and experimental results for the boiling point elevation diagram for (a) water and (b) toluene.

TABLE 26 – LITERATURE AND EXPERIMENTAL SATURATION TEMPERATURE FOR WATER AND TOLUENE.

Pressure (kPa)	Water			Toluene			
	T_{EXP} (°C)	$T_{LIT.}$ (°C)	Relative error (%)	Pressure (kPa)	T_{EXP} (°C)	$T_{LIT.}$ (°C)	Relative error (%)
8.40	44.0	41.4	6.33	5.68	37.7	37.4	0.72
13.45	51.4	49.3	4.19	13.50	54.7	50.5	8.33
24.01	62.9	63.0	0.27	23.86	68.0	64.8	5.01
44.11	76.1	80.0	4.93	43.71	84.0	84.1	0.17
69.27	86.8	90.2	3.82	64.17	95.8	96.2	0.44
90.18	97.3	94.9	2.49	79.27	102.8	102.1	0.66
91.10	97.3	95.1	2.26	91.00	107.6	106.0	1.47
		MRE	3.47			MRE	2.40

Source: The Author (2017)

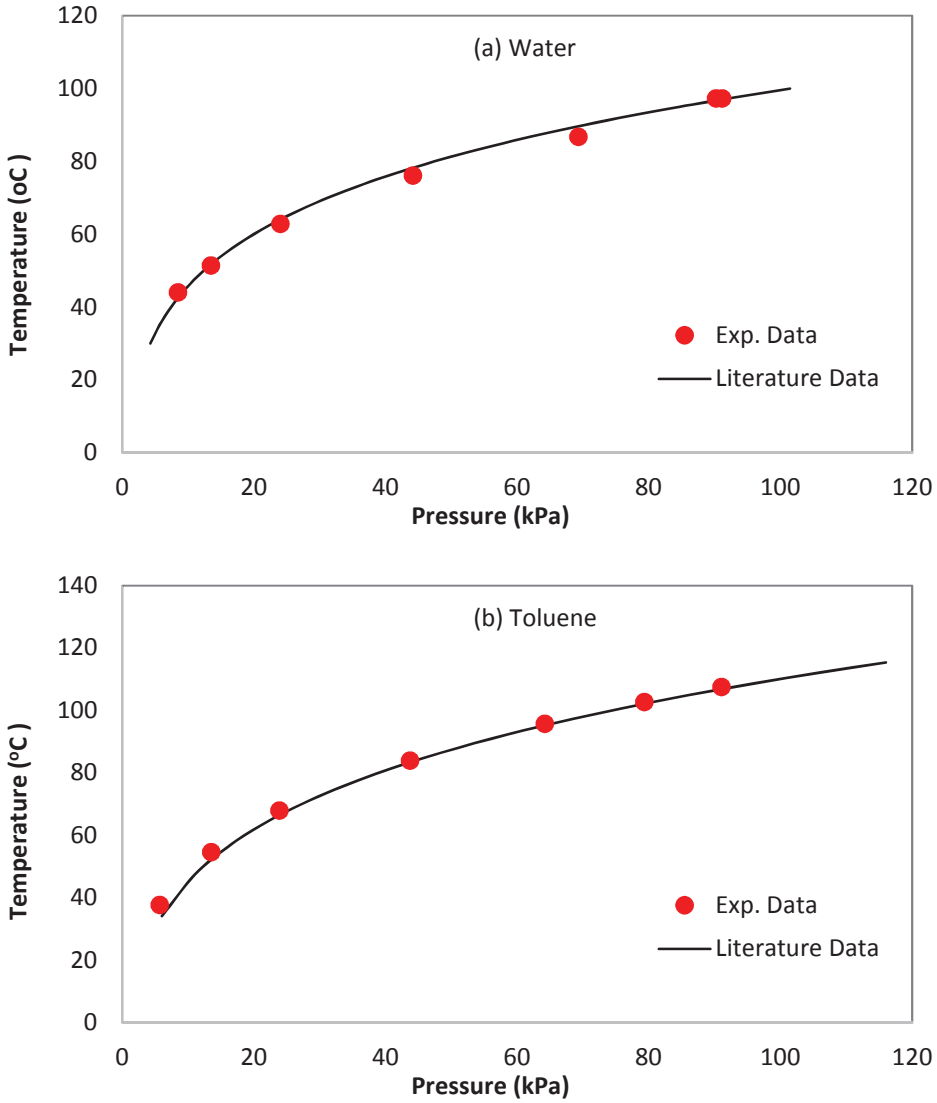

FIGURE 38 – EXPERIMENTAL AND LITERATURE DATA OF BOILING POINT ELEVATION FOR (a) WATER AND (b) TOLUENE
Source: The Author (2017)